universität wien

MASTERARBEIT/ MASTER'S THESIS

Titel der Masterarbeit / Title of the Master's Thesis

„Synthesis of Potentially Bioactive Compounds:

α-Aminophosphonates as Enzyme Inhibitors and an Improved TSPO Ligand for PET Diagnosis“

verfasst von / submitted by

Toda Stankovic, BSc

angestrebter akademischer Grad / in partial fulfilment of the requirements for the degree of

Master of Science (MSc)

Wien, 2019

Studienkennzahl lt. Studienblatt / degree programme code as it appears on the student record sheet:	UA 066 862
Studienrichtung lt. Studienblatt / degree programme as it appears on the student record sheet:	Chemie
Betreut von / Supervisor:	ao. Univ.- Prof. Mag. Dr. Michael Widhalm
Mitbetreut von / Co-Supervisor:	Dr. Katharina Pallitsch, Bakk. MSc

Acknowledgements

An dieser Stelle möchte ich mich bei alle bedanken, die zu dieser Arbeit beigetragen haben:

An erster Stelle möchte ich mich herzlich bei Kathi bedanken für ihre überwältigende Unterstützung im Labor, welche immer mit so viel Spaß und Freude von ihr erfolgte, und für die besondere Möglichkeit in diesem Labor, das für mich ein zweites zu Hause geworden ist, meine Masterarbeit zu machen.

Einen besonderen Dank auch an Thomas der mit seinem schwarzen Humor immer für gute Laune im Labor gesorgt hat und mir zur Seite stand wenn ich Hilfe gebraucht habe, wenn auch manchmal unfreiwillig.

Vielen Dank an Ao. Univ.-Prof. Dr. Friedrich Hammerschmidt für die Unterstützung bei den Fragen, welche seiner langjährige Erfahrung benötigt haben.

Ein großes Dankeschön an ao. Univ.- Prof. Mag. Dr. Michael Widhalm, ohne dessen Beteiligung diese Masterarbeit nicht möglich gewesen wäre.

Vielen Dank an die Tami, die mir große Hilfe geleistet hat im Labor.

Ich möchte mich auch gerne bei allen KollegInnen der Instituts für Organische Chemie bedanken, die für eine lustige und angenehme Atmosphäre in der Währingerstraße 38 gesorgt haben.

Danke auch an alle meine Freunde, die mir stets mit ihrer Unterstützung durch das Studium geholfen haben.

Vielen Dank auch an das Team des NMR Zentrums, der Massenspektrometrie sowie an das Mikroanalytische Laboratorium.

Ein großes Dank von Herzen an meinen Freund, welcher mir die ganze Zeit liebevoll zur Seite gestanden ist.

Zahvaljujem se mojoj dragoj familiji od srca za svu pomoc i sve sto su mi ucinili ovih zadjih godina, volim vas puno.

Ich möchte mich außerdem auch bei jenen bedanken, die hier nicht namentlich aufgezählt sind, aber dennoch einen Beitrag zur Masterarbeit geleistet haben.

“We can only see a short distance ahead, but we can see plenty there that needs to be done” [Alan Turing]

Content

1. Introduction

1.1 Organophosphonates

1.1.1 A brief classification

The availability of phosphorus has been crucial for the growth and productivity of all life forms throughout history, as it is an essential, irreplaceable macronutrient with diverse biological/biochemical functions. Amongst others, it is responsible for the primary energy transport of every cell in the form of inorganic phosphate (PO_4^{3-}, Pi) which is a functional component of ADP/ATP. The enzymatic process of phosphorylation is often used in cellular signaling cascades and regulates a variety of cellular uptake processes. Apart from these functions phosphate also plays an essential structural role. It can be found in the backbone of DNA molecules, where it is responsible for the high structural stability as well as in hydroxy apatite, which is the main component of inorganic bone matter. About 85 % of the entire amount of phosphorus in a human body can be found in bones. [1]

These well-known functionally and structurally important phosphorus containing compounds are just the tip of the iceberg. While phosphorus can be found in its highest oxidation state (+V) in all the mentioned compounds, there is also a vast number of reduced phosphorus compounds known today, where phosphorus has lower oxidation states (such as +I and +III). [2]

Phorphorus-containing compounds can be classified in different ways. One possibility is to classify them according to the elements that are directly bound to phosphorus. Considering this classification strategy, we can distinguish four groups of phosphorus-containing compounds: oxyphosphorus compounds (P–O bond-containing), carbophosphorus compounds (P–C bond-containing), azaphosphorus compounds (P–N bond-containing) and metallophosphorus compounds (P–metal bond containing). Organophosphonates are defined as phosphorus-containing compounds, attached to organic residues. They belong to the oxyphosphorus and the carbophosphorus group. A variable number of substituents of different nature attached to the phosphorus atom are possible (Figure 1).

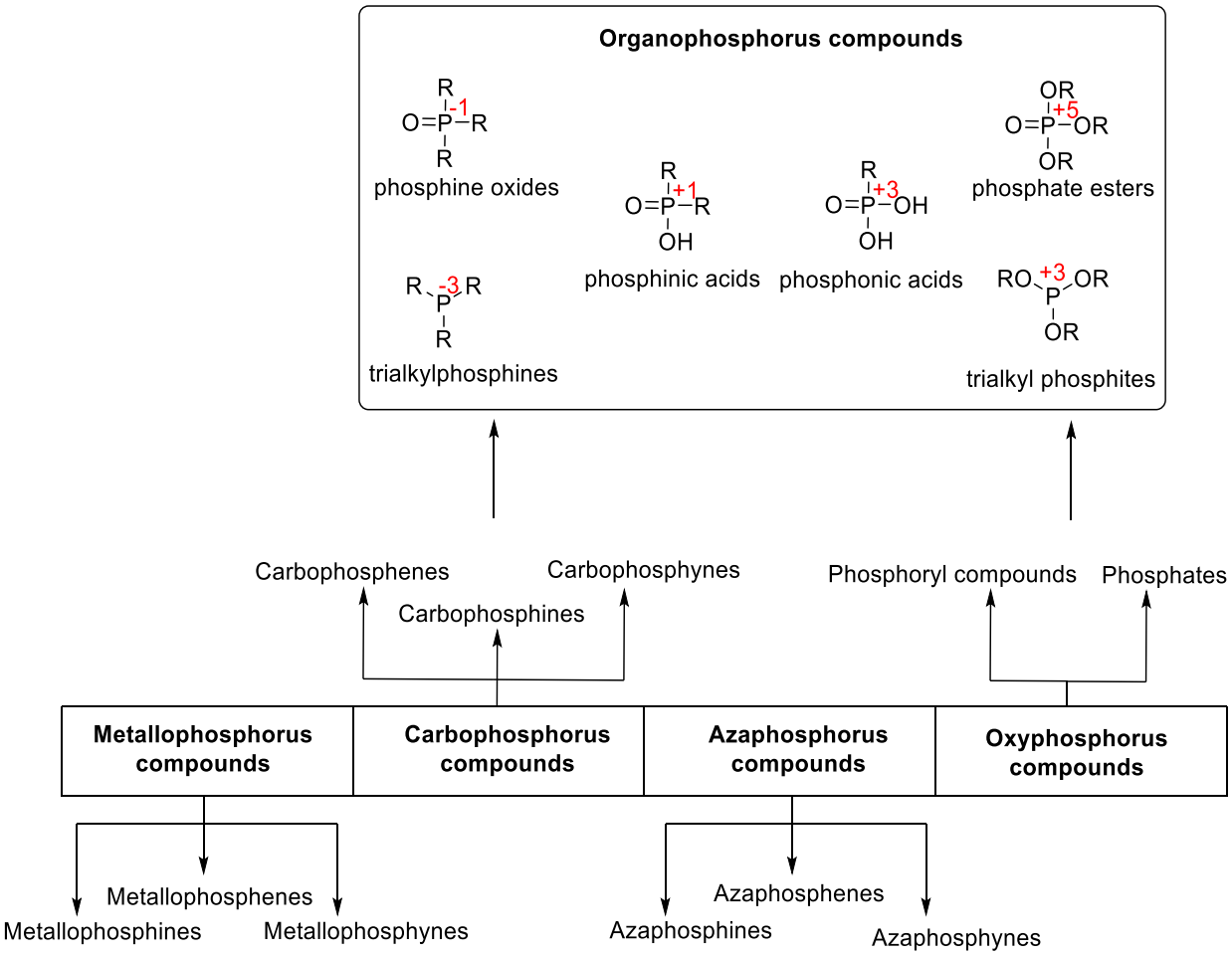

Figure 1. *Classification of phosphorus compounds into main groups and sub-groups according to the element type attached to phosphorus.*

Within the framework of this thesis, I will focus on the group of organophosphorus compounds, where phosphorus is attached to organic residues of differing nature. Within the group of organophosphorus compounds my particular interest is on phosphonic acids *aka* phosphonates (Pn). The molecules of this group are characterized by one direct, covalent phosphorus-carbon bond, while apart from this bond, phosphorus (in the oxidation state +III) is attached to three oxygen atoms.

1.1.2 The importance of organophosphonates through the ages

Organophosphorus compounds, with a direct P-C bond as seen above, have already been synthesized by alchemists in the middle ages, but systematic studies only began in 1820 [3] and it took one more century until in 1944 the first characterization of a synthetic phosphonate,

aminomethylphosphonic acid, was accomplished by Pikl *et al* . [4] Another fifteen years later the discovery of the first biogenic organophosphonate, 2-aminoethylphosphonic acid (2-AEP, **1.3**), which was isolated from sheep rumen protozoa, took place in 1959. [5] Although phosphonates have after that been found in a variety of tissue-types, [6] the first real proof of their existence in bacteria and related microorganisms was given after fosfomycin (**1.9**) was first discovered in 1969. During a search for organisms producing broad-spectrum antibiotics it was isolated from the oxygenated, drenched cultures of strains of *Streptomyces fradiae*, *Streptomyces viridochromogenes* and *Streptomyces wedmorensis*. [7]

1.1.2.1 Recent research progress

Since then, research on the chemistry of phosphonates in diverse natural and abiotic processes has progressed rapidly. It was found that the attractive properties of phosphonates range from a good resistance towards chemical hydrolysis, or against enzymatic degradation to a high thermal stability. [8] Their resistance against enzymatic degradation is also the reason why phosphonates are often found as side groups on exopolysaccharides and glycoproteins or in the polar head groups of membrane phosphonolipids in many primitive life forms. Their C–P bond can withstand the action of phosphatases and thus increases structural rigidity and stability. [4] Apart from these high molecular compounds, there is also a small, but steadily growing group of low molecular phosphonates of secondary metabolic origin. Up to 2009 there were only 20 members of this group known, [9] while nowadays already twice as many have been discovered. [10] In **Scheme 1** the eight elementary organophosphonates and some of their more complex derivatives are shown. [11]

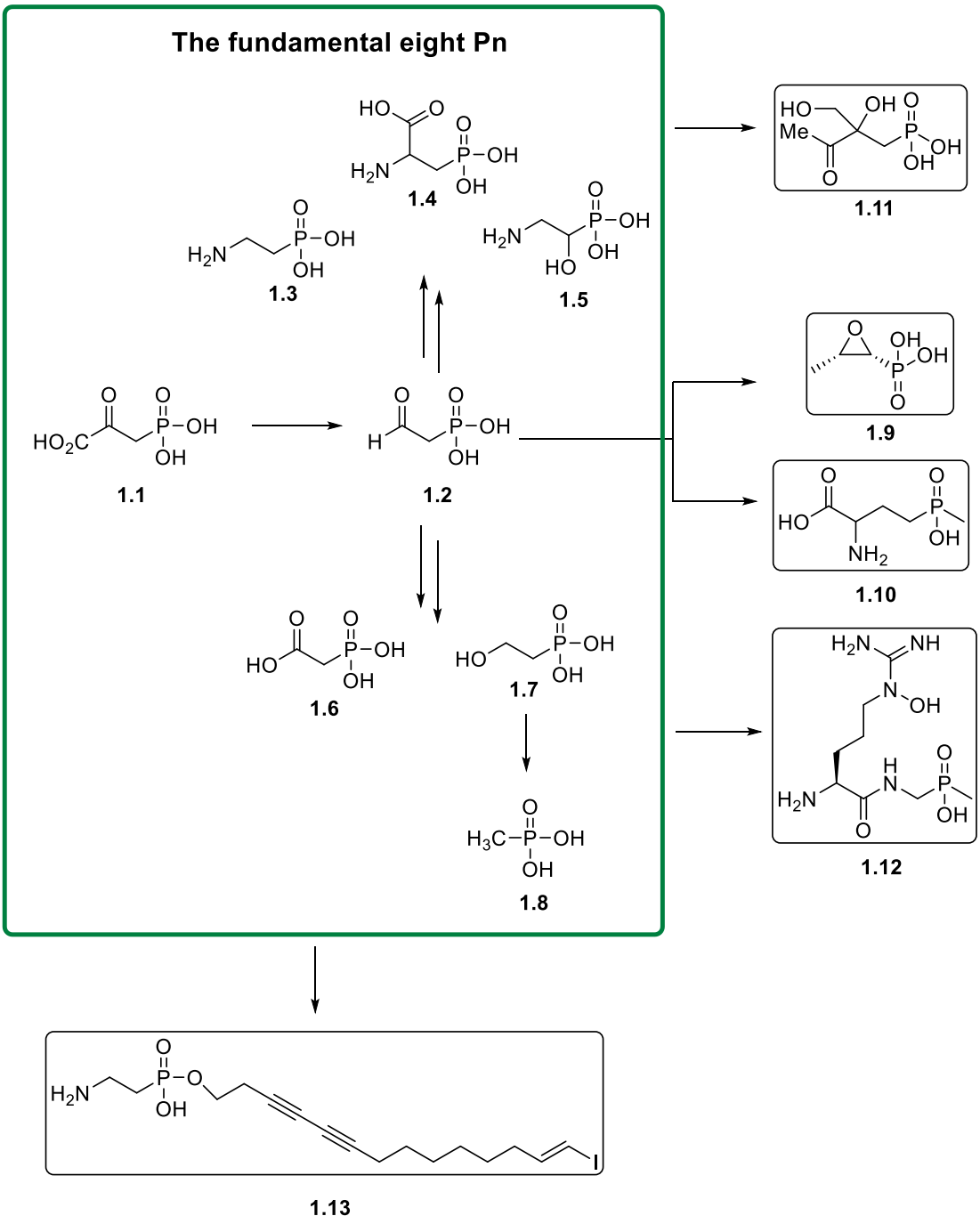

Scheme 1. *The fundamental eight Pn [phosphonopyruvate (**1.1**), phosphonacetaldehyde (**1.2**), 2-aminoethylphosphonic acid (**1.3**), phosphonoalanine (**1.4**), 2-amino-1-hydroxy-ethylphosphonic acid (**1.5**), phosphonoacetate (**1.6**), 2-hydroxyethylphosphonic acid (**1.7**), methylphosphonic acid (**1.8**)] together with some examples of phosphonates of industrial and medicinal importance [fosfomycin (**1.9**), phosphinothricin (**1.10**), phosphonothrixin (**1.11**), argolaphos B **1.12**, phosphoiodyn A (**1.13**)]; the biosynthetic relationships are represented by arrows.*

Even if they are quite simple looking compounds, phosphonates still have remarkable bioactivities. Phosphonic acid natural products have thus an immense pharmaceutical and industrial potential, with a commercialization rate of about 15%, which is massively higher than the 0.1% average for all isolated natural products. [10] Their useful properties range from antibiotic [fosfomycin (**1.9**) and argolaphos B (**1.12**)], to herbicidal [phosphinothricin (**1.10**) and phosphonothrixin (**1.11**)]. [12] There are even phosphonates known which inhibit the human transcription factor gamma (hPPARγ) [phosphoiodyn A (**1.13**)]. Phosphonoalanine (**1.4**) for example has been proved in experiments to inhibit amino acid receptors in the hippocampus of rats. [13] The useful properties of biogenic phosphonates are nowadays highly explored for applications in medicine, industry and agriculture.

Considering the effectiveness of all those biogenic phosphonates as well as the mentioned stability of the carbon−phosphorus bond, it was no surprise that over the decades manifold synthetic phosphonates and analogues to the biogenic compounds were designed and synthetized. [14]

1.1.3 Phosphonates of industrial importance

1.1.3.1 Antibiotic and herbicidal phosphonates

Fosfomycin (**1.9**) combines two interesting structural features: an epoxide ring, which is rare in antibiotics, [15] and a carbon-phosphorus bond. Fosfomycin can enter bacterial cells, due to the phosphonate group which enables it to use the L-α-glycerophosphate as well as the hexose-6-phosphate transporter systems. [16] Its antibacterial properties stem from the inhibition of the enzyme UDP-*N*-acetylglucosamine enolpyruvyl transferase (MurA), which catalyzes the first step of the bacterial peptidoglycan biosynthesis. It is responsible for the transfer of the enolpyruvyl moiety of phosphoenolpyruvate (PEP) to the 3‘-hydroxyl group of UDP-*N*-acetylglucosamine (UNAG) (**Scheme 2**). Fosfomycin binds covalently to the thiol group of the cysteine 115 residue in the active site of MurA, which leads to irreversible inhibition of the enzyme. [17]

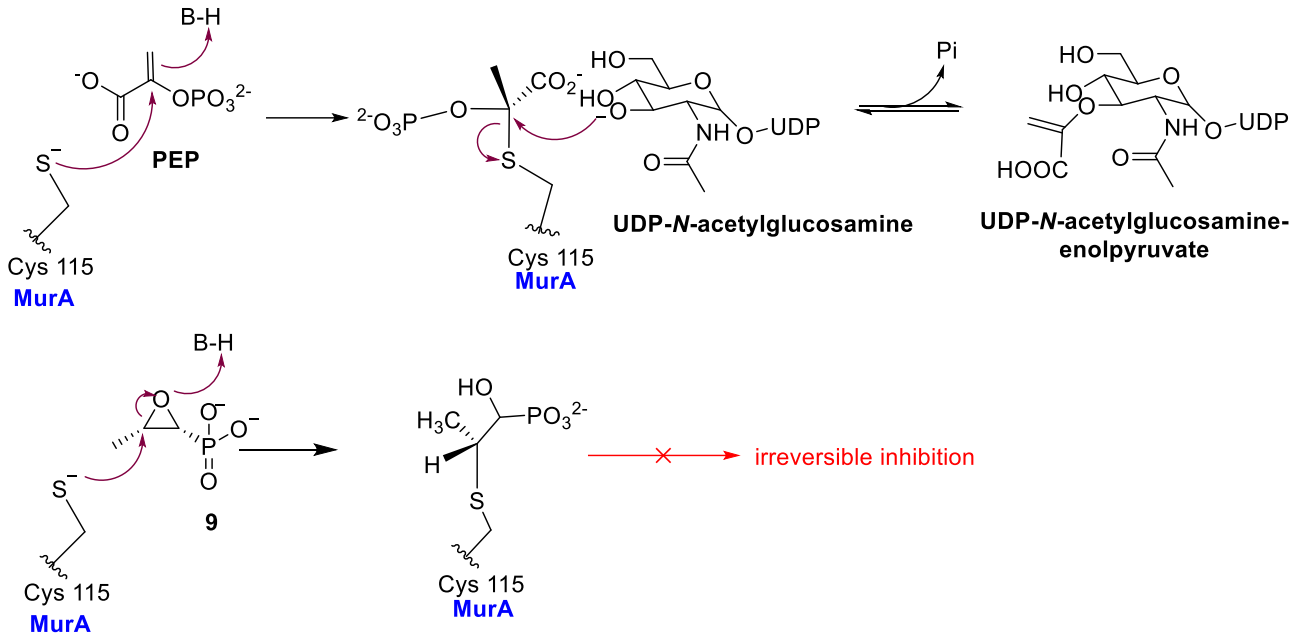

Scheme 2. *First row: Transfer of the enolpyruvyl moiety by Cys 115 of Mur A from phosphoenolpyruvate to UDP-N-acetylglucosamine; second row: the inhibition of MurA by fosfomycin (**1.9**); B-H = proton donor.*

Two years after the discovery of fosfomycin, the search for more organisms producing broad-spectrum antibiotics lead to the discovery of a novel phosphonic acid tripeptide (bialaphos, **1.14**, **Figure 2**) consisting of two L-alanine groups and an up to then unknown amino acid: L-2-amino-4-[hydroxy(methyl)phosphinyl] butyric acid. The name phosphinothricin (**1.10**) was given to the novel amino phosphinic acid by Bayer *et al.,* one of the working groups which discovered it simultaneously with Kondo *et al.* [18]

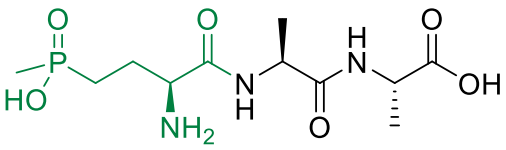

Bialaphos (**1.14**)

Figure 2. *Structure of the tripeptide bialaphos (**1.14**) with phosphinothricin (**1.10**) highlighted in green.*

Although phosphinothricin (**1.10**) was first assumed to have antibiotic properties, Hoechst AG proved that its antibiotic properties were considerably weak. [18] Following further biological screenings its herbicidal effect was discovered and after glasshouse and field trials the Hoechst AG applied for a patent 1977. The racemic ammonium salt of phosphinothricin has since been the active ingredient of a huge number of commercial herbicides under the name glufosinate ammonium (GLA). It effectively mimics glutamate and thus shows irreversible inhibition of the enzyme glutamine synthetase, which is responsible for ammonium assimilation in plants. [19] Inactivation of the enzyme leads to the accumulation of ammonia, a toxic compound, inside the thylakoid lumen. [20]

1.1.3.2 Antiviral phosphonates

As already mentioned, the useful properties of biogenic phosphonates have fueled the development of synthetic analogues and derivatives. Nowadays, one of the most famous synthetic phosphonates is certainly tenofovir (**1.16**), which acts as an acyclic nucleotide analogue of adenosine (**Figure 3**). [21] It is a very potent antiviral compound used in the treatment of HIV and hepatitis B infections. A prodrug [tenofovir disoproxil fumarate (**1.15**)] is also on the market. [22] After dephosphorylation inside the cell, it competes with deoxyadenosine 5'-triphosphate (**1.17**) for the incorporation into DNA during HIV transcription and thus inhibits the action of the HIV reverse transcriptases (RTs) and viral DNA polymerases. As those are important key factors in the viral life cycle, DNA chain elongation is stopped, and termination of the viral DNA growth takes place. [23]

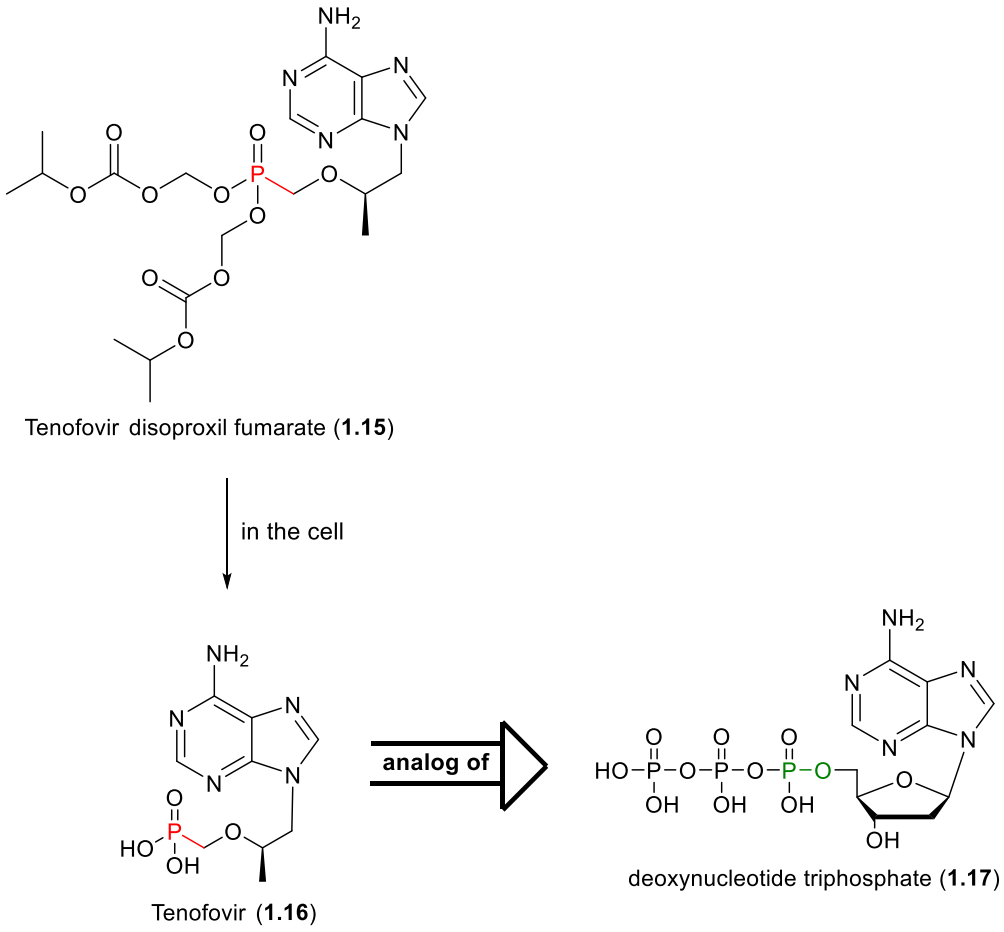

Figure 3. *Structures of the adenosine analogue tenofovir (**1.16**) and its commercially available prodrug tenofovir disoproxil fumarate(**1.15**).*

1.1.3.3 Phosphonates as warfare agents

The potential of phosphonates to effectively mimic enzymatic substrates has also been misused. The most prominent negative example certainly is the chemical warfare agent sarin (**1.18**). It inhibits the enzyme acetylcholinesterase by rapid phosphorylation of the catalytically active serine residue. The modified enzyme (**Scheme 3**) then shows complete resistance to oxime-mediated reactivation by medical antidotes. [24]

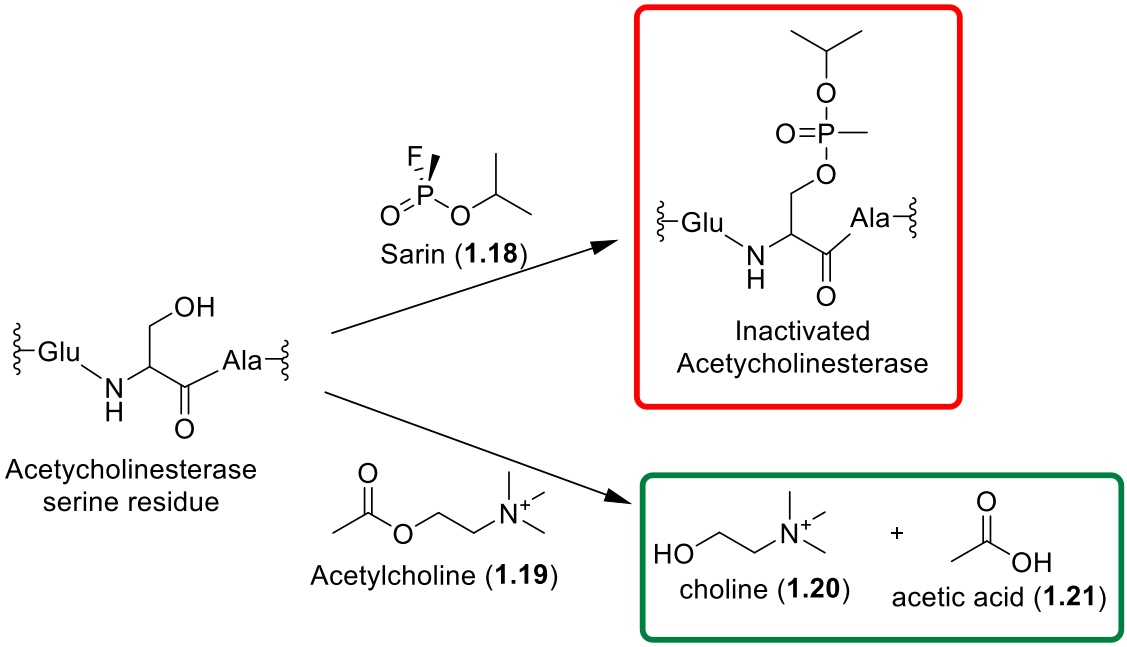

Scheme 3. *Mode of action of sarin; reaction of the active serine residue of acetylcholinesterase with its natural substrate (**1.19**), compared to the reaction with sarin (**1.18**).*

1.1.3.4 Aminophosphonic acids in medicinal chemistry

α-Aminophosphonic acids are structurally special among all phosphonic acids. α-Aminophosphonates are the phosphonic acid analogues of natural aminocarboxylic acids, where the carboxylic group is replaced by a phosphonic acid (**Figure 4**).

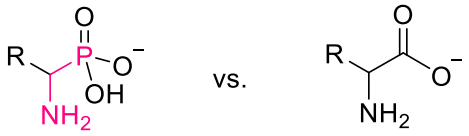

Figure 4*. General structure of α-aminophosphonic acids with the characteristic N-C-P scaffold compared to α-aminocarboxylic acids.*

Their charge and structure makes them ideal enzyme inhibitors of many different biotransformations. Even though the carboxylic- and phosphonic acid groups are different in shape (tetrahedral phosphorus and planar carbon), acidity (phosphonic acids are more acidic) and the steric bulkiness (the atomic radius of P is much larger than carbon), they are still recognized as substrates by the enzymes.

The special tetrahedral shape of the substituents around the phosphorus atom structurally resembles the high-energy transition state of ester- and amide bond formation and hydrolysis (**Scheme 4**). However, in contrast to these labile transition states it is highly stabilized by the enzyme active site. Phosphonates are thus often covalently bound by the enzyme, but cannot be cleaved again, enabling irreversible inhibition of the enzyme. This ability is known since the discovery of the inhibition of α-chymotrypsin by phosphonate analogs of alanine and phenylalanine in 1986. [25]

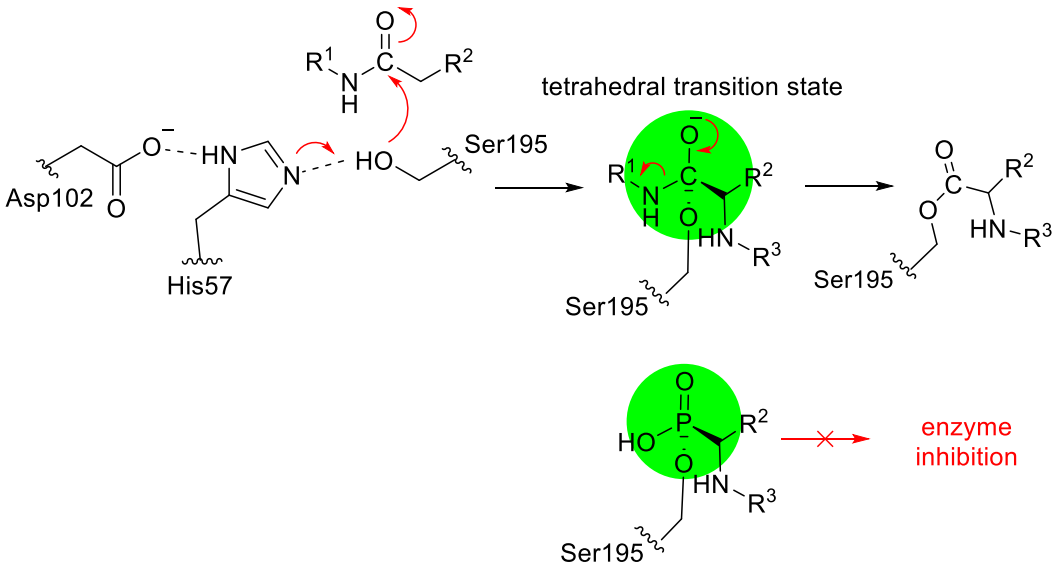

Scheme 4. *Mechanism of the cleavage of the C-N bond during amide hydrolysis by the enzyme chymotrypsin compared to a possible inhibition mode by an α-aminophosphonate.*

A commercially available drug using this mode of action-eventhough no α-aminophosphonate- is fosinoprilat (**1.23**, **Figure 5**). It is administered as a prodrug (fosinopril, **1.22**) which is metabolically converted to the active compound **1.23**. Fosinoprilat is an inhibitor of the angiotensin-converting enzyme (ACE), which converts the hormone angiotensin I to the active vasoconstrictor angiotensin II. This leads to the constriction of blood vessels and thus elevated blood pressure. Research is going on in this field at fast pace, as there has been a recent discovery in 2019 that α-carboxynucleoside phosphonates can inhibit viral DNA polymerases, mimicking their natural 2-deoxynucleotide 5-triphosphate substrates. [26] In the same year new inhibitors of 1-deoxy-d-xylulose-5-phosphate (DXP) synthase, a vital enzyme in bacterial metabolism, have been developed to prevent antibiotic resistance. [27]

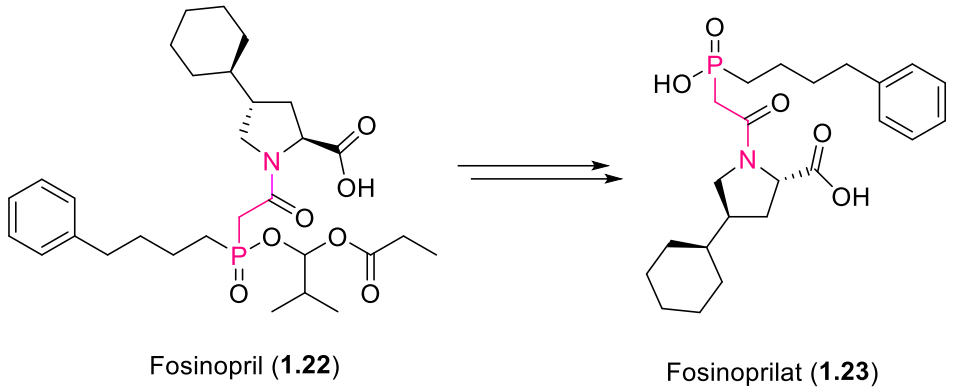

Fosinopril (**1.22**) Fosinoprilat (**1.23**)

Figure 5. *Structures of the prodrug fosinopril (**1.22**) and the active metabolite fosinoprilat (**1.23**).*

1.1.4 The environmental importance of phosphonates

Organophosphonates are present in a variety of bioactive compounds in agriculture, medicine and in common products such as laundry detergents. Despite their manifold application they were for a long time still considered to be of limited environmental importance. [4] Although it has already been known that phosphorus-containing compounds are major industrial contaminants, [28] it was only recently that the enzymology that is involved in the biosynthesis and catabolism of Pn has gained more attention. Improved analytical techniques together with genome sequencing and the manipulation of genomic and metagenomic DNA have led to the development of a better methodology for understanding C-P bond cleavage by a vast number of organisms. [11] Biogenic phosphonates play an important role as phosphorus source for microorganism especially in marine ecosystems. The availability of inorganic phosphorus in marine habitats is very limited due to the low solubility of Pi in water at room temperature, ambient pressure and pH. Thus, organophosphorus species play a vital role as alternative phosphorus source in these regions. It has been shown, that phosphonate-P makes up up to 25% of the total dissolved, organic P (DOP) in some regions of the ocean, especially in phosphate poor ocean surface waters of the Pacific Ocean. [29] This accounts for up to 80 % of the total available phosphorus in some regions. Since most marine microorganisms are thus living under Pi starvation conditions, they have developed mechanisms to cleave the C-P bond of Pns as alternative, readily available phosphorus source present in the oceans. Currently, there are three

general known enzymatic pathways for Pn catabolism, which can be grouped as follows: hydrolytic, radical and oxidative P-C bond cleavage routes. Two of those three, namely the hydrolytic and oxidative mechanisms, are very substrate specific, while the radical pathway is very flexible in terms of the accepted substrates.

1.1.5 Phosphonate biodegradation pathways

1.1.5.1 Hydrolytic C-P bond cleavage

For the hydrolytic P-C bond cleavage the substrate needs to have a carbonyl group in β-position to the phosphonate group. The β-carbonyl is used to stabilize the carbanion leaving group, formed upon nucleophilic attack of an active site water molecule at the phosphorus atom. There are three different hydrolases known today. Phosphonopyruvate hydrolase (PnPyH) was first discovered by Quinn [30] during the isolation of a *Burkholderia cepacia* species, which was able to catabolize phosphonoalanine (**1.4**). Phosphonoalanine is converted to phosphonopyruvate (**1.1**) by a transaminase in the first reaction step. The latter can then be further converted by PnPyH, with the help of a metal ion (Co^{2+}, Ni^{2+}or Mg^{2+}) cofactor to Pi and pyruvate (**1.24**) (**Scheme 5**).

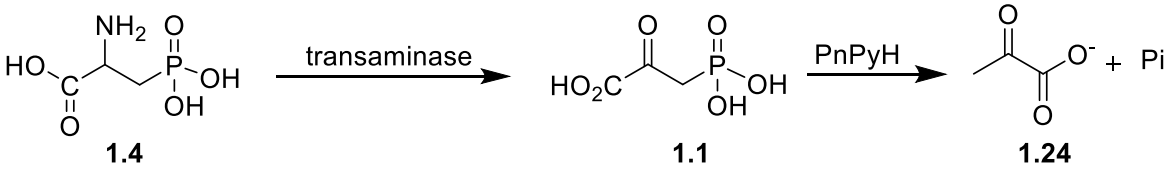

1.4 **1.1** **1.24**

***Scheme 5**. Conversion of PnPy to pyruvate by PnPyH.*

The second known hydrolase is phosphonacetaldehyde hydrolase (PnAAH), which metabolizes 2-AEP (**1.3**) in a two-step sequence to release Pi and acetaldehyde. The first step is a transamination performed by 2-AEP-pyruvate transaminase (encoded by *PhnW*). Then, phosphonacetaldehyde, (**1.2**), obtained as an intermediate and finally Pi is formed after hydrolysis by phosphonatase (PhnX). Although the exact mode of action has not been elucidated completely, La Nauze was able to demonstrate that a Schiff base intermediate was formed during catalysis. [31] The

protonated, positively charged Schiff base intermediate, which is formed with the lysine 53 residue, functions as an electron sink to stabilize the carbanion leaving group after the cleavage of the C-P bond. Afterwards, a phosphoryl-transfer to aspartate 12 is proposed to take place, which acts as the second active site nucleophile in PhnX. Thus, PhnX is one of only few enzymes that utilize bicovalent catalysis. After the hydrolysis of the intermediate imine, acetaldehyde **1.25** and Pi are released (**Scheme 6** and **Scheme 7**). [32]

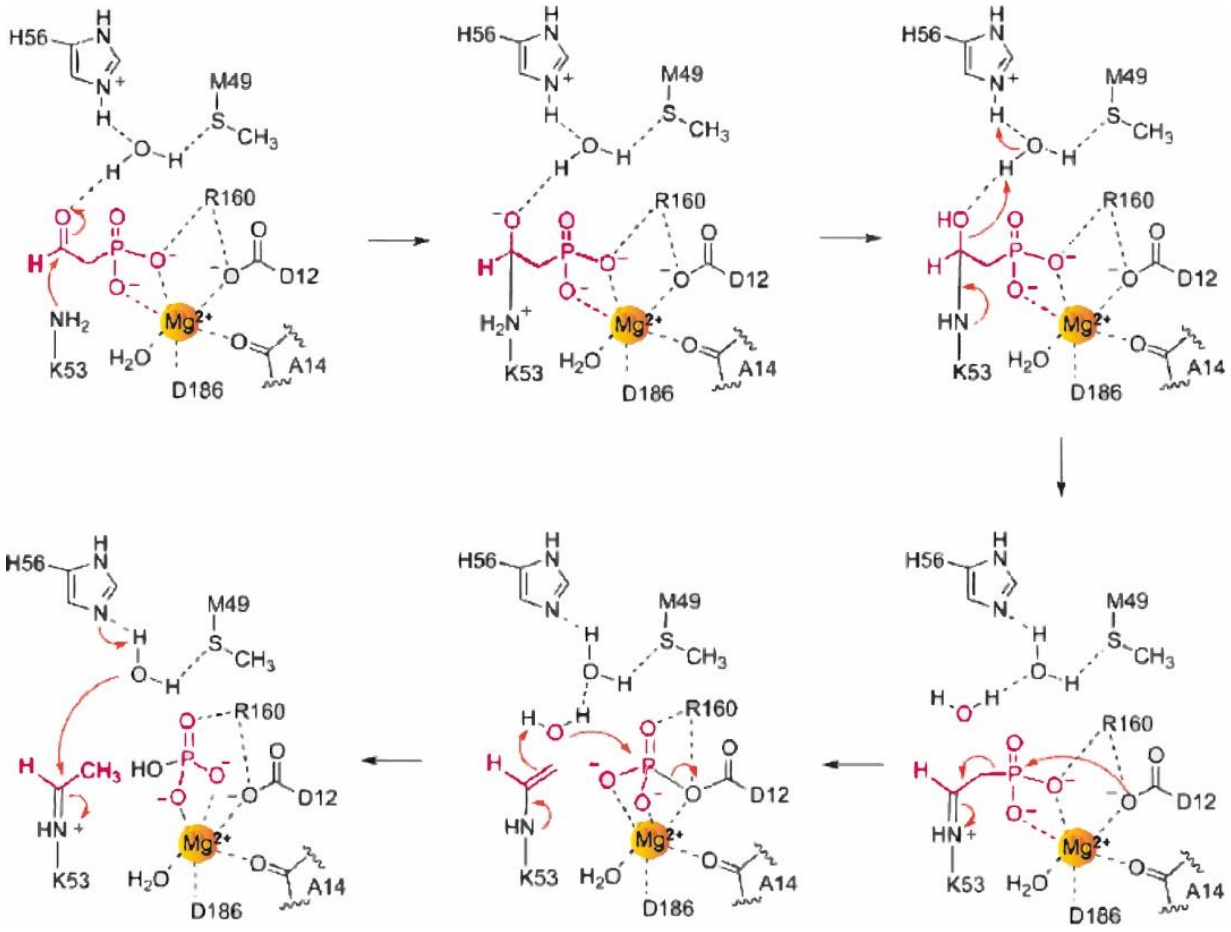

Scheme 6. *Proposed mechanism of phosphonatase (PhnX). [11]*

The third known hydrolytic P-C bond cleaving reaction is performed by phosphonoacetate hydrolase (PhnA). A three-step sequence (transamination, oxidation, hydrolysis) is used for the conversion of **1.3** to Pi and acetate. [33] The first step is again performed by the already described *phnW*-encoded transaminase to yield **1.2**. After oxidation by PhnY, which specifically uses NAD^+

as cofactor, phosphonoacetate (**1.6**) is formed as an intermediate that can be hydrolyzed by PhnA, finally yielding Pi and acetate (**1.26**, **Scheme 7**).

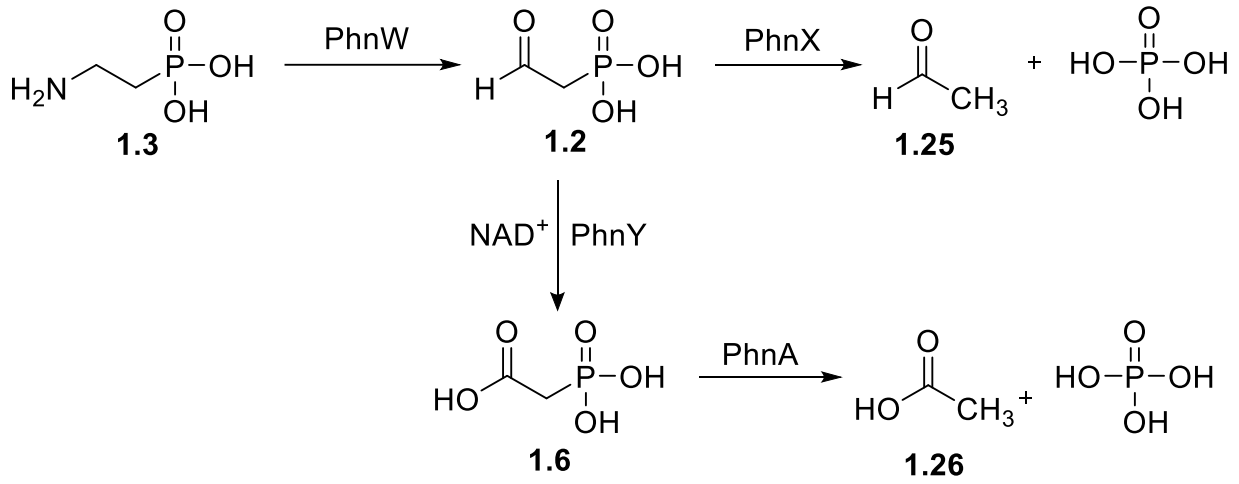

Scheme 7. *Comparison of 2-AEP degredation by PnAAH & PnAH.*

In the first step of the hydrolysis the hydroxyl group of the T68 residue attacks the P-center to form a trigonal bipyramidal transition state. Two metal ions are used to stabilize one of the equatorial oxygen-atoms of the resulting phosphate, whereas the formed enolate is stabilized by a hydrogen bridge to a water molecule, held in place by the residue I287, as well as by electrostatic interactions. After release of acetic acid, a nucleophilic water molecule, attacks the phosphate ester intermediate and Pi is formed (**Scheme 8**). Until this mechanism was found in bacteria, phosphonoacetate (**1.6**) was thought to be a purely synthetic compound. [34]

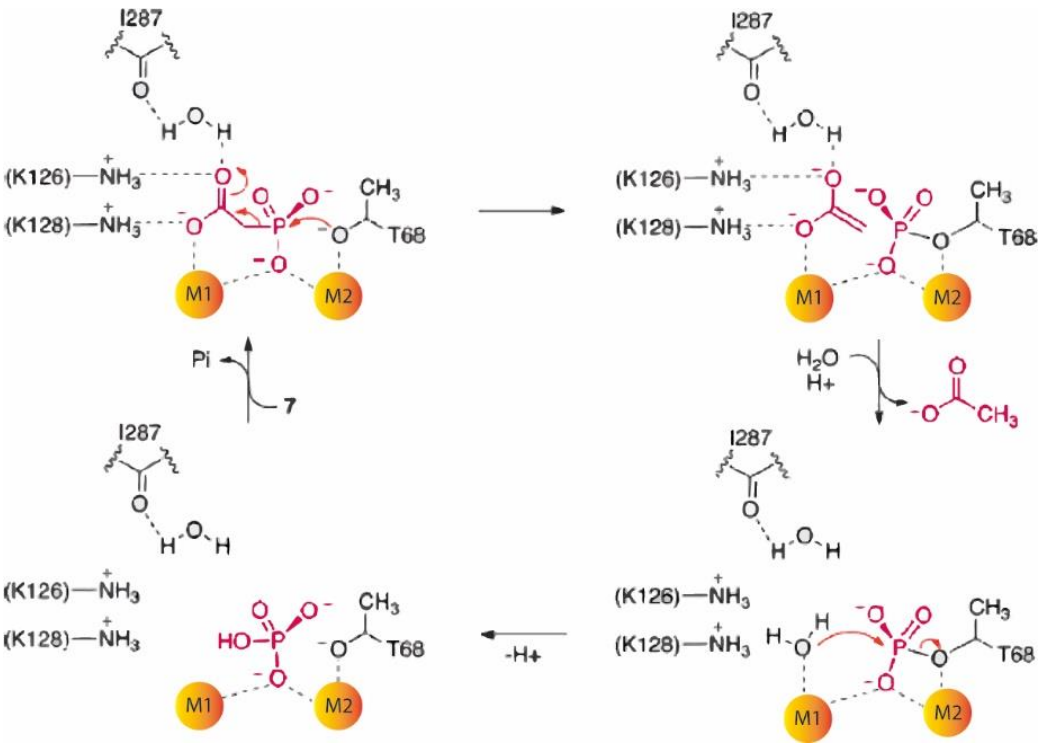

Scheme 8. *Proposed mechanism for the hydrolase PhnA. [11]*

1.1.5.2 Radical C-P bond cleavage

The radical Pn catabolism performed by the C-P lyase enzyme complex is the most abundant phosphonate degradation pathways known today. It can even cleave unactivated C-P bonds. Due to its extraordinary lack of substrate specificity, it enables bacteria to obtain phosphorus from a vast number of phosphonates such as **1.3**, **1.6**, **1.8** and **1.9** (see **Scheme 1**). This further displays the remarkable ability of nature to have multiple solutions for catabolizing the same compounds. Even nowadays there are still different substrate analogs synthesized to test the specificity of C-P lyase as well as to elucidate its detailed mechanism. C-P lyase has been shown to capture the carbon radical formed after homolytic C-P bond cleavage and is able to insert a hydrogen atom ($H^{\cdot}$) at an extremely fast exchange rate of up to $10^{11} sec^{-1}$ (**Scheme 9**). [35]

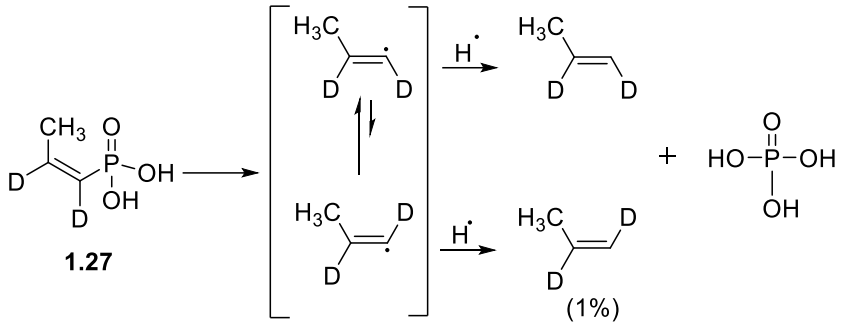

***Scheme 9**. Radical intermediates formed by C-P lyase of* K. oxytoca *from 1,2-[$^2H_1$](Z)-prop-1-en-1-ylphosphonic acid in an enzyme kinetic study. [35]*

But calling it a "simple radical mechanism" is by far too trivial to describe the complex route necessary to obtain Pi by C-P lyase. The C-P lyase pathway actually consists of 14 polypeptides, encoded by the *phnCDEFGHIJKLMNOP* operon, each of which has a very specialized biochemical function. The complex pathway is illustrated for the C-P bond cleavage of 2-aminoethylphosphonic acid (**1.3**) below (**Scheme 10**) and the function of each of the involved polypeptides is listed to illustrate the complexity of the entire process (**Table 1**). [36]

***Table 1**. Biochemical functions of the single enzymes of the* E. coli phn *operon.*

Phn polypeptide	Activity and/or function
Phn C	ABC transport system, nucleotide-binding protein
Phn D	ABC transport system, periplasmic binding protein
Phn E	ABC transport system, membrane-spanning protein
Phn F	regulatory protein, exact funtion not yet known
Phn G	purine ribonucleoside triphosphate phosphonylase component of PhnGHIJK
Phn H	purine ribonucleoside triphosphate phosphonylase component of PhnGHIJK
Phn I	purine ribonucleoside triphosphate phosphonylase component of PhnGHIJK
Phn J	C-P lyase, component of PhnGHIJK
Phn K	nucleotide-binding protein of an ABC transport system, component of PhnGHIJK
Phn L	nucleotide-binding protein of an ABC transport system
Phn M	5'-triphosphoribosyl 1'-phosphonate diphosphohydrolase
Phn N	ribosyl bisphosphate phosphokinase
Phn O	aminoalkylphosphonate *N*-acetyltransferase
Phn P	phosphoribosyl cyclic phosphodiesterase (specific)
Phn PP	cyclic phosphate dihydrolase (non-specific)
Deo B	phosphoribomutase for isomerisation
RPK	ribose-1-phosphokinase for phosphorylation

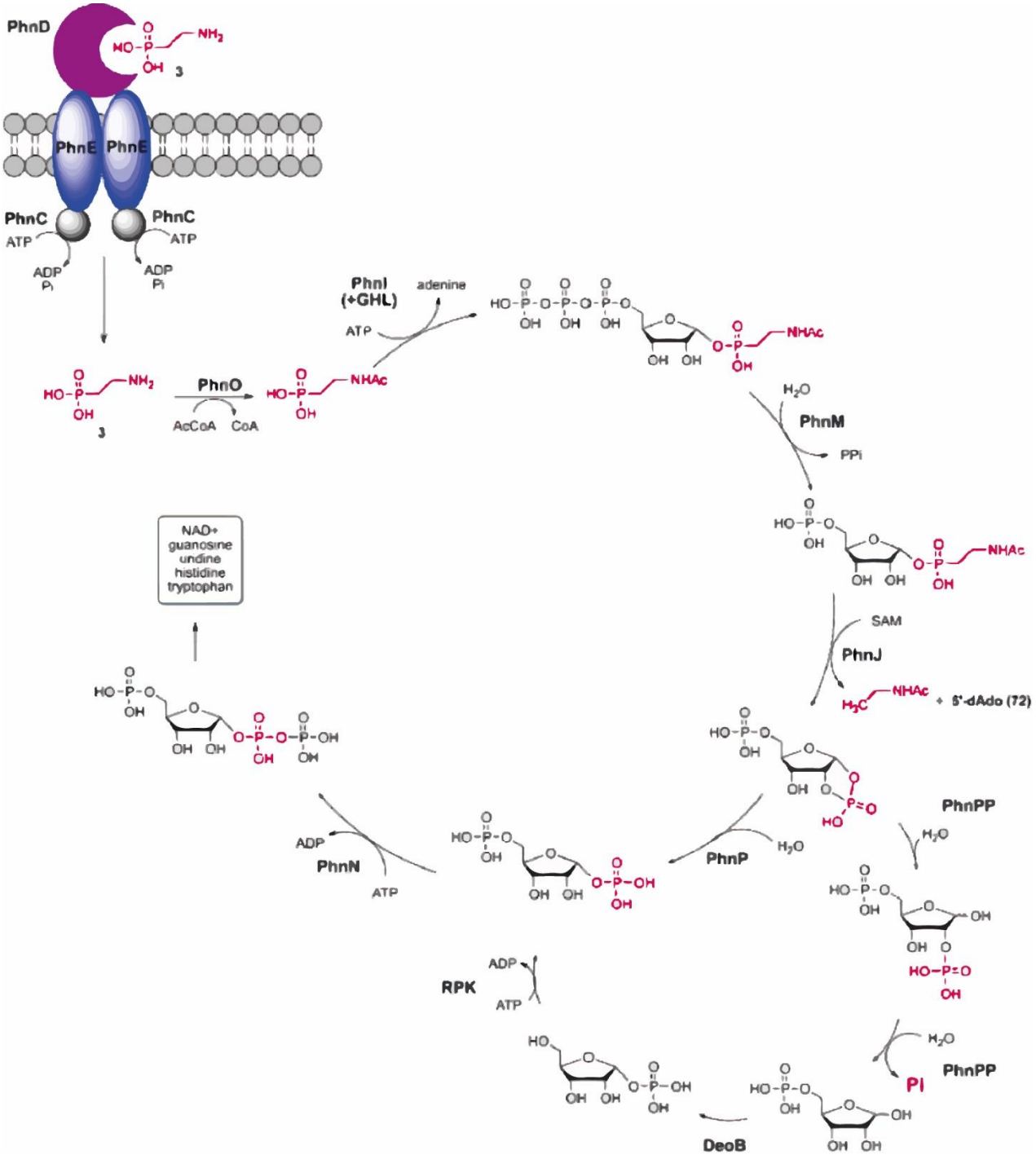

Scheme 10. *Overview of the C-P lyase catalyzed 2-AEP (**1.3**) P-C bond cleavage. [11]*

This highly complex mechanism also provided the first explanation for the observed methane supersaturation of the oxygen-rich ocean surface waters, which was a long-standing paradox. Thus, it is relevant for global warming. The methane paradox describes the phenomenon that biogenic methane production was long time considered to be limited to archaeal methanogenesis, a strictly anaerobic process, which is usually inhibited by the presence of oxygen and sulfate. Still an oversaturation of ocean surface waters with methane leading to a net flow of the latter to the atmosphere from sulfate-rich, fully oxygenated ocean surface waters, could be observed. [37] The use of methylphosphonic acid (**1.8**) by euphotic marine bacteria to obtain Pi and methane via C-P lyase, [38] is part of the explanation.

The biogenic origin of the used methylphosphonic acid (**1.8**) has been explored thoroughly and it was found by Metcalf *et al*. that the marine archaeon *Nitrosopumilus maritimus* possesses a phosphoenolpyruvate phosphomutase (*Ppm*) gene which is encoding the enzyme PEP mutase. This enzyme catalyzes the first step in the biosynthesis of most known phosphonates. *Ppm* is located within a biosynthetic gene cluster further encoding the biosynthesis of 2-hydroxyethylphosphonic acid (2-HEP, **1.7**). [39] Another enzyme, namely methylphosphonate synthase (MpnS), was shown to further convert **1.7** to **1.8**, releasing CO_2 as a side product. MPnS shares two histidine residues with 2-hydroxyethylphosphonate dioxygenase (HEPD, **Figure 6**). [40] HEPD is an enzyme responsible for the conversion of 2-HEP to hydroxymethylphosphonate (HMP) during the biosynthesis of phosphinothricin (**1.10**).

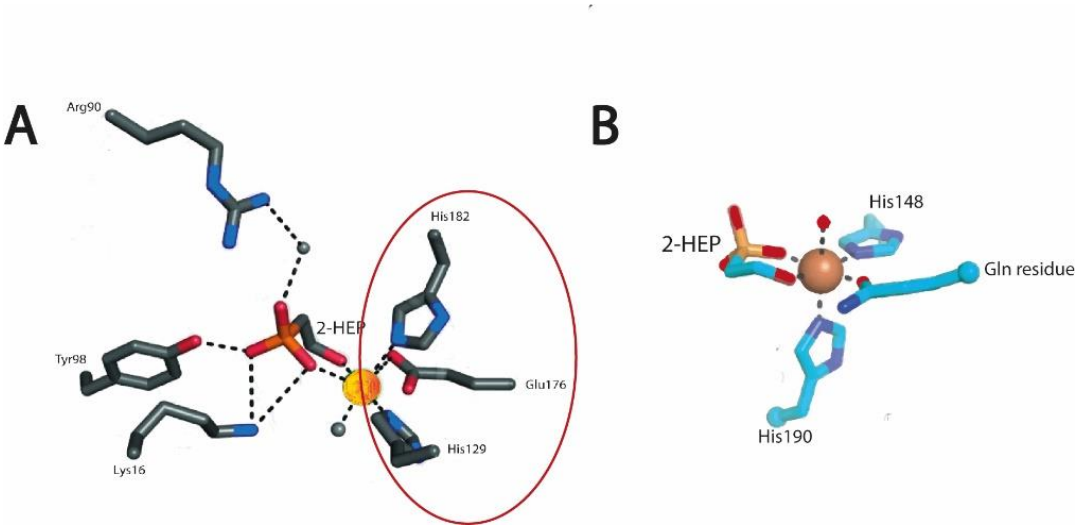

Figure 6. *(A) Illustration of the active site of HEPD, where the 2-His-1-carboxylate triad binds a divalent cation, coordinating 2-HEP.*
(B) Active site of MPnS of N. maritimus *showing strong similarities to HEPD. [41]*

The definite mechanism of MpnS has still to be elucidated. Based on recent studies a possible mechanism, can be proposed (**Scheme 11**). [11] It has been suggested that **1.7** binds to the Fe(II) cofactor and after formation of a superoxide species with molecular oxygen, a ketyl-like radical can be formed by hydrogen abstraction (**Scheme 11**, A). The ketyl radical can then reduce the ferric ion from Fe(III)-O−OH to Fe(II)-O−OH and form an aldehyde during the process (**Scheme 11**, B). The reductive homolytic cleavage of the peroxide bond yields an alkoxyl radical, which is then able to form a methylphosphoryl radical and formate (C) by β-scission of the C1−C2 bond. From this point there are two possible directions, one of which is leading to the formation of methylphosphonic acid (**1.8**, D).

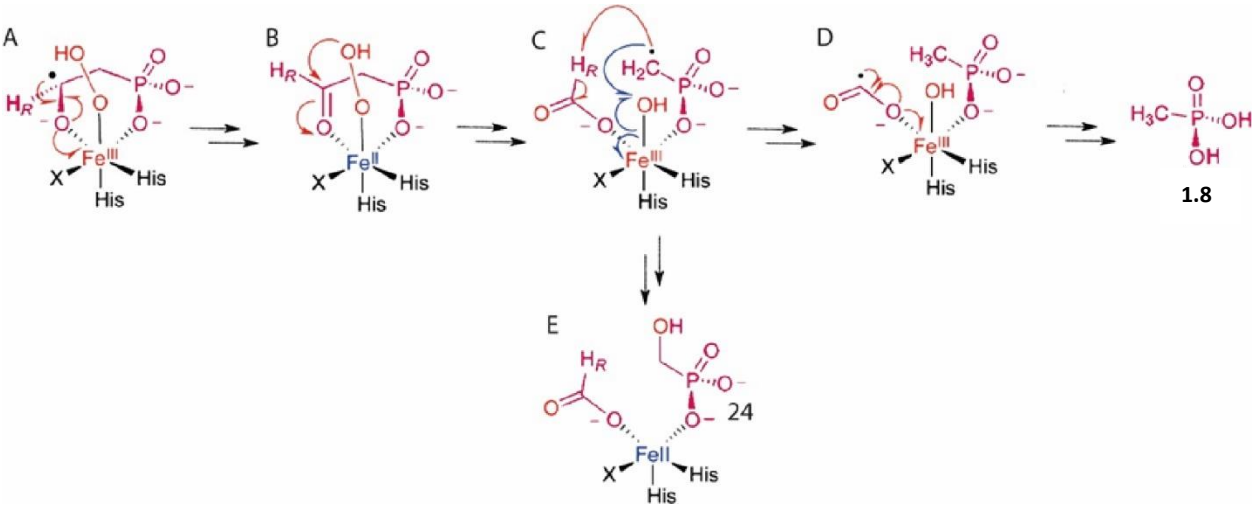

Scheme 11. *Proposed key steps of the biosynthesis of* ***1.8*** *by MpnS.*

1.1.5.3 Oxidative C-P bond cleavage

The third known pathway for P-C bond cleavage, the oxidative pathway, is encoded by two genes, namely *PhnY** and *PhnZ*. PhnY* is a nonheme iron dioxygenase and should not be mistaken for the NAD^+ dependent dehydrogenase PhnY mentioned before. PhnY* utilizes a highly reactive ferryl oxygen to catalyze a stereospecific α-hydroxylation, where **1.3** is converted to (*R*)-**1.5** (**Scheme 12**). [42]

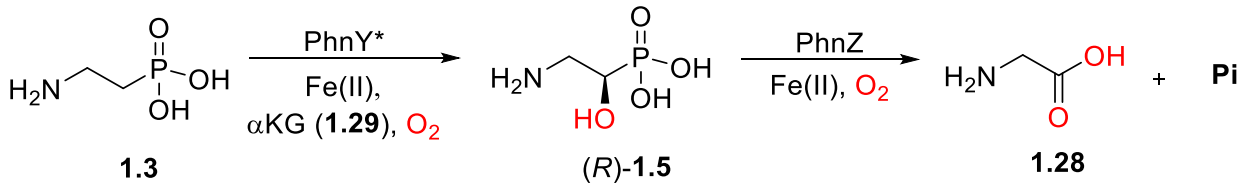

Scheme 12*. Oxidative catabolism of* ***1.3*** *by the enzymes PhnY* and PhnZ.*

In the first step α-ketoglutarate (**1.29**) and molecular oxygen are bound by the active site Fe(II), reducing molecular oxygen to a superoxide species. Fe(IV)=O is then obtained by the oxidative decarboxylation of α-ketoglutarate to succinate (**1.30**, **Scheme 13**). It is used to abstract the α-hydrogen next to phosphors to form a carbon-centered radical and an Fe(III)-bound hydroxide (**1.31**). The latter in turn reacts once more with the radical to give the intermediate product (*R*)-**1.5** and Fe(II).

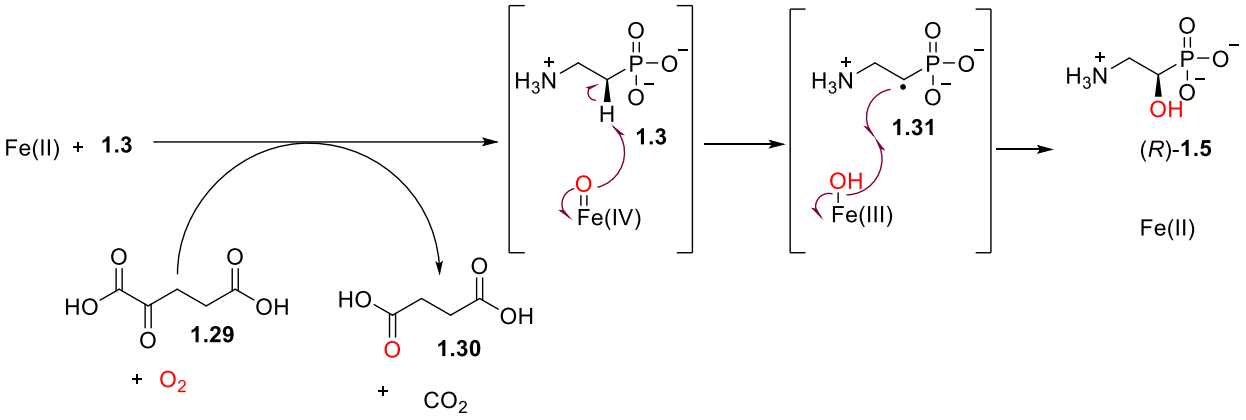

Scheme 13. *Reaction mechanism of the PhnY*- catalyzed hydroxylation of* ***1.3*** *to (R)-****1.5.***

The next catabolic step is performed by an Fe(II) dependent monooxygenase, which specifically converts the (*R*)-enantiomer of **1.5** to glycine and Pi, namely PhnZ. The active site of the enzyme contains two Fe ions, where (*R*)-**1.5** is bound in a bidentate fashion to one of the ions through its α-hydroxyl and one of the phosphonyl oxygens (***Figure 7***).

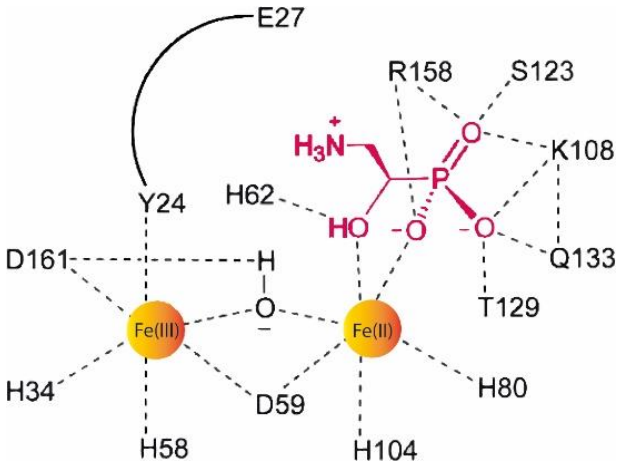

Figure 7. *Active site of PhnZ with the bound substrate (R)-****1.5.***

After the formation of a ferric-superoxide, it can cleave the C-P bond. The two metal ions are further coordinated to four histidine residues, two aspartates, and a bridging water molecule. The residues H58 and D59 make up the "HD" motif of the HD phosphohydrolase superfamily. However, there are slight differences between PhnZ and other members of that superfamily.

Only recently it has been found that oxidative P-C bond cleavage is not limited to 2-AEP (**1.3**) as a substrate, but MePn (**1.8**) can also be cleaved oxidatively in a similar pathway. [43]

Despite the useful properties of natural phosphonates and their more complex synthetic analogues, research in this area has for a long time been limited to the elucidation of the degradation of phosphonates of high economic importance. Nowadays we know twice as many biogenic phosponates as some years ago and only start to understand the environmental importance of this compound class. After decades of research it was only possible to touch the surface of the fascinating biochemistry of Pns. Our knowledge on the metabolic pathways for phosphonate breakdown has already expanded drastically, but there are still lots of obstacles to overcome on the way towards a detailed understanding of phosphonate metabolism.

In order to understand the enzymatic degradation pathways involved in phosphonate metabolism, it is necessary to develop straightforward synthetic strategies to easily access chiral phosphonates. This will further enable the development of new synthetic phosphonate-based drugs for application in medicine, agriculture and other biochemical fields.

1.2 TSPO

1.2.1 Positron emission tomography

The visualization of biochemical processes on a molecular level in all different kinds of living systems is still one of the biggest challenges faced by modern life sciences. Understanding metabolic pathways and protein expression levels in all tissue types is important to gain a deeper understanding of their involvement in a vast number of pathological conditions. That knowledge can then be used to develop important, non-invasive, early stage diagnostic approaches as well as therapeutic strategies against severe pathologies. The gained knowledge can further be used to develop new and more selective (chemo)therapeutic drugs. Currently there are some highly sensitive imaging techniques known that allow - together with highly selective tracers or biomarkers - the visualization of molecular processes and biochemical pathways under *in vivo* conditions. Today the most sensitive and specific technique known for this purpose is positron emission tomography (PET). [44]

Today PET is one of the major methods for tomographic imaging together with single photon emission computed tomography (SPECT), nuclear magnetic resonance tomography (MRT), and X-ray computed tomography (CT). It gives quantitative information about the distribution of administered radiopharmaceuticals as well as about their pharmacokinetic properties, and their effects on the metabolism by monitoring the relative signal change over time. [45]

1.2.2 Types of used radionuclides

The huge amount of PET tracers known today, can be divided into two categories: inorganic and organic tracers. The group of inorganic tracers comprises complexes formed with radioactive metal isotopes. One of the most well-known inorganic PET tracers is ^{68}Ga-DOTA (**Scheme 14**). It is usually combined with a biomolecule such as a pseudopeptide to specifically target tumor tissue or other diseases-specific tissue types. [46] Another frequently used inorganic tracer is Rubidium-82 chloride used for myocardial perfusion imaging.

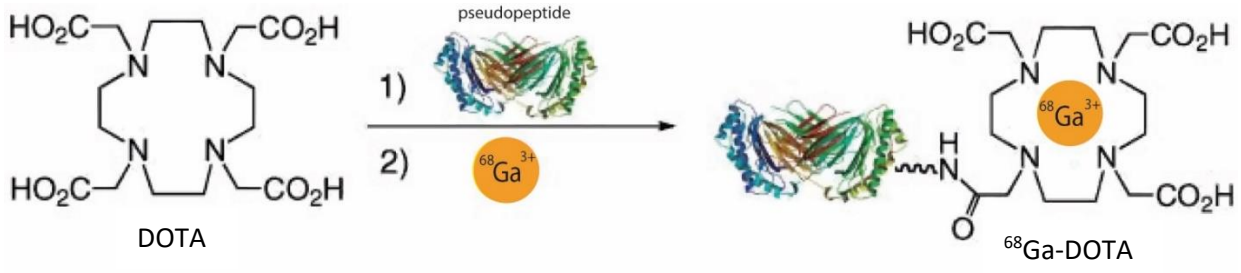

Scheme 14. *Formation of a PET tracer by combining $^{68}Ga^{3+}$ with 1,4,7,10-tetraazacyclododecane-1,4,7,10-tetraacetic acid (DOTA) and a pseudopeptide.*

Organic tracers are obtained by substitution reactions on organic molecules, using nucleophiles that contain cyclotron derived positron emitting radioisotopes like carbon-11, fluorine-18 or nitrogen-13. Substitution reactions for the organic tracers can be performed using different nucleophiles for the incorporation of the radioisotope like $^{11}CH_3I$, $^{11}CH_3OTf$, $^{18}F^-$ and $^{13}NH_3$. There are different possibilities on how to incorporate the radioisotopes, but one factor must be kept in mind during all reactions: time. While ^{18}F has a half-life of 109 minutes, ^{11}C has already decayed by 50% in just 20 minutes. The synthesis of the nucleophile $^{11}CH_3OTf$ uses cyclotron-derived $^{11}CO_2$. The latter has first to be produced by irradiation of $^{14}N_2$ with a proton beam. There is usually a small amount of O_2 added to ensure the formation of $^{11}CO_2$ after the nuclear $^{14}N(p,\alpha)^{11}C$ reaction. The vast majority of ^{11}C containing compound syntheses use $^{11}CO_2$ as a starting point. After a satisfying activity yield is reached, $^{11}CO_2$ is transferred to a fully automated synthesizer module (**Figure 8**), where it is trapped on molecular sieves to be reduced to $^{11}CH_4$ by a nickel catalyzed hydrogenation. [47] After reaction with sublimated iodine, $^{11}CH_3I$ can be either used directly as methylating agent or passed through a column containing silver triflate to obtain $^{11}CH_3OTf$. $^{11}CH_3OTf$ is more reactive than $^{11}CH_3I$ and can thus be used for labeling a larger variety of compounds. [48]

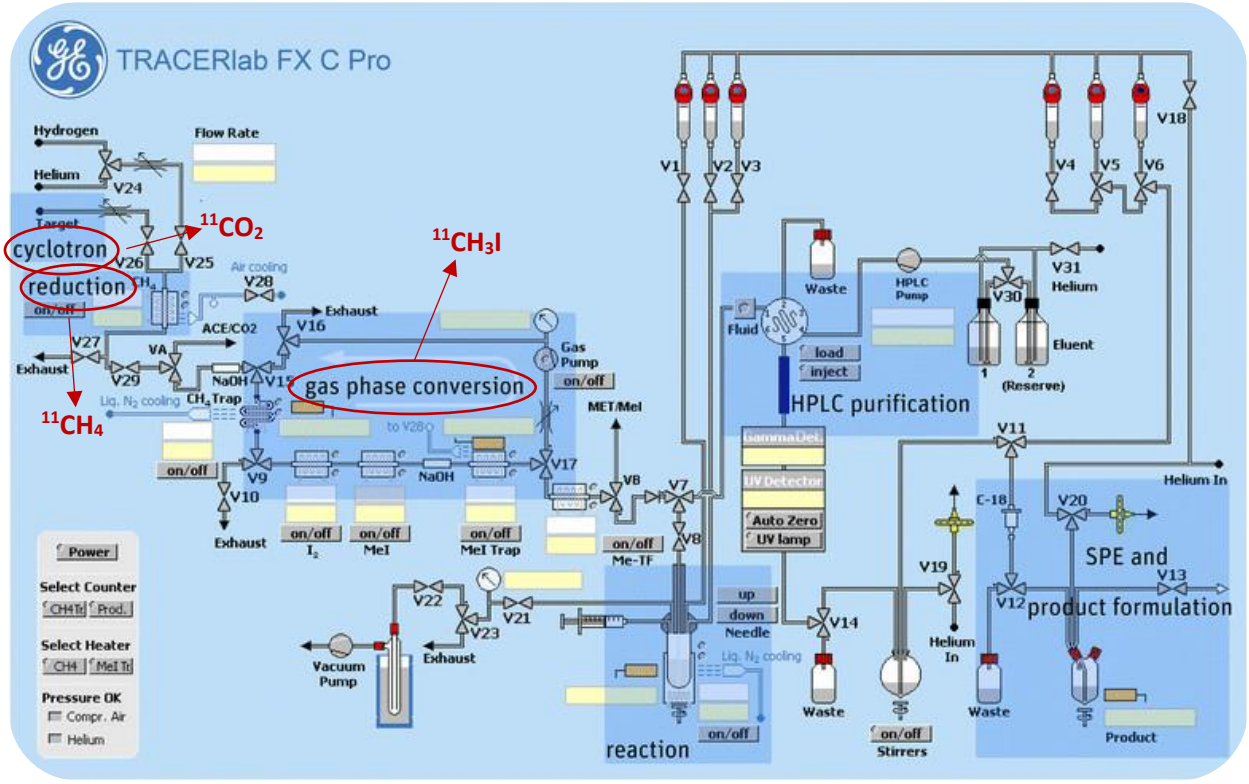

Figure 8. *Typical control panel of an automated preparation of $^{11}CH_3I$ and following labeling reactions for TracerLab synthesis modules and facilitated quality control by analytical HPLC as used by the Vienna General Hospital.*

A very important radiotracer in which ^{11}C is incorporated is 4-propyl-3,4,4a,5,6,10b-hexahydro-2H-naphtho[1,2-b][1,4]oxazin-9-ol, also known as (+)-PHNO [(+)-**1.34**], a very potent and highly selective dopamine D_2 receptor agonist. [49] The commercially used synthetic route towards (+)-[^{11}C]-PHNO is depicted below (**Scheme 15**). The D_2 receptor is a membrane-spanning protein belonging to a subfamily of the G protein-coupled receptors (GPCR) superfamily. This superfamily is responsible for the pharmacological properties of dopamine. D_2 receptor dysfunction has been shown to be involved in a variety of neuronal diseases, like Parkinson's disease and schizophrenia. An agonist like (+)-PHNO is used, because it binds only to the D_2-high state. An antagonist would show the same affinity to D_2-high as to D_2-low, making it impossible to distinguish a proportional shift between the two states, which is an indication for a disease. [50] However, this can have severe side-effects on the patient during diagnosis. (+)-PHNO is also a very good example showing that even multi-step organic synthesis is possible using short-lived radioisotopes.

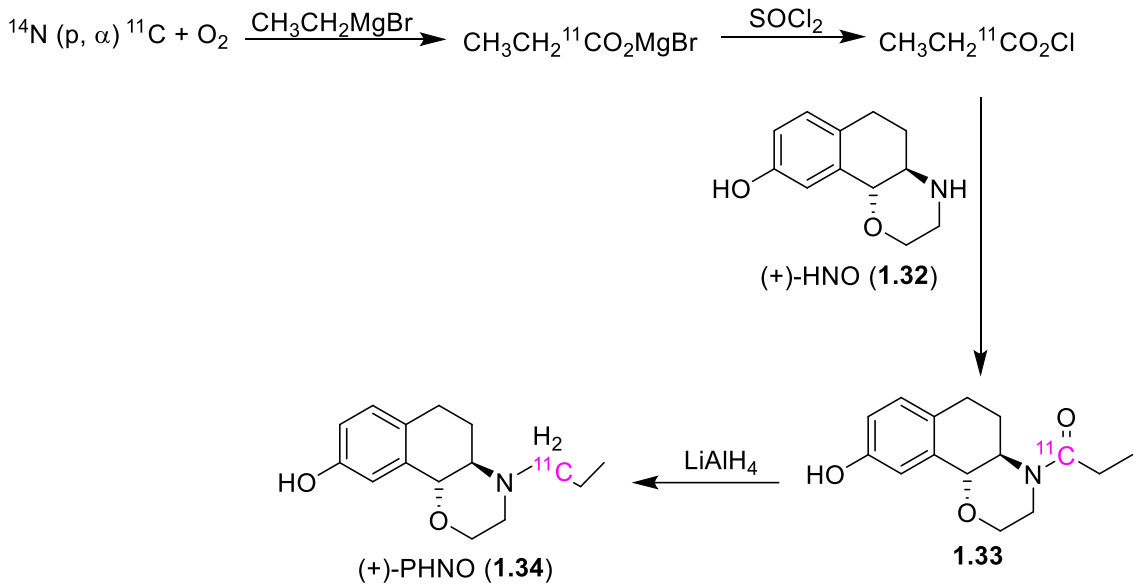

Scheme 15. *Synthesis of the ^{11}C-radiolabeled PET tracer (+)-PHNO.*

^{13}N labelling is rarely used due to a very short half-life of nitrogen-13 of only 9 minutes. Still there are a few possible applications, mainly using [^{13}N]NH_3. ^{13}N can be either produced from isotopically enriched [^{13}C]carbon powder in an ^{13}C(p,n)^{13}N reaction, or by using natural carbon powder and a ^{12}C(d,n)^{13}N reaction. Alternatively, water can be used in an ^{16}O(p,α)^{13}N reaction. [51]

Another diagnostically very important radioisotope is fluorine-18. It is used to synthesize the most commonly used PET tracer: 2-[^{18}F]fluoro-2-deoxyglucose ([^{18}F]FDG, **1.36**). ^{18}F is commonly produced by one of two reactions: either ^{20}Ne(d,α)^{18}F in a neon gas target or ^{18}O(p,n)^{18}F using ^{18}O enriched O_2 gas or water is used as target. In the first variant O_2 is removed after irradiation and the target is filled with argon, containing traces of F_2. This enables target irradiation, where the fluorine in the gas phase and the ^{18}F, previously caught on the walls of the target undergo isotopic exchange. The resulting mixture of [^{18}F]F_2 in argon can then be used for electrophilic fluorination. However, this strategy is problematic due to the corrosive properties and dangers arising from fluorine gas. [52]

Thus, an aqueous solution of [^{18}F]fluoride, which can be used as a nucleophilic fluorine source, is often preferred. [^{18}F]Fluoride can either be used directly for synthesis or the water can be removed by azeotropic distillation. The reactivity of the fluoride can further be increased by

combining it with a crown ether or with tetrabutylammonium salts. This leads to an increased solubility in organic solvents and thus to higher reaction rates. [52]

The above-mentioned PET tracer, [^{18}F]FDG, has been used as a major clinical tool in cancer diagnosis since it was first synthesized in 1980. It preferably accumulates in tumor tissue and other tissue types with an elevated need of carbohydrates by metabolic trapping. [53] It is an analog of glucose, where the hydroxy group at the C-2 position is substituted by ^{18}F. This enables it to use the glucose transport pathway for distribution inside the body. After it reaches the cytosol, it is phosphorylated by hexokinase. However, it is no suitable substrate for phosphohexose isomerase, and thus cannot enter the mitochondria, but is trapped in the cytosol. [54] The radioactive decay of [^{18}F]FDG can then be monitored by PET imaging. In **Scheme 16** the metabolism of FDG is compared to that of glucose (**1.35**). The injected PET tracer constantly emits positrons, which only travel for a short distance inside the tissue, before they annihilate with an electron. During the annihilation two 511 keV gamma quanta (or photons) are emitted in opposite directions. These energy beams can then be detected by the PET scanner and the position of the decay event can be used to localize the area of accumulation of the PET tracer within the body (**Figure 9**). [55]

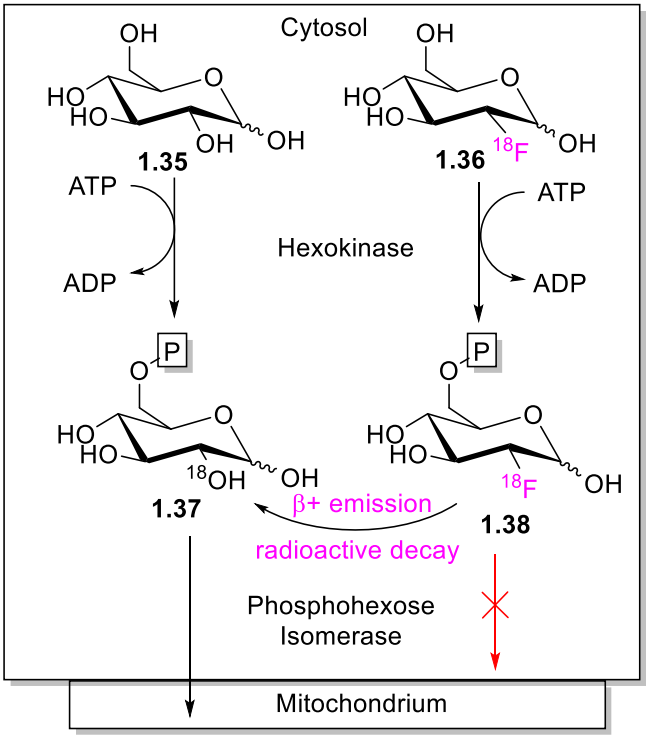

Scheme 16. *Metabolism of glucose and [^{18}F]FDG in comparison,* P *symbolizes phosphate.*

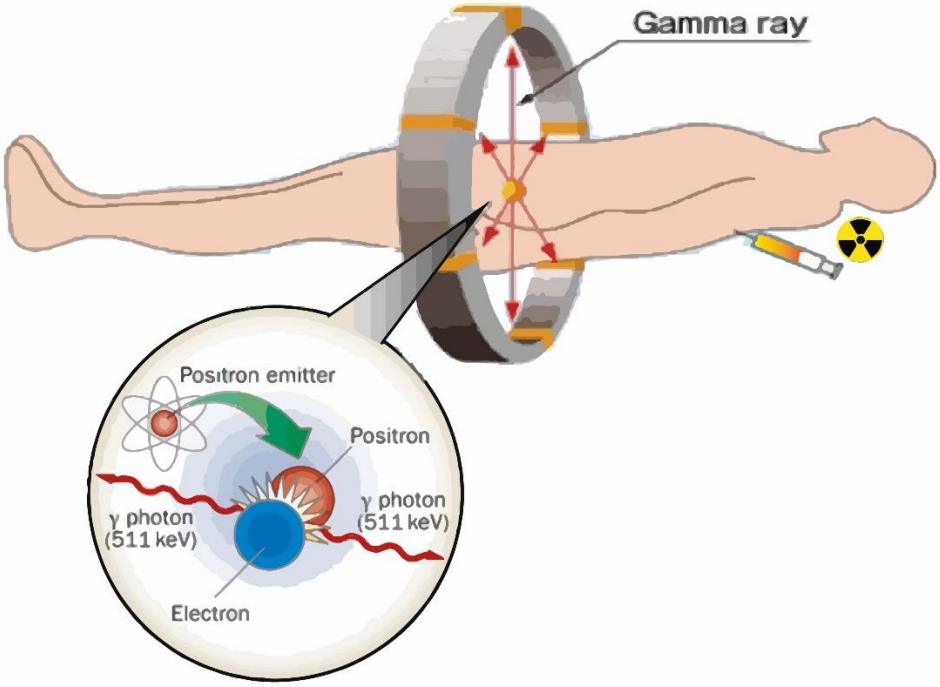

Figure 9. *Illustration of the principle of PET imaging. [56]*

1.2.3 The translocator protein

The so-called translocator protein (18 kDa, TSPO) was formerly known as the peripheral-type benzodiazepine receptor (PBR). It has been developed to study a benzodiazepine binding site to understand the pharmacokinetics of drugs like Valium®. [56] It is localized in the outer mitochondrial membrane and is highly abundant in steroid-synthesizing tissues such as the lung, liver, kidneys and heart. TSPO is responsible for a variety of different mitochondrial functions like cholesterol transport and steroid hormone synthesis and it even influences apoptosis and cell proliferation. [57] Even more interestingly, TSPO was found to be overexpressed in a variety of neurodegenerative diseases such as, Multiple sclerosis (MS) or Alzheimer's disease. The difference in TSPO expression levels between a healthy brain and the brain of a person suffering from one of these diseases can thus be used for diagnostic purposes (**Figure 10**). However, not only neurodegenerative disorders show dysregulated TSPO levels but also a vast number of heart insufficiencies and endocrine syndromes. [57]

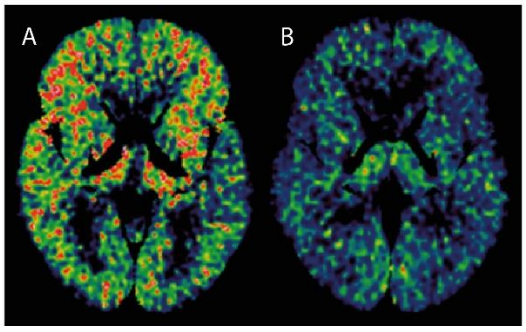

***Figure 10**.Comparison of PET scans of the (A) brain of an Alzheimer's patient, where TSPO is overexpressed (B) a healthy brain using the radiolabeled TSPO ligand [^{11}C]PBR28 {[^{11}C]**1.40**} [58]; regions low in TSPO expression are depicted in blue, while higher expression levels are represented by a red-shift.*

1.2.4 The development of new TSPO PET tracers – some challenges

Currently there is a huge number of TSPO ligands that are used as PET tracers. Since 1994, (*R*)-[^{11}C]PK11195 ([^{11}C]-**1.39**) has been the gold standard for TSPO PET imaging (**Figure 11**). [59] Despite its importance, it suffers from considerable drawbacks such as a high level of nonspecific

binding. This leads to a poor signal-to-noise ratio and makes quantification very difficult. [60] This drawback led to the design and synthesis of the so called “second generation” of TSPO ligands. These use PK11195 as a template and can be grouped according to their structural features (isoquinoline/carboxamide-,pyrazolopyrimidine- and pyridine scaffolds). The second generation of TSPO ligands, comprising compounds such as [^{11}C]PBR28 (**1.40**), [^{18}F]FEPPA (**1.41**), and [^{11}C]DPA-713 (**1.42**), sorted out the described drawbacks successfully (**Figure 11**). They all have a lower lipophilicity and thus higher specific TSPO affinity. However, they suffered from another major drawback: It was found in early clinical studies, that some of the subjects lacked specific binding to [^{11}C]PBR28 (**1.40**), although there was no obvious difference in demographics or medical history. [61] The same was found for [^{18}F]FEPPA (**1.41**) [62] and even for [^{11}C]DPA-713 (**1.42**) [63].

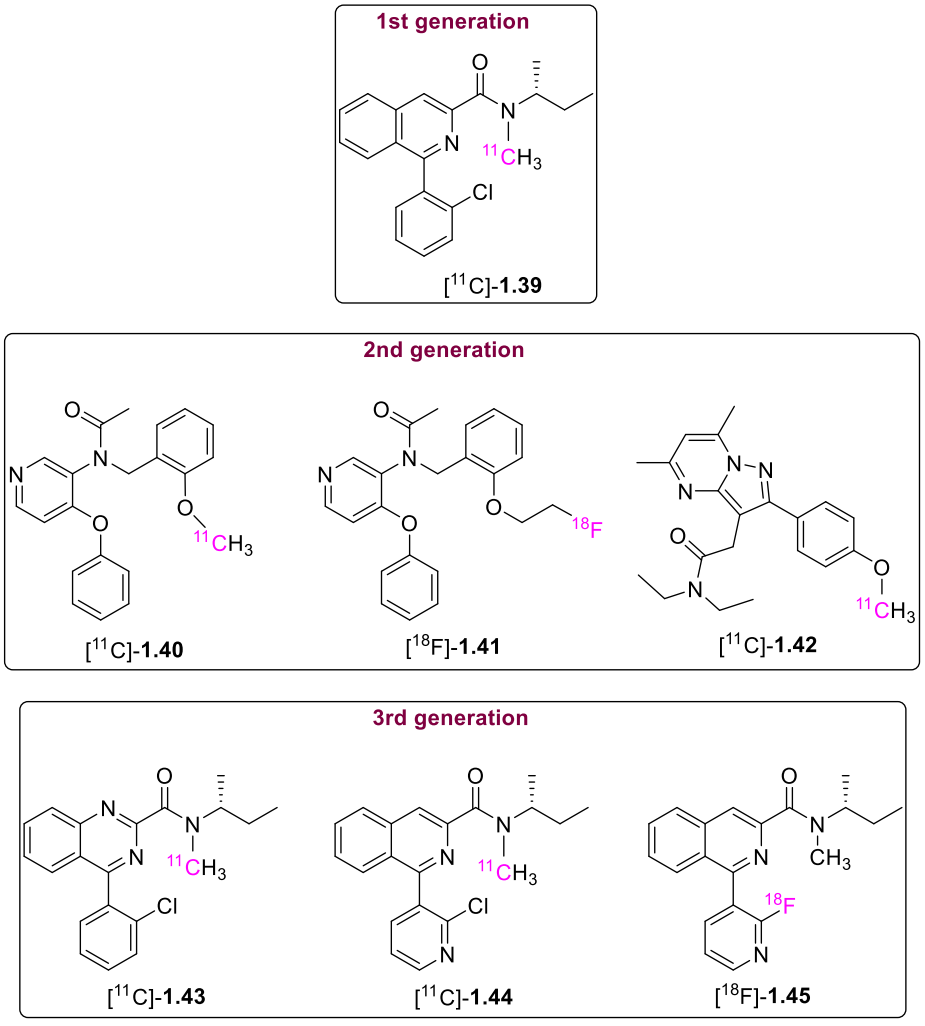

***Figure 11**. Structures of some important 1st,2nd and 3rd generation TSPO ligands.*

This heterogeneous binding behavior could later be explained by a single nucleotide polymorphism (rs6971) in the TSPO gene. [64] The polymorphism is located on exon 4 of the TSPO gene, resulting in an amino acid substitution from alanine to threonine at position 147. [65] This leads to three different phenotypes in the Caucasian-European population regarding TSPO. We can distinguish so-called high-affinity binders and low-affinity binders (HABs and LABs), showing one single binding site with high or low affinity towards the known PET tracers. The so called mixed-affinity binders (MABs) express almost equal numbers of the high- and low-affinity binding sites. The phenotypes are distributed as follows among the population: 66% high-affinity-binders, 5% low-affinity-binders, 29% mixed-affinity-binders. [64] Diagnosis of TSPO-related diseases by means of the established PET tracers is not possible in LABs and MABs. To reduce the effect of those differences in binding affinity as well as to improve pharmacokinetic properties, development of new TSPO ligands has still been a very important and highly discussed topic in the last years. The newest "third generation" of TSPO ligands includes the quinazoline derivative [^{11}C]ER-176 [^{11}C]-**1.43** [66] as well as a novel radiotracer (*R*)-[^{11}C]Me@NEBIQUINIDE ([^{11}C]-**1.44**) and its fluorine-18 labeled analogue (*R*)-[^{18}F]NEBIFQUINIDE ([^{18}F]-**1.45**) recently developed by our working group in cooperation with the Medical University of Vienna. [67] They showed improved binding properties in all known human TSPO phenotypes together with a high metabolic stability in first preclinical *in vitro*, *in vivo* and *ex vivo* trials. In **Table 2** the preclinical evaluation results of the newly developed compounds [^{11}C]-**1.44** and [^{18}F]-**1.45** are compared to the established PET tracer [^{11}C]-**1.39**. (*R*)-[^{18}F]NEBIFQUINIDE shows an even higher affinity to TSPO than the ^{11}C labeled compound [^{11}C]-**1.44**. Both compounds beat the "gold standard" PK11195 in terms of inhibition constant (K_i) and lipophilicity. (*R*)-[^{18}F]NEBIFQUINIDE further showed outstandingly low sensitivity toward the TSPO polymorphism [K_i(HAB)/K_i(LAB) = 0.93] in first *in vitro* experiments.

***Table 2**. K_i and logP values of (R)-[^{11}C]-PK11195 ([^{11}C]-**1.39**) [68] in comparison to the newly developed compounds [^{11}C]-**1.44** [67] and ([^{18}F]-**1.45** [69]. The values presented below are arithmetic means ± standard deviations of at least 3 independent experiments.*

Compound	K_i(HAB) (nM)	K_i(MAB) (nM)	K_i(LAB) (nM)	LogP
1.39	28±4	22±2	24±6	3.25±0.03
1.44	16±3	21±4	17±4	2.27±0.14
(*R*)-**1.45**	5.1±0.3	5.3±0.6	5.5±0.4	2.35±0.14

Currently further investigations and clinical trials concerning the *in vivo* sensitivity of (*R*)-[^{18}F]NEBIFQUINIDE towards the polymorphism rs6971 in humans are ongoing.

2. Aims of the thesis

During the course of my master thesis I was working on the synthesis of a variety of different compounds. All of them have a high potential for future medicinal applications. Their structure suggests a possible biological activity, either as mechanism-based enzyme inhibitors or as highly selective protein ligands.

On the one hand the synthesis of three different, chiral α-aminophosphonic acids was planned: phosphaserine [(*R*)-**3.18**], phosphacysteine [(*R*)-**3.39**] and phosphaisoserine [(*R*)-**3.45**], deuterated at the C-1 position (**Figure 12**). These compounds are intended to be synthesized by a very similar synthetic strategy, which we are currently optimizing to make it a valuable and general synthetic route towards all phosphonic acid analogues to the proteinogenic amino acids. The already known synthesis pathway was - while sticking to the same key-steps - adjusted to fit to the specific functionalities present in the molecules. On the other hand, considering the highly promising results for the two PET tracers already developed in our working group, our aim was to synthesize an even more potent TSPO ligand [(*R*)-**3.56**] with improved properties. In order to lower the lipophilicity and increase the specific binding, it was decided to synthesize a similar compound to (*R*)-[^{11}C]Me@NEBIQUINIDE (**1.44**), but to add one more pyridine ring instead of the benzene ring, to further improve the properties. For this purpose, a new synthesis approach was designed.

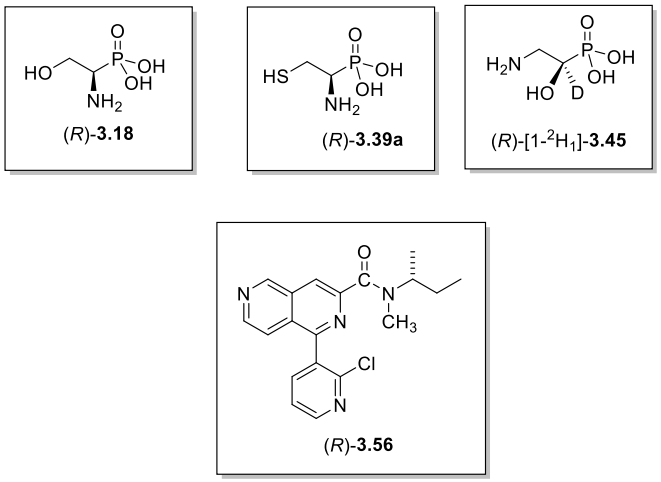

Figure 12. *Target compounds.*

3. Results and Discussion

3.1 Synthetic strategy to access chiral α-aminophosphonic acids

Despite the uncontested importance of phosphonates for the global P-cycle and for the development of new drugs, the literature known methodologies for their synthesis still suffer from severe drawbacks.

Several chemo-enzymatic syntheses for the enantiopure α-aminophosphonic acid analogues to the known proteinogenic α-aminocarboxylic acids have been reported in literature.[40] The ees obtained during chemo-enzymatic synthesis of α-aminophosphonic acids can be over 98% [70].However, these approaches suffer from severe drawbacks, including a maximum yield of 50 % due to the chiral resolution step. Also, the availability and substrate scope of the used enzymes are limiting the general application of these methods for the synthesis of analogs. The substrate specificity of the enzyme has to be considered, limiting the number of compounds that can be synthesized by one enzyme. Furthermore, enzymes can only be used under almost physiological conditions, where selectively only one enantiomer is converted. Thus, there is still the need for a robust, tolerant (in terms of functional groups present in the molecule) and cheap, method for the synthesis of chiral α-aminophosphonates from achiral starting materials.

The method shown in **Scheme 17** is currently optimized for the synthesis of chiral α-amino phosphonic acid analogues to the 21 proteinogenic amino acids. This system was chosen due to the varied nature of functional groups that are present in proteinogenic amino acids, which will help to give a detailed picture on the advantages and limitations of the method. The method should finally be suitable for a large variety of substrates.

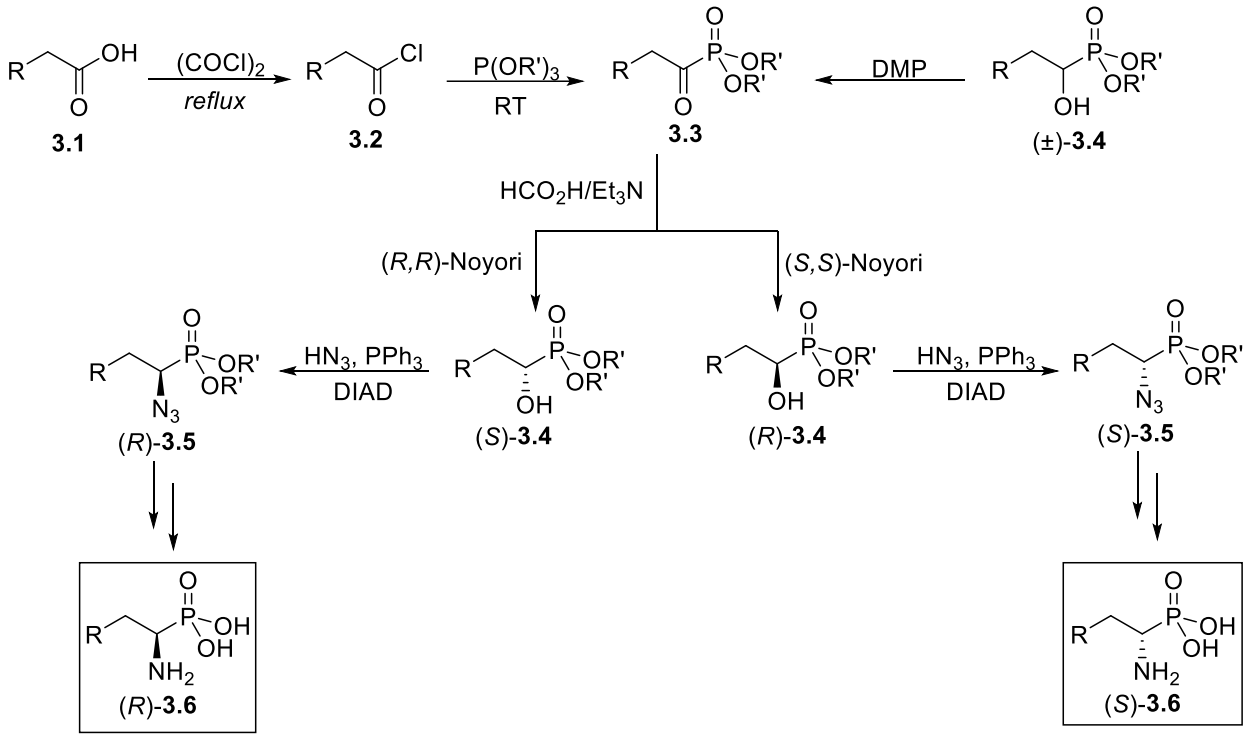

***Scheme 17**. General suggested pathway for the synthesis of enantiopure α-aminophosphonic acids.*

The first step of the synthetic procedure is the conversion of a carboxylic acid **3.1** to the corresponding acyl chloride **3.2**. A following Michealis-Arbusov reaction with a trialkyl phosphite afterwards gives the ketophosphonate **3.3**.

As ketophosphonates tend to be very labile, alternative approaches to access these key-intermediates might become necessary from time to time. One alternative for more labile molecules, which cannot withstand the harsh conditions needed for acyl chloride formation uses the racemic α-hydroxyphosphonates [(±)-**3.4**] as intermediates. They can be obtained by an Abramov reaction using an appropriate aldehyde and a dialkyl trimethylsilyl phosphite at low temperatures. The racemic alcohols can then be oxidized to the ketophosphonate (**3.3**) in the presence of Dess–Martin Periodane (DMP).

The ketophosphonate (obtained by either route) is then, reduced in an asymmetric transfer-hydrogenation in the presence of a Noyori-type catalyst. The resulting stereochemistry of the product can be defined by either using an (*R*,*R*)- Noyori catalyst (*R*,*R*)-**3.8** to yield the (*S*)-1-

hydroxyphosphonate [(*S*)-**3.4**], or a (*S,S*)- Noyori catalyst (*S,S*)-**3.8** for the (*R*)-1-hydroxyphosphonate (*R*)-**3.4**. [71] The commercially available catalysts need to be activated in the presence of base prior to use to obtain their catalytically active form (**Figure 13**). A subsequent Mitsunobu-reaction leads to the formation of an azide (**3.5**) with inverted stereochemistry (S_N2 reaction). Reduction to the amine and global deprotection finally gives the desired α-aminophosphonic acids (**3.6**).

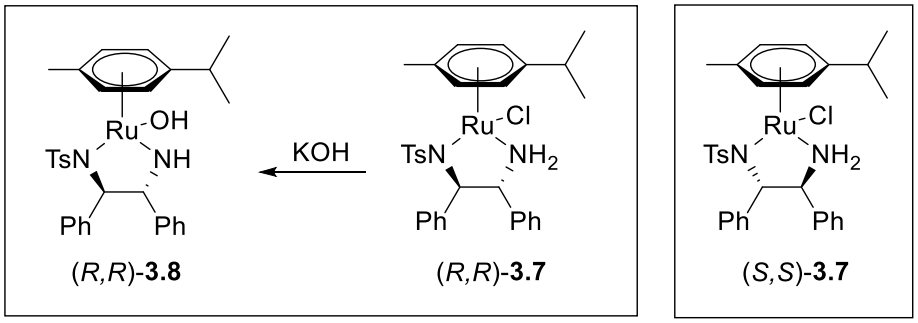

***Figure 13**. Structures of the commercially available catalysts (R,R)- and (S,S)-RuCl[(p-cymene)-TsDPEN] and the activated form of (R,R)-**3.8**.*

3.1.1 Detailed discussion of the synthesis of enantiopure (*R*)-phosphaserine [(*R*)-**3.18**]

One of the key steps of the synthesis of chiral phosphonates is always the P-C bond forming reaction. Today, a variety of P-C bond forming reactions is known (**Scheme 18**).

One of these is the Pudovik reaction (a). The Pudovik reaction, where dialkyl phosphites react with deprotonated aldehydes at low temperatures under basic conditions is often problematic due to decomposition of the formed P-C bond to again give the starting materials. [72]

Alternatively, the three-component Kabachnik Fields reaction (b) is a straightforward strategy for synthesizing α-aminophosphonates, but it proceeds via a very reactive imine intermediate and can usually only be performed satisfyingly by either using of a catalyst or microwave conditions. [73] Thus, these reactions can be problematic during the synthesis of chiral α-phosphonates starting from labile substrates.

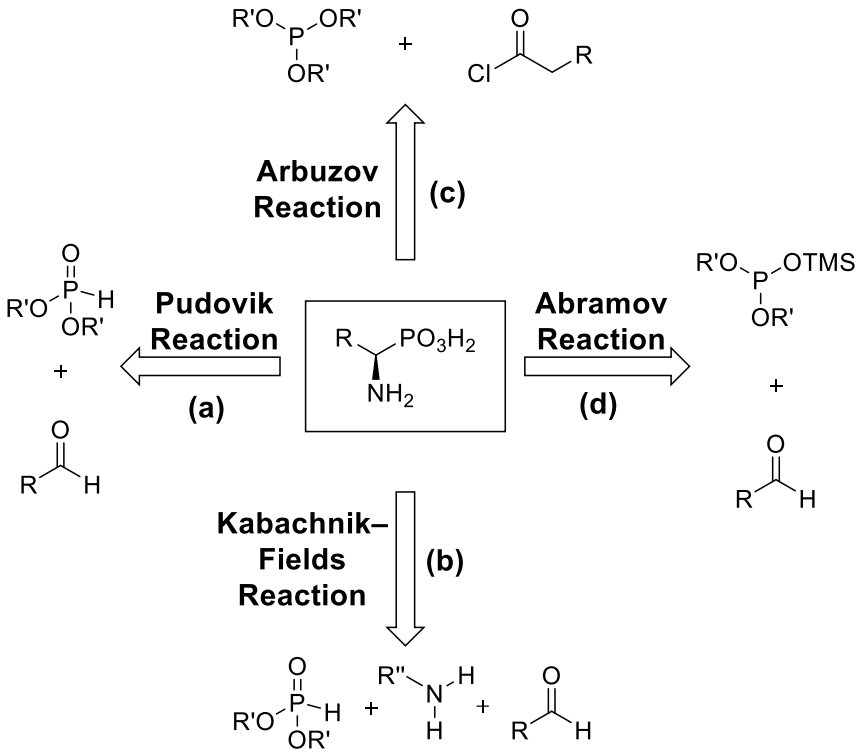

***Scheme 18**. Overview of synthetic strategies for P-C bond formation.*

The Arbuzov reaction (c), between trialkyl phosphites and alkyl/acyl halides, was developed more than one hundred years ago, and is still used today to manufacture tons of organophosphoryl compounds every year. However, it also has considerable drawbacks, like the use of toxic alkyl halides as well as harsh reaction conditions (temperature) leading to numerous side reactions. [74] Many starting materials do not withstand the harsh reaction conditions required for acyl chloride formation which was also the case for 2-benzyloxyacetic acid. Attempts to convert the acid to the corresponding acyl chloride, led to attack of the reagent at the benzylic position and thus decomposition of the starting material. The standard approach for the synthesis of an α-ketophosphonate via an Arbusov reaction was thus not possible in the case of 2-benzyloxyacetic acid (3.9, **Scheme 19**). A viable alternative can be found in the Abramov reaction (d). It has proved to provide a very mild access to racemic α-hydroxyphosphonates in very good yields under easy to handle reaction conditions. [75] The nucleophilic addition of the phosphorus center to an aldehyde without spontaneous decomposition of the obtained product proved to be very reliable. It is only possible using silylated phosphites, where the TMS ether acts as a readily transferable protecting group (**Scheme 19**). [3]

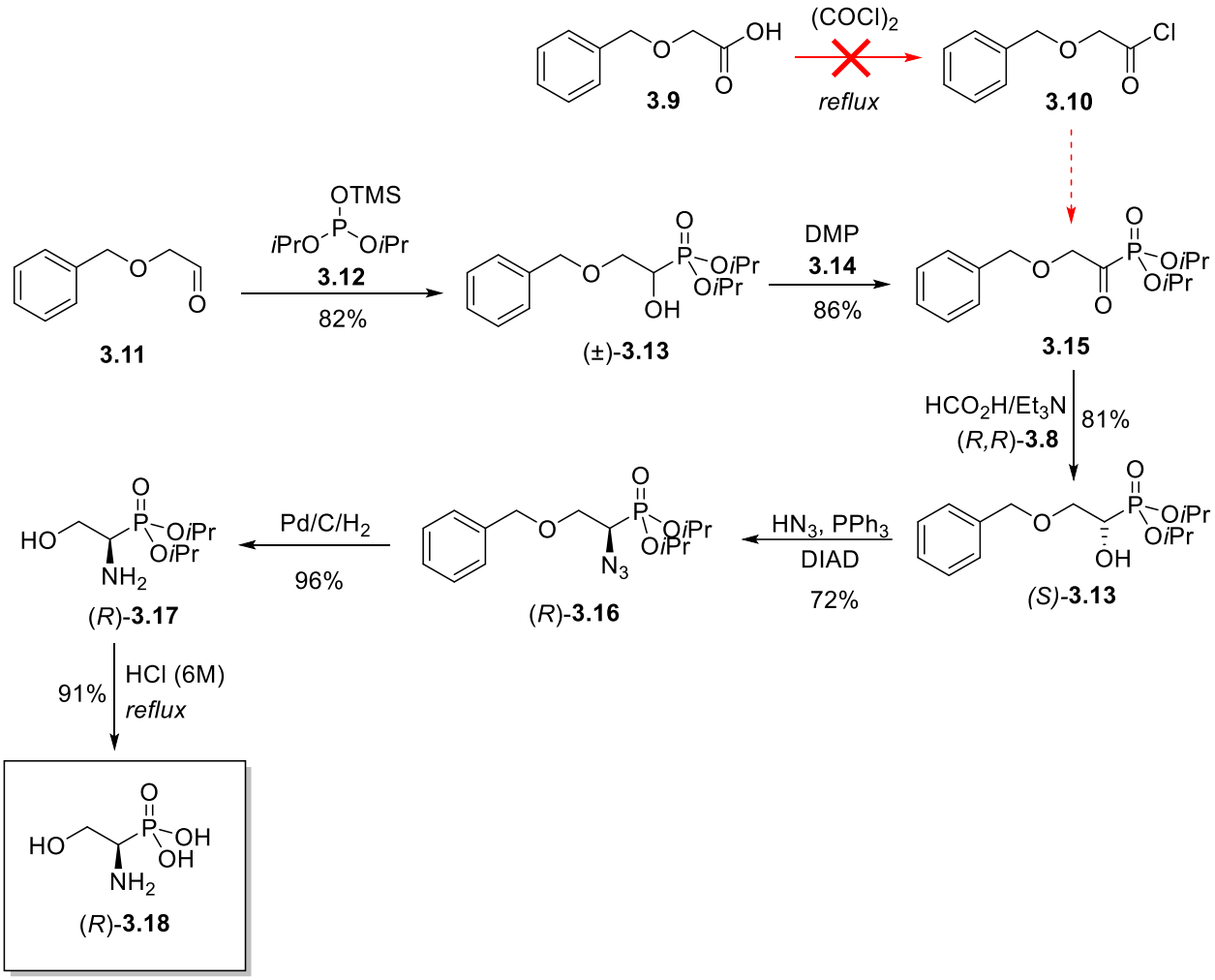

***Scheme 19**. Optimized synthesis pathway for (R)-(1-amino-2-hydroxyethyl)phosphonic acid [(R)-**3.18**].*

Thus, the second discussed strategy to obtain the desired ketophosphonate intermediate **3.15** was used (**Scheme 19**). The desired dialkyl trimethylsilyl phosphite (**3.12**) had to be prepared first. Diisopropyltrimethylsilyl phosphite, the starting material for the synthesis of enantiomerically pure phosphaserine, was obtained by a very reliable, literature known method), developed by a former group member. [75]

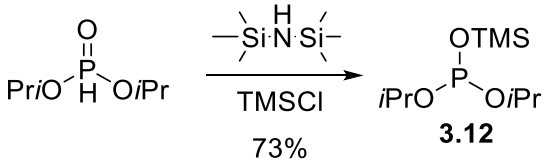

***Scheme 20**. Synthesis of **3.12**.*

Unreacted diisopropyl phosphite could be removed by adding additional equivalents of hexamethyldisilazane after half of the reaction time. Despite several purification attempts, minimal traces of diisopropyl phosphite could not be removed entirely from the product after distillation.

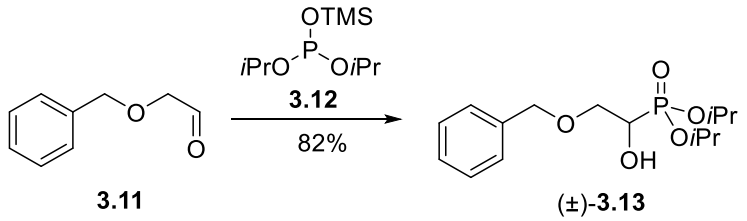

Scheme 21. *Synthesis of the racemic α-hydroxyphosphonate (±)-**3.13**.*

To obtain the α-ketophosphonate **3.15** for the transfer hydrogenation, the racemic α-hydroxyphosphonate (±)-**3.13** was synthesized by an Abramov-reaction (**Scheme 21**) starting from benzyloxyacetaldehyde (**3.11**) and diisopropyl trimethylsilylphosphite (**3.12**) at –78 °C in satisfying yields and purity (82%) after cleavage of the TMS protecting group using 2 M HCl in THF. It could be oxidized to the desired ketophosphonate **3.15** with DMP (**3.14**, **Scheme 22**).

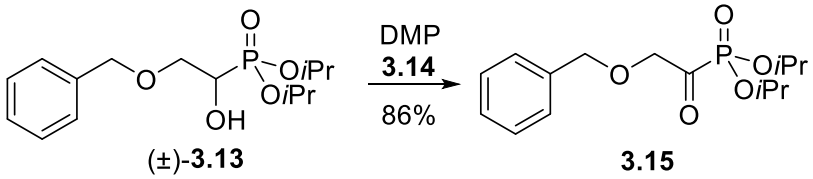

Scheme 22. *Synthesis of the ketophosphonate **3.15**.*

The Dess–Martin Periodinane (DMP) (**3.14**) for the oxidation was synthesized according to a literature known procedure. [76] The ketophosphonate was obtained in good yields and sufficient purity by this method (**Scheme 22**).

Excess DMP has to be removed after completion of the reaction. This was first attempted by extraction with a sat. aqueous solution of $NaHCO_3$ and $Na_2S_2O_3$ from the reaction mixture. However, thereby DMP could not be removed sufficiently. Therefore, the solvent was removed *in vacuo* at room temperature and the residue was taken up in diethyl ether. DMP is insoluble in

diethyl ether and it became thus possible to remove excess DMP from the product by extraction with a 1:1 mixture of a sat. aqueous solution of $NaHCO_3$ and $Na_2S_2O_3$. Although handled with care, the final compound was still very labile, and decomposition could not be avoided entirely. Minimal traces (about 8 mol% in total) of several decomposition products were visible in the ^{1}H NMR as well as in the ^{31}P NMR. The crude compound was used directly for the next step. Due to the instability of the product and the fact that the impurities did not interfere with the next reaction step, no further purification of the ketophosphonate was needed.

The crude keto-phosphonate was thus reduced to a chiral α-hydroxyphosphonate. The asymmetric hydrogenation of carbonyl compounds has been already known for over half a century. [77] One of the most important breakthroughs for catalytic reactions was the highly enantioselective reduction of aromatic ketones by Noyori *et al.* [78] using a new chiral hydride – transfer reagent and later using newly designed Ru-complexes. [79] These are of high importance today for the synthesis of enantiopure intermediates and bioactive drugs. [80] Reduction of a variety of α-ketophosphonates with (*R,R*)-RuCl[(*p*-cymene)-TsDPEN] [(*R,R*)-**3.7**] or (*S,S*)- **3.7** a new generation Noyori catalyst, was already achieved with ees of over 98% by several groups. The catalyst makes it possible to access both enantiomers of the desired α-hydroxyphosphonates depending on the stereochemistry of the catalyst. In the case of the α-ketophosphonate (**3.15**) (*R,R*)-**3.7** yields the (*S*)-hydroxyphosphonate and the (*S,S*)-**3.7** gives only the (*R*)-hydroxyphosphonate. [71]

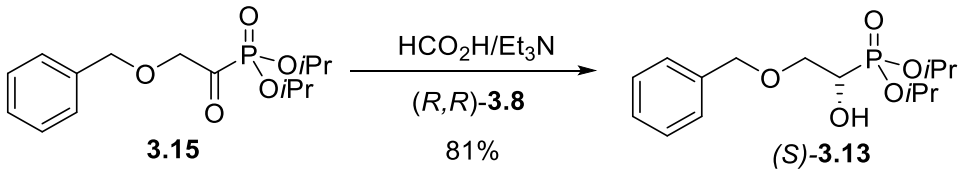

***Scheme 23**. Synthesis of the (S)-hydroxyphosphonate (S)-**3.13**.*

The catalyst needs to be activated with a base first and then a hydride source is needed for reduction. [81] There are many possible hydride sources, such as isopropanol. It became a popular hydride source due to its many advantages. It is a stable, easy to handle, non-toxic, cheap and commercially available compound. [82] However, there are still some drawbacks to be considered. Both, the product and the used isopropanol, are secondary alcohols with similar

stereochemistry, which occasionally leads to a steadily degrading enantiomeric purity of the product, to mention just one. Another possible hydride source is a mixture of formic acid and triethyl amine. [83] And indeed, previous experiments with the (*R,R*)-**3.8** performed by our working group show satisfying conversion rates as well as high enantiomeric purity of the desired products using this system.

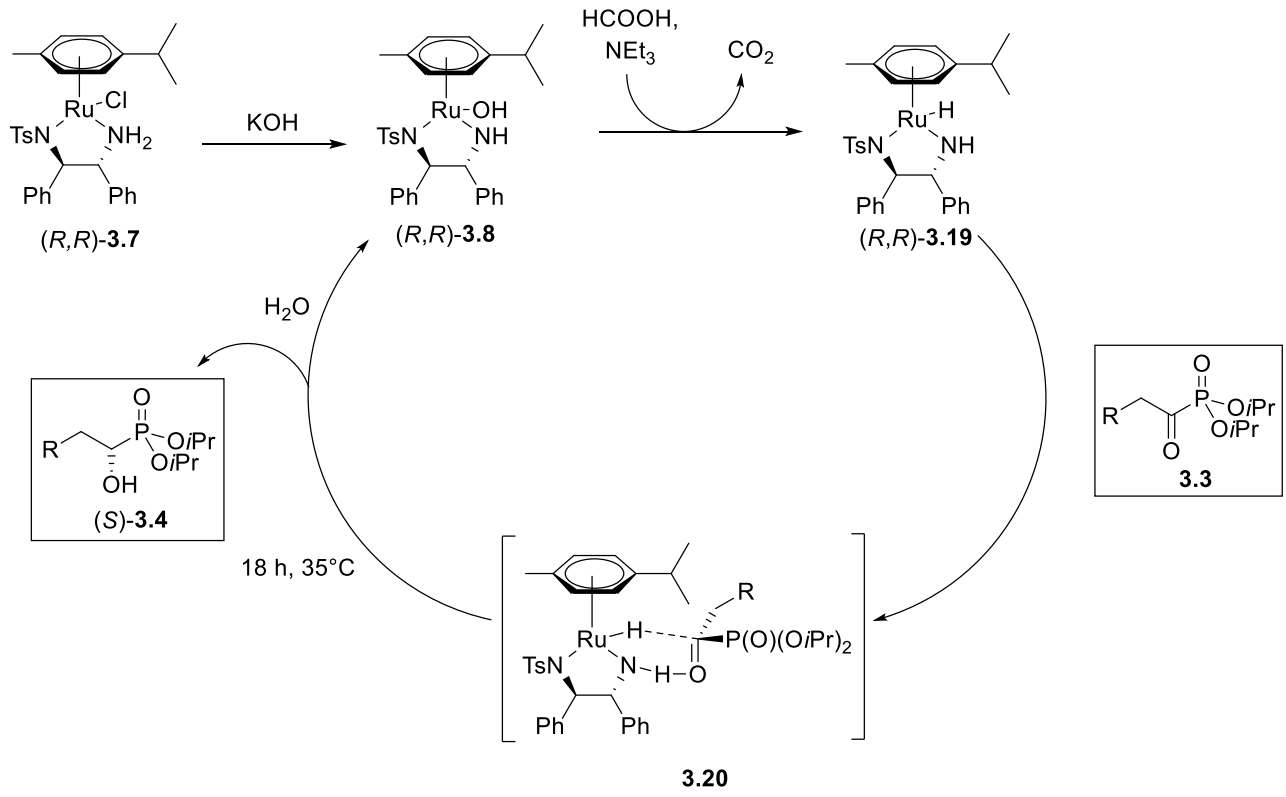

Scheme 24. *Reaction pathway of a typical Noyori-type asymmetric reduction of a ketophosphonate with (R,R)-RuCl[(p-cymene)-TsDPEN] [(*R,R*)-**3.7**].*

In the specific case of the reduction of diisopropyl (2-(benzyloxy)acetyl)phosphonate (**3.15**) to (*S*)-(2-(benzyloxy)-1-hydroxyethyl)phosphonate [(*S*)-**3.13**, **Scheme 23**] just 0.02 equivalents of the catalyst were sufficient to accomplish a conversion of 100 %. The pure product could be obtained in very good isolated yields of over 80 % with ees over 98% after purification via MPLC. The ee was determined by means of $^{1}H/^{31}P$ NMR spectroscopic techniques using the chiral solvating reagent (*S*)-**3.21** (**Figure 14**).

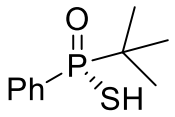

(*S*)-**3.21**

Figure 14. *Structure of the used chiral solvating agent (S)-tert-butyl-phenyl-phosphinothioic acid.*

In order to finally obtain the desired α-aminophosphonic acid, an azide was installed on the carbon next to the phosphorus atom under inversion of configuration (**Scheme 25**).

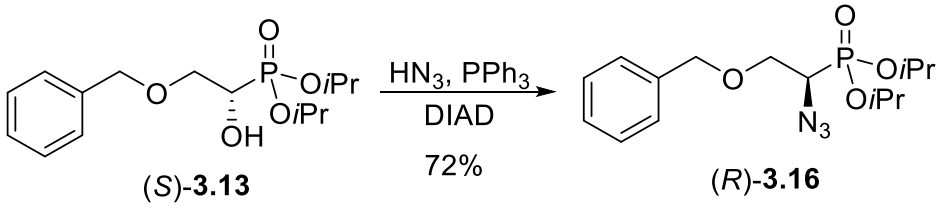

(*S*)-**3.13** (*R*)-**3.16**

Scheme 25. *Synthesis of the (R)-azide.*

The inversion of the stereochemical configuration of a primary or secondary alcohol by the use of different nucleophiles together with azodicarboxylates and triphenylphosphine is a classical S_N2-type reaction that proceeds with a high enantiomeric excess of over 98%. [84] This makes it very important in enantiopure synthesis of biological compounds. Since the first published manuscript about the Mitsunobu reaction in 1967 [84] huge advances were made that led to an improvement of the reaction conditions and broadened substrate scope. Nowadays a variety of different azo-esters can be chosen depending on the type of nucleophile and alcohol to replace (**Figure 15**).

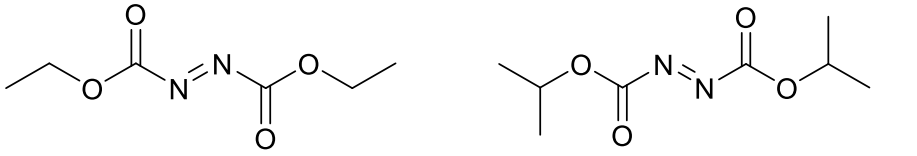

Diethyl azodicarboxylate (**3.22**) Diisopropyl azodicarboxylate (**3.23**)

Figure 15. *Structures of the two azo-esters DEAD and DIAD.*

The variety of accepted nucleophiles in a Mitsunobu reaction ranges from aromatic alcohols to amides with sufficient acidity, imides, azides, thiols, or carboxylic acids. [85]

In the first step of a Mitsunobu reaction the azo-ester is attacked by PPh_3, which leads to the deprotonation of the nucleophile - in our case hydrazoic acid. The positively charged phosphorus-atom is then attacked by the alcohol compound and a hydrazo-ester derivative is formed. Due to the steric hindrance of the leaving group, a complete inversion of configuration at the stereocenter of interest occurs.

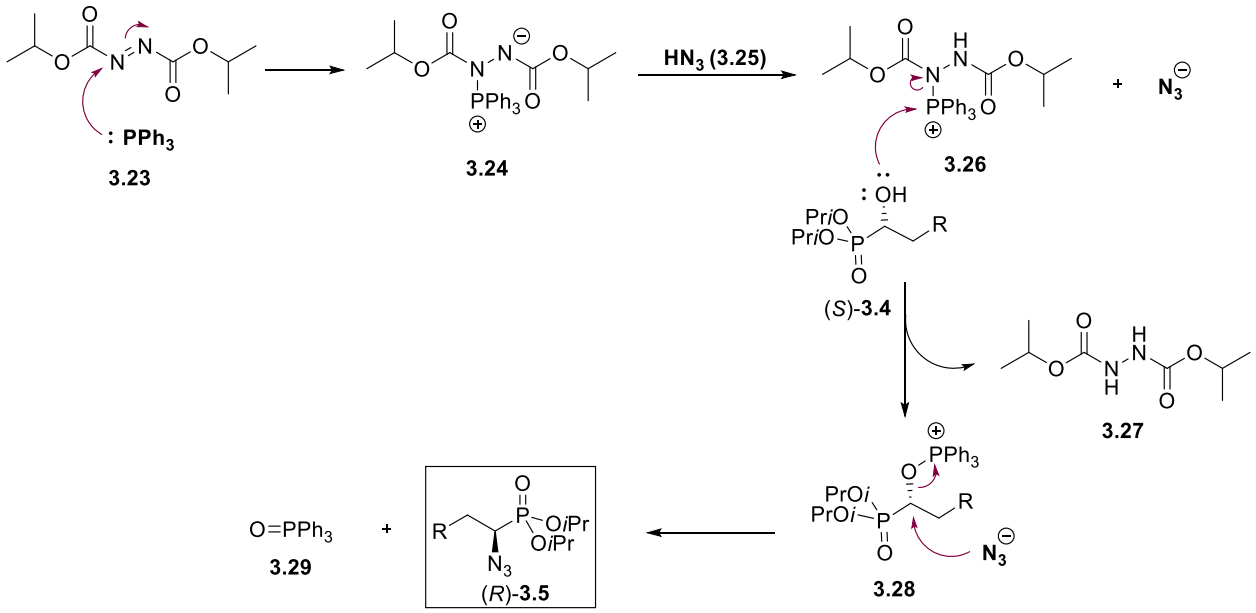

Scheme 26. *General mechanism of the Mitsunobu reaction.*

In the specific case of the conversion of (*S*)-**3.13** to (*R*)-**3.16** DIAD was used as the azo-ester, a solution of HN_3 in toluene provided the nucleophile and CH_2Cl_2 was the solvent of choice. The reaction mixture was first stirred at 0 °C, followed by stirring at room temperature. However, full conversion could not be achieved, even after an extended reaction time. Thus, different nucleophiles, including phthalimide were tested, which did not lead to improved results. Neither did changing the azo-ester (substituting DIAD with di-*tert*-butyl azodicarboxylate) or the solvent (toluene instead of CH_2Cl_2 or mixtures of these two). None of those changes led to a considerable change in the conversion rate. Raising the molar equivalents of hydrazoic acid and the used azo-ester from 1.4 to 1.9 eqiuv. had a slightly positive effect on the isolated yield. However, the most

significant effects were observed for longer reaction times and higher temperatures. Quantitative conversion (determined by NMR spectroscopy) could be obtained after stirring for 2 days at 35 °C and good yields could finally be isolated after purification (72%, ee ≥ 98%).

Finally, the obtained azide had to be converted to the amine (*R*)-**3.17**. A benzyl ether (Bn) was originally chosen as protecting group due to its stability towards acidic and basic conditions as well as towards many reducing and oxidizing agents like DMP. This makes it the protecting group of choice for our synthetic approach. [86] Cleavage was possible under very mild hydrogenolytic conditions, avoiding racemization or P-C bond cleavage of the chiral intermediate.

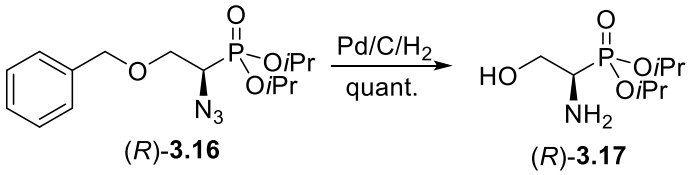

(*R*)-**3.16** (*R*)-**3.17**

***Scheme 27**. Reduction to the protected α-aminophosphonic acid.*

Catalytic reduction of the azide to the amine occurred simultaneously with quantitative yields, which is another advantage (**Scheme 27**). In case of the transformation of (*R*)-**3.16** palladium on charcoal in ethanol under a hydrogen pressure of 3 bar was sufficient to achieve complete deprotection of the protecting group and reduction of the amine within 4 h at room temperature. Addition of a catalytic amount of conc. HCl (1-2 drops) proved to make the reaction faster.

Finally, the protecting groups attached to phosphorus were removed. There are many different kinds of alkyl ester phosphorus protecting groups. If stable protection over numerous steps is necessary, bulkier groups like isopropyl esters are preferred. They are less labile towards nucleophilic cleavage but can still be cleaved easily under acidic conditions. Thus, the isopropyl protecting group, which was chosen for phosphorus protection in this case. It could be cleaved by refluxing the compound in 6 M HCl.

Purification of the resulting residue by ion exchange chromatography (using Dowex 50W × 8, H^+-form) was performed to remove impurities and isolate the pure α-aminophosphonic acid (*R*)-**3.18** (96%). The purified aminophosphonic acid can be dissolved in water, and the pH adjusted to 7 with a 0.5 M aqueous NaOH solution. The sodium salt of (*R*)-**3.18** can then be obtained after

lyophilization [96%, calculated yield from NMR, 2-AEP (**1.3**) used as internal standard]. Alternatively, the product can be (re-)crystallized after ion exchange chromatography from water/EtOH to give the free phosphonic acid (*R*)-**3.18**.

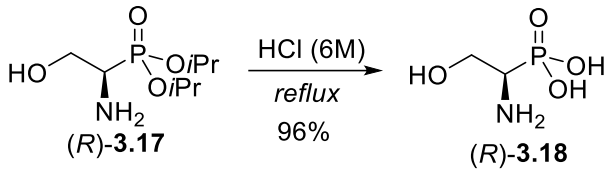

Scheme 28. *Deprotection to the α-aminophosphonic acid (R)-**3.18**.*

In conclusion, it was possible to synthesize the *R*-enantiomer of the phosphonic acid analogue of serine with an ee of over 98% and an overall yield of 36% over just six reaction steps in excellent purity. The obtained specific rotation of + 30.13 (*c* 0.75, H_2O) was in agreement to that reported in the literature. [87]

3.1.2 Detailed discussion of the synthesis of enantiopure (*R*)-phosphacysteine [(*R*)-and (*S*)-3.37a]

The synthesis of chiral phosphacysteine could be accomplished following the general synthetic strategy outlined in **Scheme 17**. The synthesis of the desired acyl chloride from thiobenzyl acetic acid in the presence of excess oxalyl chloride could be performed easily and was complete after 5 hours (**Scheme 29**).

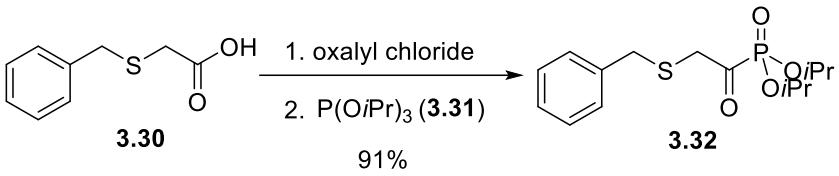

***Scheme 29**. Synthesis of the ketophosphonate 3.32.*

The ^{1}H NMR of the crude compound showed some impurities after the conversion, which could be removed via fractional bulb-to-bulb distillation [K_p (product) = 80-100 °C, 0.3 mbar]. The purified acyl chloride reacted neatly with triisopropyl phosphite in an Arbusov reaction to give the desired ketophosphonate in sufficient yield and purity for the next reaction step. Lowering the reaction temperature to 0 °C (or lower) for the Arbusov reaction did not lead to lower side product formation. The ketophosphonate could be crystallized for characterization purposes. However, we observed drastic losses in terms of the isolated yield. Thus, the crude product was used without further purification for the next reaction.

Diisopropyl (*S*)-(2-(benzylthio)-1-hydroxyethyl)phosphonate (**3.33**) could be obtained by using a Ru-mediated Noyori-type transfer hydrogenation [(*R,R*)-**3.8** as catalyst, see Figure 13 with a mixture of HCO_2H/Et_3N as hydride source in good yields (70%) and excellent ee (98%) (**Scheme 30**).

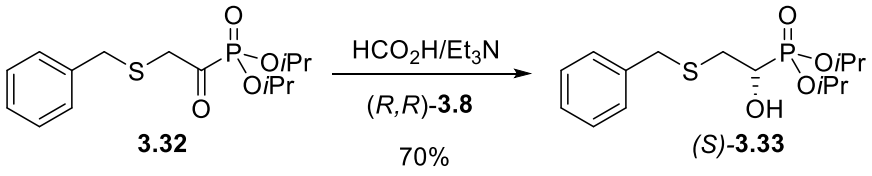

***Scheme 30.** Reduction of the ketophosphonate **3.32**.*

The same reaction procedure could be used to obtain (*R*)-(2-(benzyloxy)-1-hydroxyethyl)phosphonate by simply using the catalyst of opposite stereochemistry [(*S,S*)-**3.8**]. 5 mol% of the catalyst had to be used in both cases, as sulfur-containing species are known to be catalyst poisons. [88] Lower amounts of catalyst did not show full conversion. The ee for both compounds was determined using the chiral solvating reagent (*S*)-**3.21** and was above 98% in both cases.

The first approach for the subsequent Mitsunobu-reaction was done under standard conditions using PPh_3, DIAD, HN_3 as reagents and CH_2Cl_2 as solvent. The ^1H NMR spectrum showed the formation of two very similar compounds in a molar ratio of 1:3 differing in the shifts for the hydrogen atoms attached to the carbon atom next to the phosphorus (**Figure 16**).

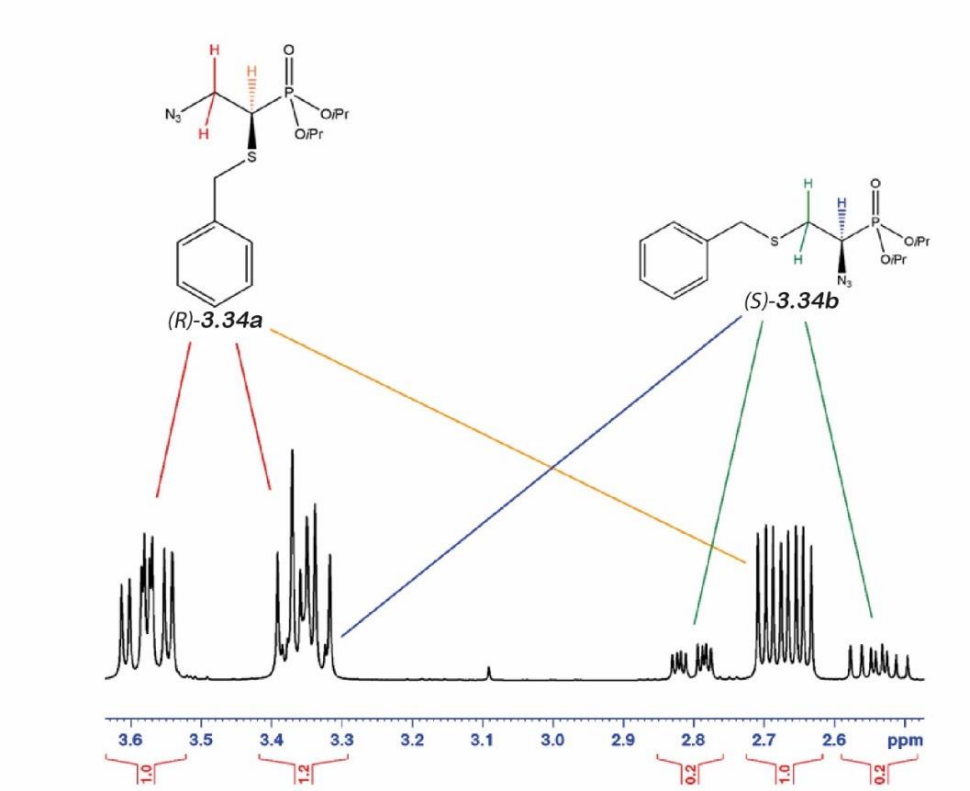

***Figure 16**.[1]H NMR of a mixture of compounds (R)-**3.34a** and (S)-**3.34b** in a 3:1 ratio.*

The two products could also be distinguished easily by comparing their ^{13}C NMR spectra (**Figure 17**). The α-carbon atom signal, which shows a coupling to the phosphorus, is found in the area around 40 ppm for (*S*)-**3.34b**, whereas it can be found at a shift value of around 60 ppm for (*R*)-**3.34a** where an azide is directly attached. This is in agreement to the literature. [89]

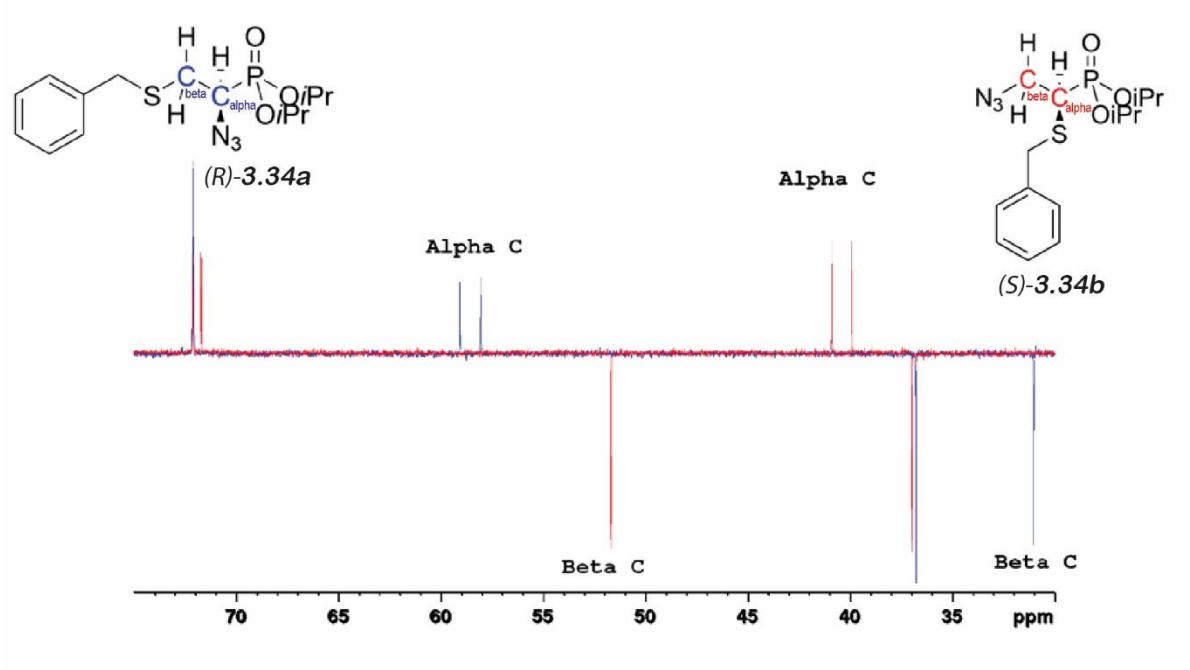

Figure 17. *Overlaid ^{13}C NMR of the two regioisomers (R)-**3.34a** and (S)-**3.34b**.*

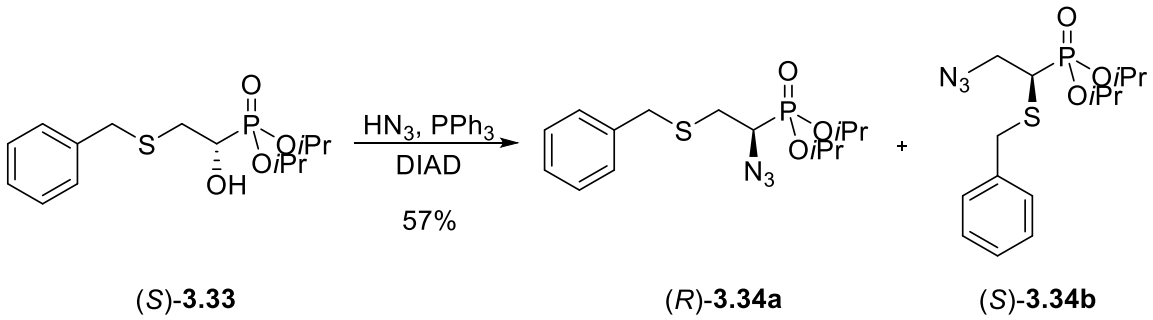

Scheme 31. *Synthesis of compounds (R)-**3.34a** and (S)-**3.34b** via Mitsunobu reaction.*

These two main products were separated, and a structural analysis revealed a rearrangement during the course of the Mitsunobu-reaction to give the two products shown in **Scheme 31**. The putative mechanism for this rearrangement is outlined in **Scheme 32**.

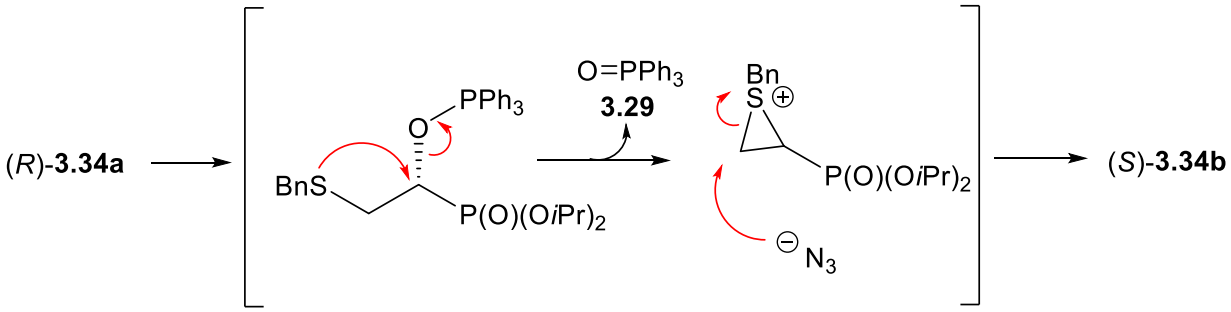

Scheme 32. *Possible mechanism for the rearrangement of the sulfide (S)-**3.34**.*

We assume that this rearrangement occurred due to the nucleophilic character of the sulfide. The calculated ratios were 1:3 in favor of the rearrangement product (*S*)-**3.34b**. Therefore, the reaction conditions were altered in order to achieve a higher conversion rate towards the desired compound (*R*)-**3.34a**. Different azo-compounds such as diethylazodicarboxylate, and di-*tert*-butylazodicarboxylate, as well as a variety of solvents (THF, toluene, 1,4-dioxane) were tested. Best results were obtained using D*t*BAD and THF as solvent, which favoured the desired product by a 4:1 ratio. However, complete removal of the formed hydrazoester (derived from D*t*BAD) proved to be very difficult and also the conversion rates were lower. Thus, as a compromise, DIAD was the azoester of choice, even though this led to slightly worse product/side product ratios (3 : 1 = (*R*)-**3.34a** : (*S*)-**3.34b**).

After optimization of the reaction conditions, the separation of the two molecules proved to be very problematic. In order to find a practical system for chromatographic separations of the two regioisomers, a variety of different solvent systems was tested (Table 3).

Solvent 1	Solvent 2	Ratio	R_f (*R*)-3.34a	R_f (*S*)-3.34b	R_f of other impurities	
n-Heptane	EA	1:1	0.55		0.67	0.34
Aceton	CH_2Cl_2	1:19	0.67		0.48	
Aceton	CH_2Cl_2	1:39	0.42		0.46	
n-Heptane	Et_2O	1:1	0.21		0.50	0.08
n-Heptane	Et_2O	2:1	0.15		0.19	0.11
Et_2O	/	/	0.88	0.74	0.62	
CH_2Cl_2	Et_2O	1:1	0.78		0.95	0.75
CH_2Cl_2	Et_2O	1:2	0.79		0.95	0.63
CH_2Cl_2	Et_2O	2:1	0.80		0.98	0.70
CH_2Cl_2	Et_2O	5:1	0.75	0.67	0.8	0.47
CH_2Cl_2	Et_2O	9:1	0.53	0.44	0.61	0.23
CH_2Cl_2	Et_2O	19:1	0.52	0.42	0.58	0.33
CH_2Cl_2	Et_2O	39:1	0.25	0.22	0.12	

Table 3. *Compared R_f values of (R)-**3.34a** and (S)-**3.34b** in different solvent systems.*

After comparing the R_f values of the two stereoisomers for different eluents, it was concluded that a mixture of CH_2Cl_2 : Et_2O (19 : 1) is ideal for separation. However, it was still not possible to separate the isomers after only one chromatographic run, but partial separation was possible. In order to obtain pure compound samples for analysis, several subsequent chromatographic runs were performed to finally yield the two products in good to moderate yield [81% combined for (*S*)-**3.34b** and (*R*)-**3.34a**].

However, separation is not mandatory at such an early stage. It is a well known fact that the retention time for α- and β-aminophosphonic acids differs drastically on strongly acidic cation exchange resins. This is for example the case for (*R*)-(1-amino-2-hydroxyethyl)phosphonic acid

and its regioisomer (*R*)-(2-amino-1-hydroxyethyl)phosphonic acid. Thus, a mixture of both regioisomers can be used in the next steps without separation and the regioisomers can then be separated after final global deprotection. While we used a mixture of both compounds, only the desired regioisomer is shown in all subsequent schemes.

Attempts to reduce the azide (*R*)-**3.34a** and cleave the benzyl protecting group at the same time, using H_2/Pd/C as for compound (*R*)-**3.17** failed. Again, it has to be taken into consideration that sulfur is poisonous for transition metal catalysts. Even very high amounts of palladium on charcoal did not lead to the formation of the desired product. While the azide was fully reduced to the amine, the benzyl group could not be cleaved hydrogenolytically by reacting (*R*)-**3.34a** with hydrogen using a palladium catalyst. Different solvents and pressures were tested. However, only diisopropyl (*R*)-(1-amino-2-(benzylthio)ethyl)phosphonate could be obtained by reacting the azide in THF with the palladium catalyst at room pressure. An elevated pressure led to decomposition of the starting material and other solvents (ethanol, methanol, CH_2Cl_2) had a negative effect on the degree of conversion of the azide.

Thus, it was decided to remove the protecting group via a Birch-type reaction (**Scheme 33**).

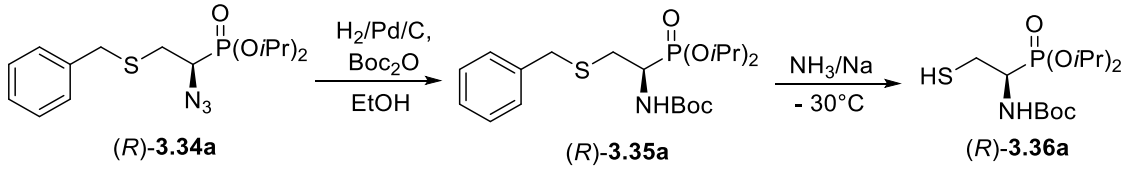

(*R*)-**3.34a** (*R*)-**3.35a** (*R*)-**3.36a**

Scheme 33*. Reduction of (R)-**3.34a** to the corresponding amine with simultaneous Boc-protection, followed by Birch reduction for removal of the benzyl ether protecting group of (R)-**3.35a**.*

To do so, a Boc-protecting group had to be installed, which was easily possible by adding Boc_2O to the reaction mixture for hydrogenation. This led to a faster reaction and gave the protected α-aminophosphonate (*R*)-**3.35a** for the subsequent Birch reduction. This protection is necessary to avoid an undesired α-aminophosphonate/phosphoamidate rearrangement that could easily occur under the strongly basic reaction conditions used for the Birch reduction. [91]

The Birch reduction with dissolving metals has been used for the synthesis of partially unsaturated six-membered rings and many other compounds for a long time. [90] Desogestrel, a

progestin medication, is an example for the application of the Birch reduction in drug development. [91] However, catalytic hydrogenation over various palladium catalysts was used preferentially for the majority of reductions until today because of the more convenient implementation. [92]. Due to the sulfide, which is poisonous to the palladium catalysts, the older Birch reduction had to be chosen. As sodium dissolves in liquid ammonia, it produces a deep blue solution, which shows reductive properties linked to the presence of metal cations and solvated electrons (**Scheme 34**). [93] The solvated electrons initiate the radical reductive cleavage of the benzyl (thio-)ether. During the course of the reaction, the blue color fades again, showing consumption of the solvated electrons.

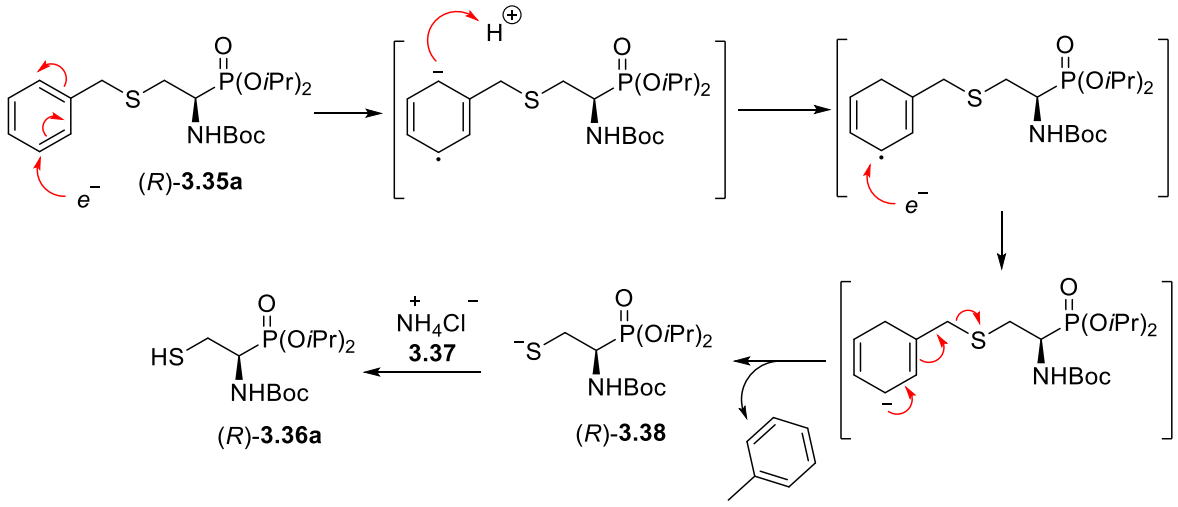

Scheme 34. *Reaction mechanism of the removal of the benzyl ether protecting group of (R)-**3.35a**.*

The reaction is complete after the blue color persists, which means that no further electrons are used. Afterwards, NH_4Cl can be added to quench the reaction and to full discoloration of the solution. The final deprotection of the isopropyl groups and the Boc-group was possible using the same approach as described for compound (*R*)-**3.17** and proceeded smoothly (**Scheme 35**).

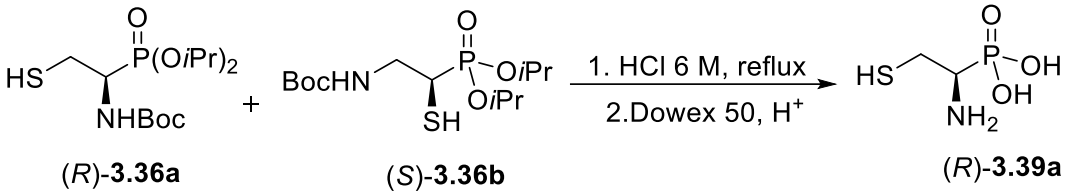

Scheme 35. *Global deprotection of a mixture of both regioisomers (R)-**3.36a** and (S)-**3.36b.***

However, due to the stereoisomer (*S*)-**3.36b** still being present in the reaction mixture, the desired product (*R*)-**3.39a** was formed in a mixture with (*S*)-**3.39b** (phosphaisocysteine). Thus, special care has to be taken during the ion exchange chromatographical purification. The column length was adapted to separate the two compounds successfully and avoid the leakage of the β-aminophosphonic acid alongside the α-aminophosphonic acid. Compound (*R*)-**3.39a** was obtained using water as eluent, whereas the other regioisomer (*S*)-**3.39b** had to be eluted with aqueous acetic acid (3 %). Both the compounds could be recrystallized from EtOH/H_2O to yield colorless crystals.

Summarized, the synthesis outlined above is the first described synthetic pathway to access phosphacysteine and phosphaisocysteine in high ee. The overall yield of the synthesis might not seem very high (8%), but all reaction steps could be performed with ≥60% yield, except for the Mitsunobu reaction. Future improvement of the yield in this step can thus have a dramatic effect on the overall yield. The ees calculated for the intermediate hydroxyphosphonate using the chiral solvating reagent (*S*)-**3.21** was over 98%. The exact ee of the final products will be determined by our cooperation partners by chiral stationary phase HPLC after derivatization. As the compound (*R*)-**3.39a** was synthesized for the first time, it was not possible to compare its specific rotation to literature values.

3.1.3 Detailed discussion of the synthesis of deuterated (*R*)-phosphaisoserine [(*R*)-1-[$^2H_1$]-**3.44**]

Kinetic and mechanistic studies of phosphonate degrading enzymes often need isotopically labelled substrates. However, these are often difficult to access. Delicate synthetic techniques or expensive starting materials are often needed for their synthesis. Thus, we decided to adapt the already established Noyori-transfer hydrogenation for these purposes, which will allow it to introduce deuterium instead of hydrogen. This will provide an easy access to chiral, deuterated phosphonates starting from cheap, commercially available sources using the same reactions as for the non-deuterated analogs. This methodology was tried in the synthesis of deuterated (*R*)-phosphaisoserine. [95]

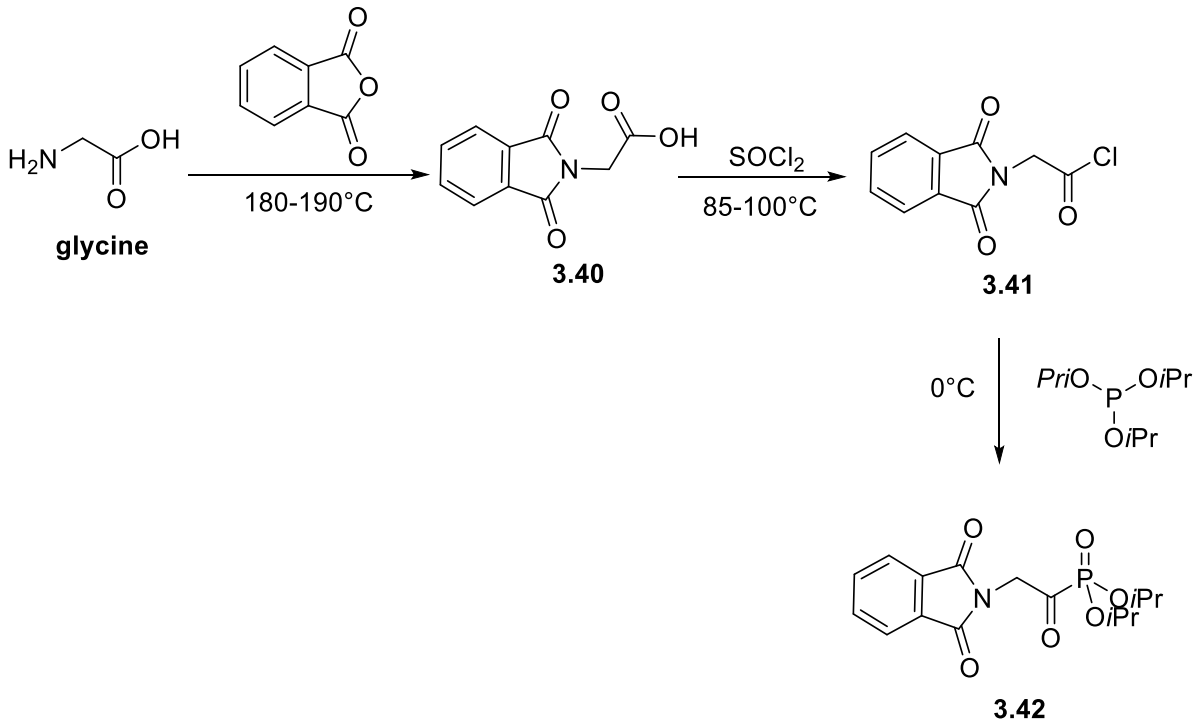

Scheme 36. *Reaction overview for the synthesis of* ***3.42****, starting from glycine.*

For this purpose, compound **3.42** was synthesized according to a method developed by a group member. Therefore, **3.40** was converted to the corresponding acyl chloride **3.41** using thionyl chloride after protection. The ketophosphonate **3.42** was then obtained in an Arbusov-type reaction as shown above (**Scheme 17**). [95]

The already described, very reliable method for catalytic transfer-hydrogenation of the keto phosphonate to give a (*R*)-**3.43** was already successfully used on this molecule. [96] The generated product was the key-intermediate in the synthesis of (*R*)-phosphaisoserine. Studies on the detailed mechanism and reaction kinetics of the individual steps of the PhnY*/PhnZ phosphonate degradative enzyme complex are currently ongoing in our collaborators laboratory using this compound. For these and other purposes, there is an urgent need for deuterated analogues to this biogenic phosphonic acid.

Thus, we adapted our already established transfer-hydrogenation method to allow to access deuterated compounds of this kind in a reliable fashion, using cheap reagents. And most importantly: using this approach the deuterated analogue (*R*)-[1-$^{2}H_{1}$]-**3.43** becomes accessible from the same precursors as the non-deuterated compound (*R*)-**3.44**. This allows a maximal flexibility in the synthesis of this compounds (**Scheme 37**).

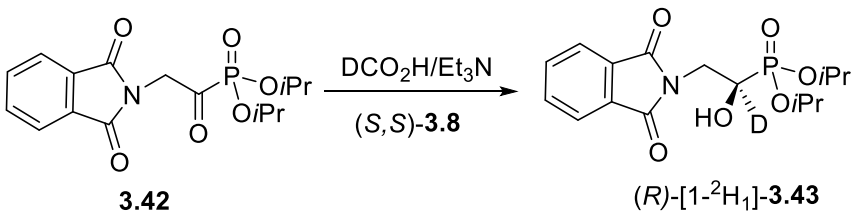

***Scheme 37**. Reduction using deuterated formic acid.*

The desired chiral, deuterated α-hydroxyphosphonate could be obtained from the keto-phosphonate precursors **3.42** by slightly adapting the synthetic protocol. First attempts, where DCOOD (an easily available and cheap deuterated acid) replaced formic acid in the Noyori catalytic transfer-hydrogenation, showed incorporation of deuterium not only in α- but also in β-position to the phosphorus atom. The ^{1}H NMR spectrum showed that the hydrogen atoms in β-position were partly exchanged with deuterium as well (**Figure 18**) as indicated by the integration of the β-hydrogen atoms.

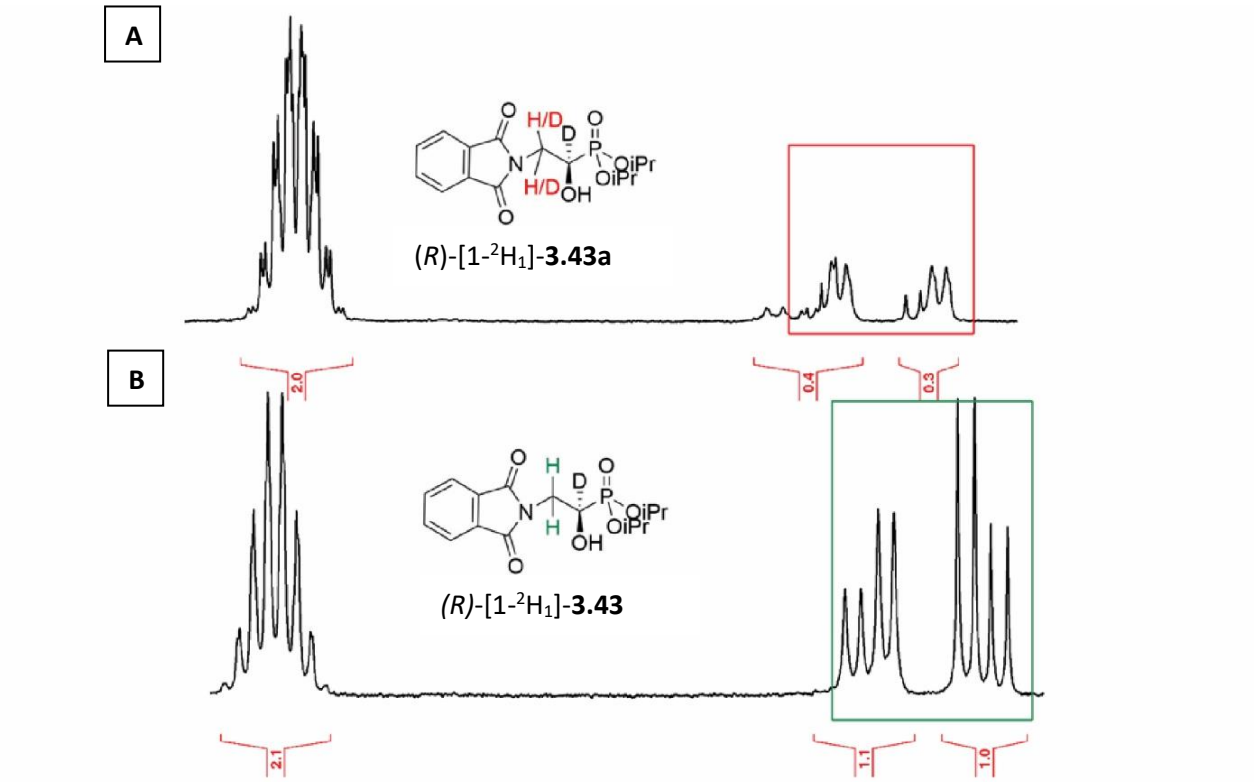

Figure 18. *Comparison of the ^{1}H NMR of the products obtained from catalytic transfer hydrogenation using either DCOOD (A) or DCOOH (B).*

This can be attributed to a fast equilibrium between the keto- and enol-form of the used α-oxo-phosphonate. In these experiments, one of the limitations of the method becomes quite clear: if the enolisation process is faster than the attempted reduction, there will be potential loss of chirality on the β-position to phosphorus. However, using monodeuterated formic acid (DCOOH), we could successfully generate the desired product (*R*)-[1-$^{2}H_1$]-**3.42**. All subsequent steps were carried out in agreement with the already established synthesis for (*R*)-phosphaisoserine (**Scheme 38**). [96]

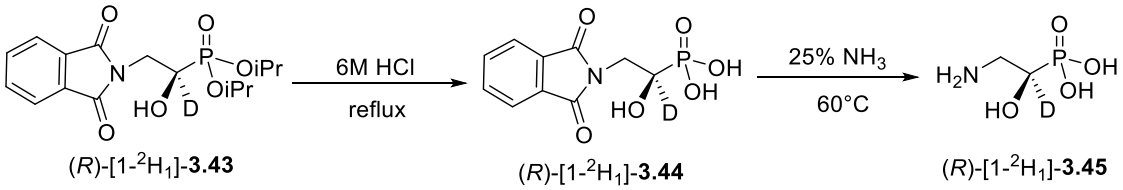

Scheme 38. *Global deprotection of (R)-[1-$^{2}H_1$]-**3.43**.*

After the reaction with NH_3 (to cleave the phthalimide group), it was difficult to distinguish if the phthalimide was still bound to the product or already cleaved by ^1H NMR spectrum (**Figure 19**).

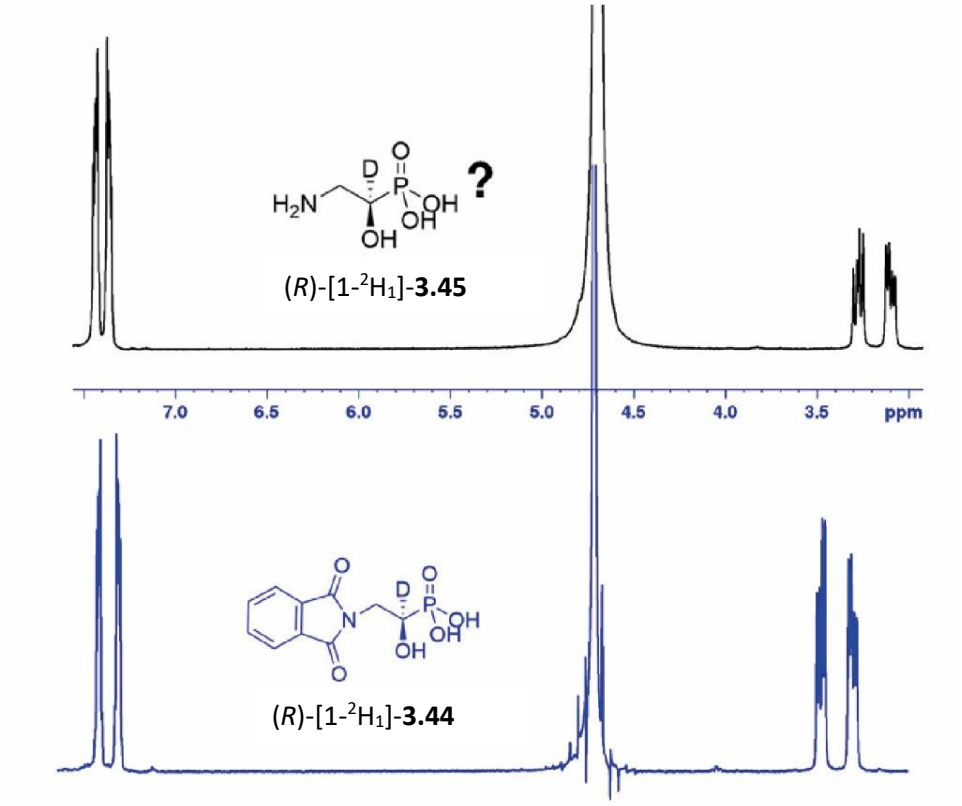

Figure 19. *^1H NMR before and after deprotection of (*R*)-[1-$^2H_1$]-**3.43** with NH_3.*

However, TLC showed the cleavage to be complete. [While the product shows a rather small R_f-value (0.18), the phthalimide is not as polar and shows a higher R_f (0.73)]. Most of the cleaved phthalimide could finally be removed from the product solution by extraction with EtOAc. However, even after vigorous shaking, traces of the cleaved protecting group remained in the sample. Thus, a rather long column for ion exchange chromatography was chosen to ensure a good separation.

Applying this strategy we could obtain the deuterated compound of (*R*)-[1-$^2H_1$-**3.44**] in an overall yield of 37% in the same number of steps and applying an identical synthetic sequence as for the non-deuterated analog (*R*)-**1.5**.

3.2 Synthetic strategy to access a novel TSPO ligand

3.2.1 The first synthetic approach

The “first generation” TSPO ligand, PK11195 (Figure 20), which suffers from high non-specific binding due to its immense lipophilicity [97], is still the most prominently used template for the synthesis of new TSPO –PET ligands.

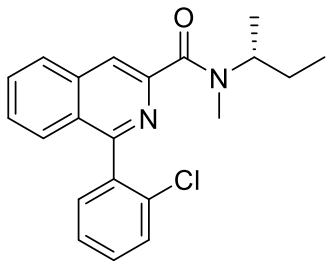

1.39

***Figure 20**. PET tracer (R)-[^{11}C]PK11195*

The subsequent generation of TSPO ligands successfully sorted out these drawbacks but showed a very heterogeneous binding behavior, among a group of patients, explained by a single nucleotide polymorphism in the TSPO gene. [64] To eliminate differences in binding affinity caused by the different TSPO genotypes, as well as to improve pharmacokinetic properties, new TSPO ligands are still developed. One of the most prominent recent advances was the synthesis of a novel radiotracer (*R*)-[^{11}C]Me@NEBIQUINIDE (**1.44**) as well as of its fluorine-18 labeled analogue (*R*)-[^{18}F]NEBIFQUINIDE (**1.45**) by Kalina *et al*. (**Figure 20**) [67].

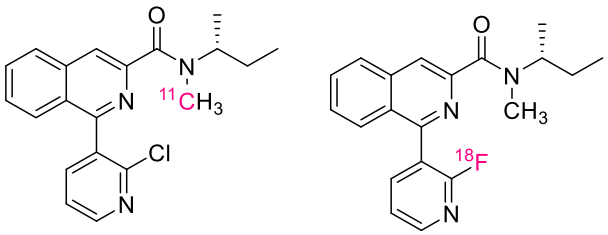

1.44 **1.45**

***Figure 20.** Structure of ^{11}C- and ^{18}F- radiolabeled (R)-Me@NEBIQUINIDE.*

These already showed improved binding properties in all known human TSPO phenotypes in addition to a high metabolic stability in first preclinical *in vitro*, *in vivo* and *ex vivo* trials.

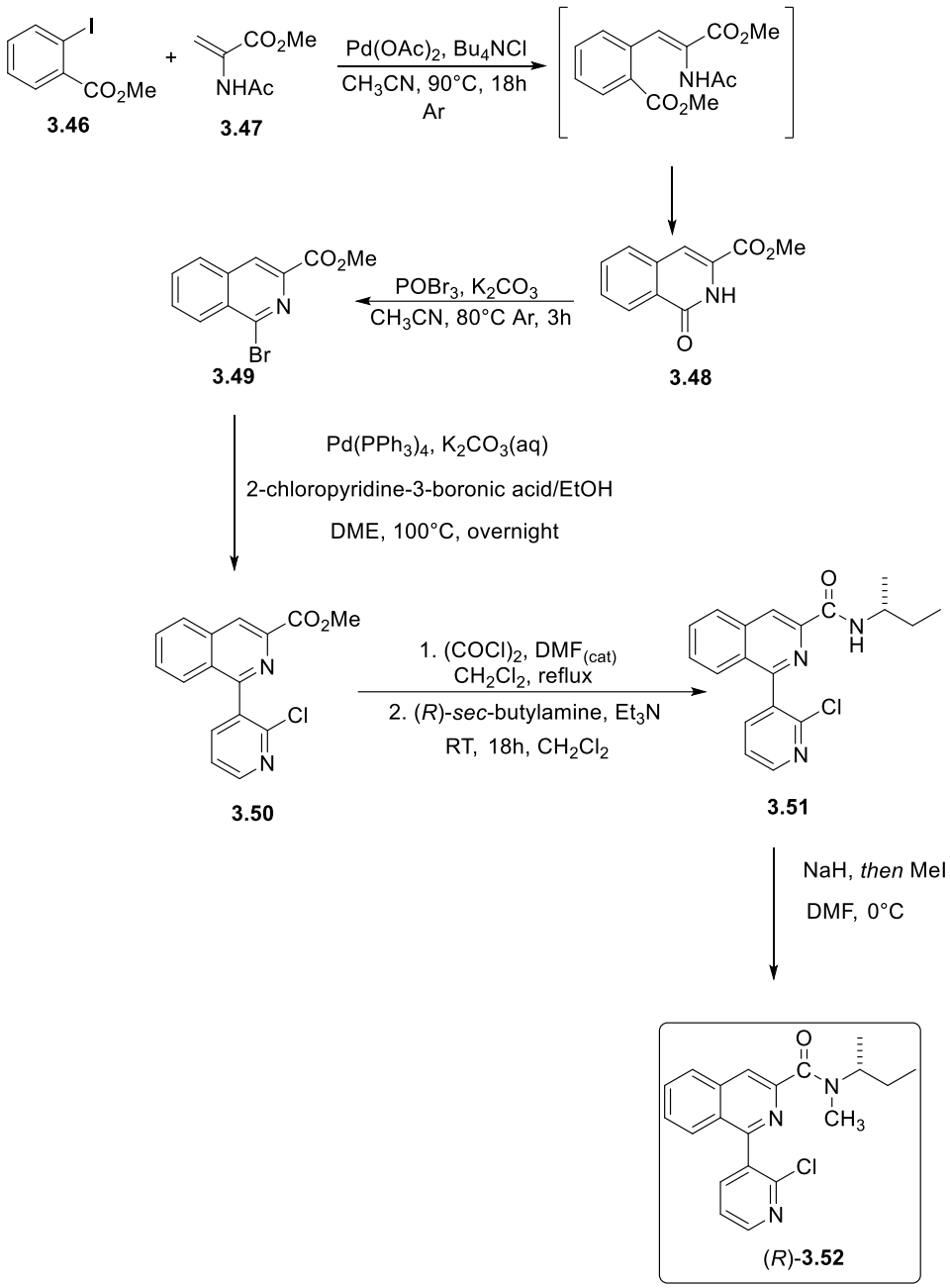

Scheme 39. *Synthesis scheme for (R)-Me@NEBIQUINIDE (easily adaptable to give NEBIFQUINIDE by using a different boronic acid for the Suzuki coupling). [67]*

The synthesis pathway shown in **Scheme 39** shows the optimized, straightforward approach to access both Me@NEBIQUINIDE and (*R*)-NEBIFQUINIDE. It could possibly also be used for the synthesis of other, similar molecules such as the target compound of this work: (*R*)-*N*-(*sec*-butyl)-1-(2-chloropyridin-3-yl)-*N*-methyl-2,6-naphthyridine-3-carboxamide [(*R*)-**3.55**] (**Scheme 40**) .

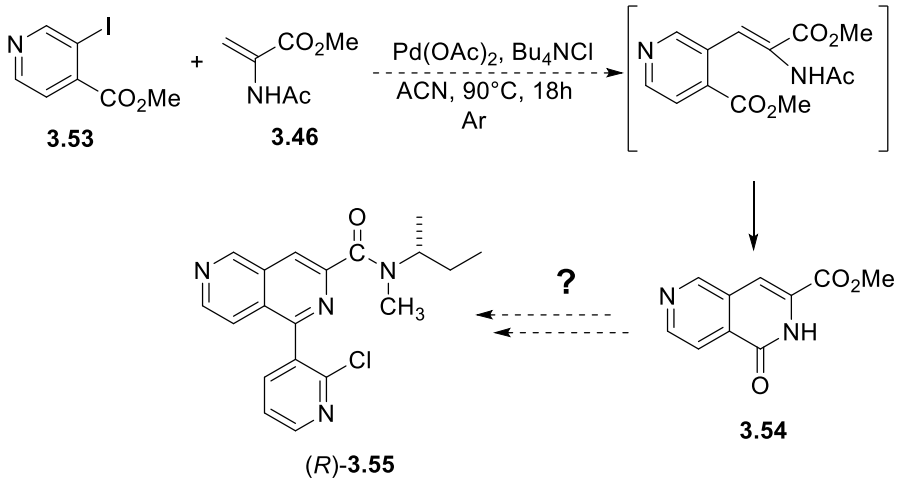

***Scheme 40**. Adaption of the general reaction approach in the attempted synthesis of (R)-**3.55**.*

The first attempt to obtain the desired key-intermediate **3.54** for the synthesis of the less lipophilic compound (*R*)-**3.55**, via a commonly used Heck reaction, was not successful by using any of the noted reaction conditions (Table 4).

Catalyst	Solvent	Reaction Temperature [°C]	Reaction Time [h]	Yield [%]
$Pd(OAc)_2$	ACN	90	24	0
$Pd(PPh_3)_4$	DMF	120	24	0
$Pd(dppf)Cl_2$	DMF	120	24	0
$Pd(dppf)Cl_2$	ACN	130 (Microwave)	2	0
$Pd(OAc)_2$	DMF	120	24	0

Table 4.** Different applied reaction conditions to obtain the desired compound (*R*)-**3.55.

3.2.2 Adapted synthetic procedure

Since none of the applied reaction conditions were successful, a new approach was developed to evade the occurring problems. (**Scheme 41**)

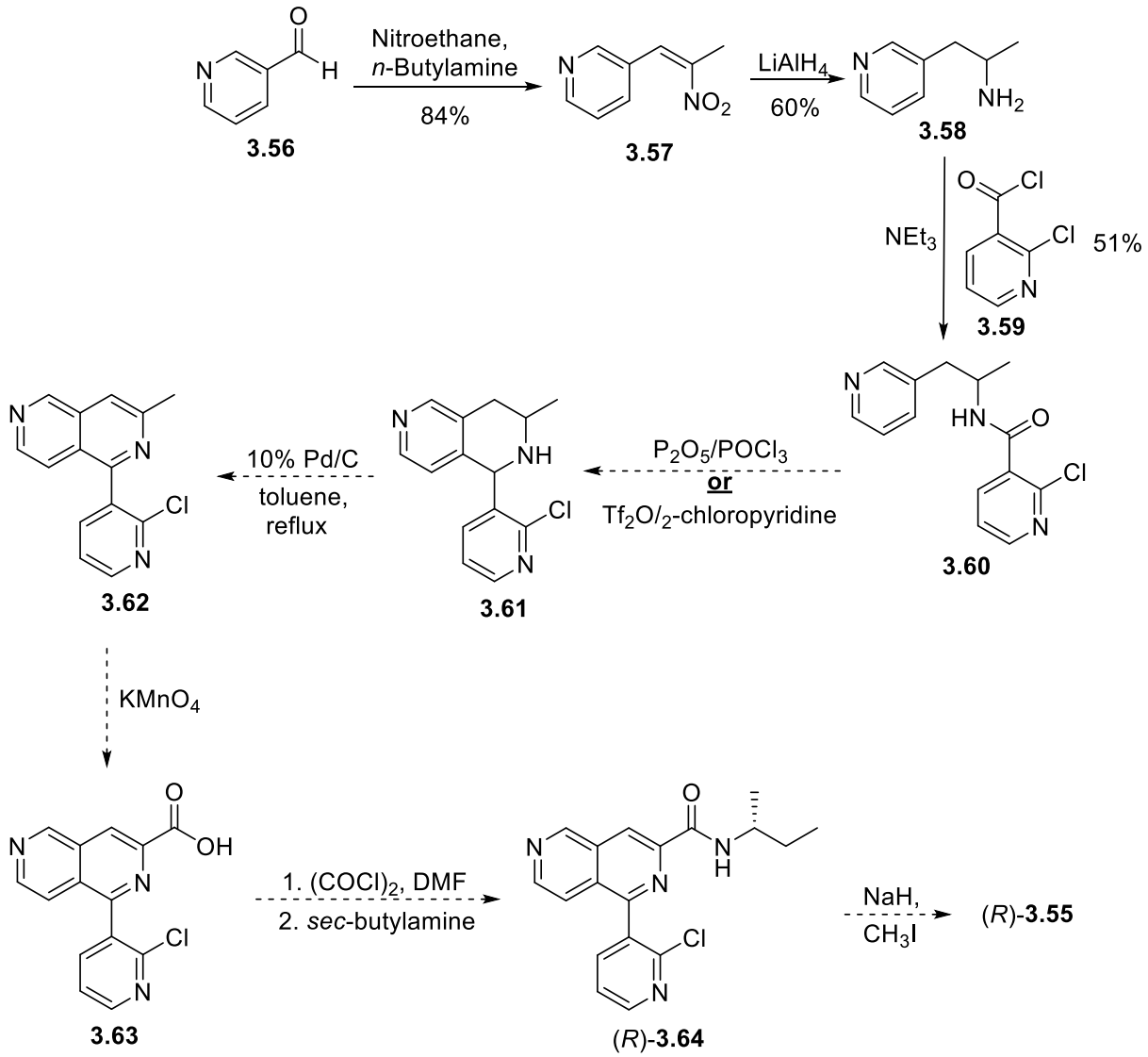

Scheme 41. *New synthesis approach to obtain (R)-**3.54**; successful transformations are depicted using full arrows, while dashed arrows are used for transformation that were not carried out.*

In order to obtain the amine **3.58** for a subsequent coupling reaction, a Knoevenagel reaction between nicotinic aldehyde and nitroethane was envisaged, giving the nitro compound **3.57**, which was planned to be reduced further with $LiAlH_4$ to the desired amine **3.58**. Using acyl chloride **3.59**, the coupling reaction to give the key-intermediate **3.60** could be performed with

a mild base such as NEt_3 in 51% yield. The Bischler-Napieralski reaction was chosen to perform a ring closure, which usually achieves good, reliable results. After reduction with Pd/C it was planned to oxidize the methyl group with $KMnO_4$ to selectively give the corresponding acid **3.63.** The latter can then possibly be converted to a reactive acyl chloride and coupled with an amine. The resulting amide (*R*)-**3.64** was meant to be finally methylated.

3.2.3 First results

At first, an approach for the nitro compound **3.57** was chosen, published by Gotor *et al*. [98] For this synthesis nitroethane was used as a reactant as well as a solvent. This led to unsatisfying yields and made a very difficult purification procedure necessary. Even after numerous separation attempts, nitroethane could not be entirely removed from the product, meaning that we could not reproduce the published strategy successfully, even after numerous attempts. Changing the base to *n*-butylamine (0.05 eq) and reducing the amount of nitroethane to 1 eq. as described by Person *et al*. [99] yielded the desired product **3.57** in good yields after refluxing the reaction mixture in toluene for 6 days (**Scheme 40**).

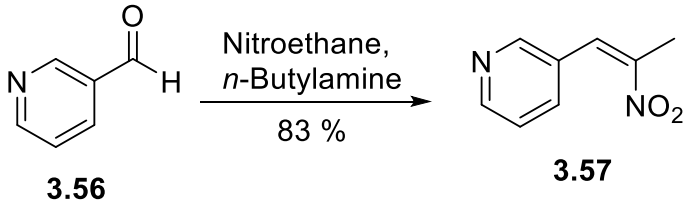

3.56 **3.57**

Scheme 42. *Reaction to form the nitro compound* ***3.57****.*

After purification by column chromatography, a pure - now almost colorless and crystalline - product, could be obtained in yields over 80%.

Although, according to the literature a reduction to the amine can be achieved quantitively by refluxing the starting material (**3.56**) in the presence of $LiALH_4$ in dry THF overnight. However, a satisfying yield could not be obtained by that procedure. After numerous approaches in different solvents such as Et_2O and DCM, we found that the maximum yield is 60% (**Scheme 43**).

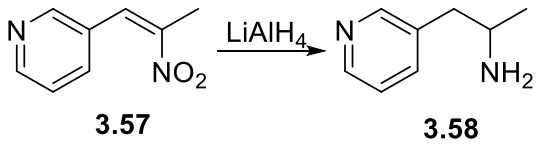

3.57 **3.58**

Scheme 43. *Reduction of* ***3.57*** *to the amine* ***3.58****.*

Decomposition of the product can already be observed in the reducing reaction environment, while there is still unreacted starting material present. It was found that the perfect reaction conditions are stirring the nitro compound for 2 h at room temperature in THF under Ar. Conducting the reaction at 0 °C did not yield any detectable amount of amine **3.58**, while stirring it for more than 2 h at room temperature lead to the decomposition of the product. There are two possibilities for the subsequent reaction step: either by using an acyl chloride as reactant (which can be attacked more easily by the nitrogen atom following basic activation) or reacting the amine with the corresponding acid **3.64** (**Scheme 44**).

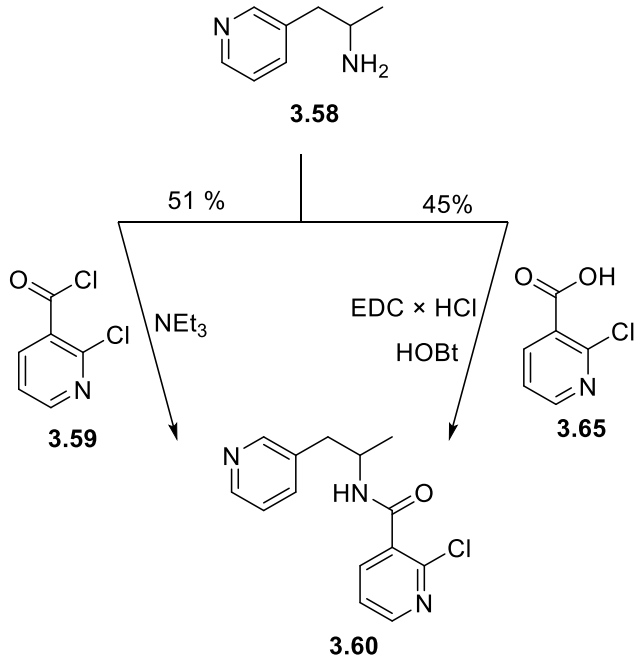

Scheme 44*. Coupling of the amine* ***3.58*** *with 2-chloronicotinoyl chloride/2-chloronicotinic acid.*

The coupling reaction is performed using common coupling agents (mixture of HOBt, EDC × HCl) in the second case. Both approaches gave similar yields (51 % and 45 % respectively). Optimization of the yield was postponed to a later time and the feasibility of the next reaction step was tested first.

3.2.4 Attempting the ring closure

The first approach was a Bischler-Napieralski reaction, which is known for mild reaction conditions (**Scheme 45**). [100]

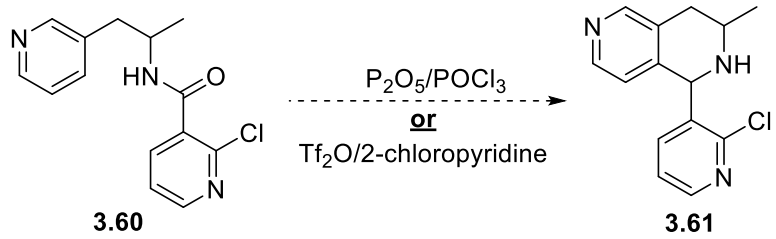

***Scheme 45**. Attempted ring closure by Bischler-Napieralski conditions.*

However, this did not give the desired product. Different literature sources for the synthesis of isoquinolines using this method [101] all either show an electron donating residue or an unsubstituted aromatic ring. The nitrogen-atom in the pyridine ring is therefore presumably too electron withdrawing for ring closure as presented in **Scheme 46**.

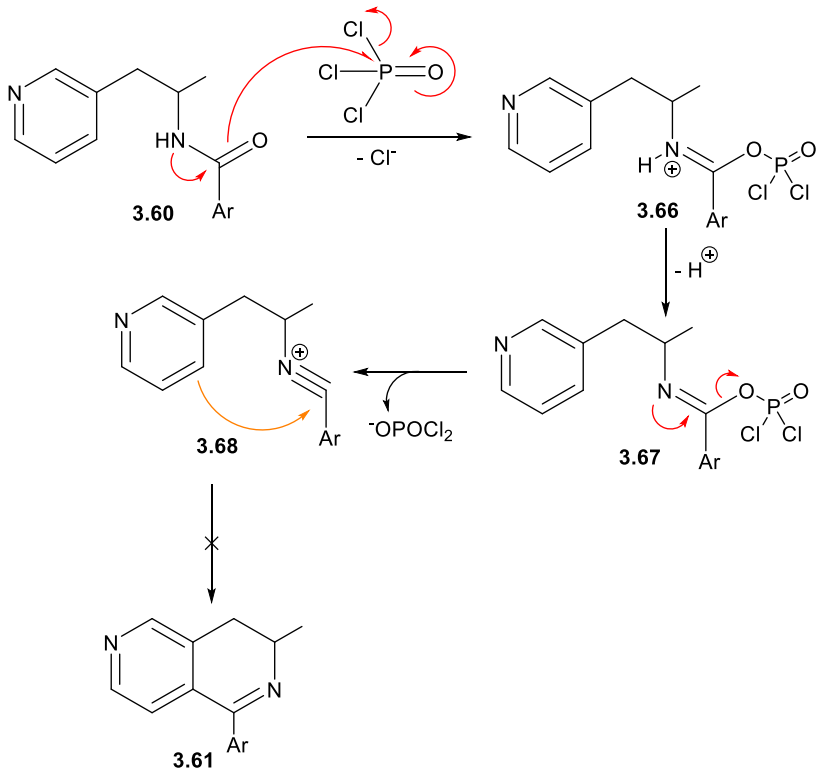

***Scheme 46**. Reaction mechanism of the attempted Bischler-Napieralski cyclization.*

3.2.5 Outlook

Since the second synthetic approach faced major difficulties which could not be solved either, another method was designed.

The general idea is to facilitate the ring closure by changing from an intermolecular problem to an intramolecular Heck reaction (**Scheme 47**).

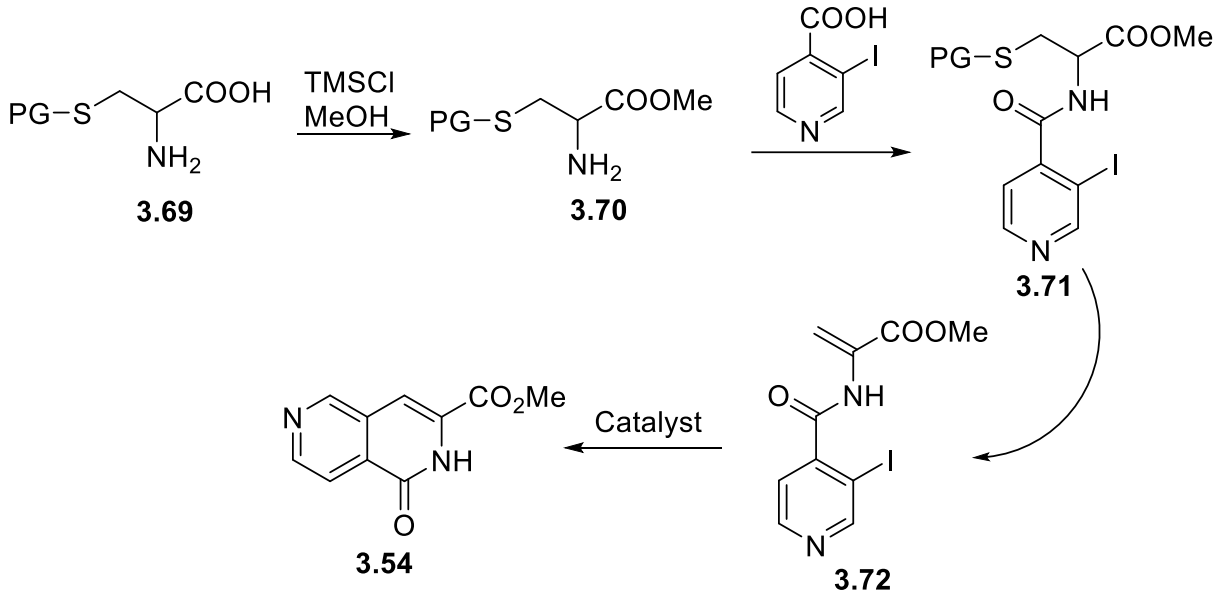

***Scheme 47**. Future suggested synthetic approach towards **3.54**; PG = protecting group.*

This should drastically improve the yield by increasing the reaction rate by several orders of magnitude. This will, if successful, provide highly improved reaction kinetics, for which even the electron withdrawing effect of the additional nitrogen atom in the ring should not be an obstacle. For a successful synthesis of the desired compound **3.54** it is necessary to find an appropriate protecting group for the sulfide of 3.69, since side reactions could occur with the iodide substituent during the coupling step. In order to convert the sulfide group to the needed double bond, several literature known approaches can be envisaged. [102] This new synthetic approach still has to be analyzed in detail concerning the exact stereochemistry of our compounds and is planned to be tested in the near future.

4. Experimental Part

4.1 Instrumentation and general experimental part

Characterization data were obtained on the following devices:

IR Spectra:

Vertex 70 IR spectrometer in ATR mode.

Specific Rotation:

Perkin-Elmer 341 polarimeter (d = 1 dm, at given temperature).

Melting point:

Leica Galen III Reichert Thermovar; all melting points are uncorrected.

NMR spectra:

Bruker Avance AV III 600 (^{1}H: 600.25 MHz, ^{13}C: 150.93 MHz, ^{31}P: 242.99 MHz);

Bruker Avance AV 400 (^{1}H: 400.27 MHz, ^{13}C: 100.65 MHz, ^{31}P: 162.03 MHz).

The spectra were referenced to the following solvent (residual) peaks:

^{1}H NMR spectra: $CDCl_3$: $CHCl_3$ (δ_H = 7.24 ppm), D_2O: HOD (δ_H = 4.80 ppm), d_4-methanol: CHD_2OD (δ_H = 3.31ppm), d_6- dimethyl sulfoxide: $(CD_2H)SO(CD_3)$ (δ_H = 2.50 ppm), d_8-toluene: $(C_6D_5)CHD_2$ (δ_H = 2.08 ppm).

^{13}C NMR spectra: $CDCl_3$: δ_C = 77.23 ppm, d_4-methanol: δ_C = 49.15 ppm, d_6- dimethyl sulfoxide: δ_C = 39.51 ppm.

^{31}P NMR spectra: external H_3PO_4 85% aqueous solution: δ_P = 0.00 ppm.

Chromatographic separations were carried out using the following equipment:

Medium pressure liquid chromatography (MPLC):

Column Chromatography was either performed manually or on a Biotage Isolera Prime (Biotage) flash purification system. Separation cartridges (depending on the substance amount): KP-Sil 10 g – KP-Sil 100 g, filled with Merck silica gel 60 (230-400 mesh) or Chromabond Flash RS 15 SiOH, or RS 80 (pre-packed).

Thin layer chromatography (TLC):

Merck silica gel 60 F_{254} glass plates (coating 0.25 mm thick)

TLCs were stained using the following solutions:

Molybdate solution: 23 g $(NH_4)_6Mo_7O_{24} \times 4\ H_2O$, 1 g $Ce(SO_4)_2 \times 4\ H_2O$ in 500 mL 10% aqueous H_2SO_4.

Ninhydrin solution: 0.2% ninhydrin in ethanol (98%).

Iodine chamber

UV detection (254 nm)

Chemicals:

THF was dried over potassium and distilled prior to use.

All other chemicals were bought from Sigma-Aldrich, ABCR, Fluka or Acros and were used without any further purification.

4.2 Synthesis of (*R*)-phosphaserine

4.2.1 Synthesis of Dess-Martin periodinane (DMP, 3.14) [103]

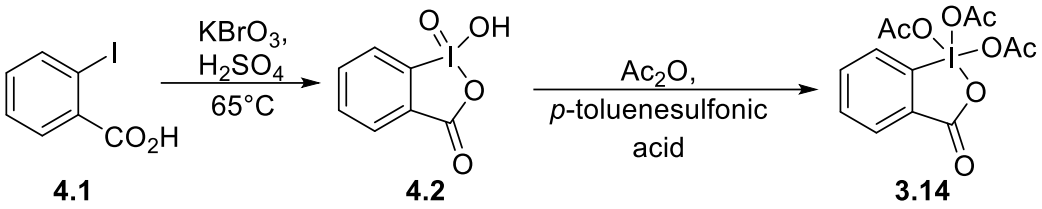

Iodobenzoic acid **4.1** (20 g, 80 mmol) was dissolved in H_2SO_4 (165 mL, 0.73 M) and $KBrO_3$ (20 g, 120 mmol) was added in portions over 30 min, while heating the reaction mixture to 65 °C. After stirring for 6 h, the reaction mixture was cooled to 0 °C. The precipitate was filtered and washed with H_2O (250 mL) followed by EtOH (2 × 50 mL) and dried *in vacuo* to yield iodoxybenzoic acid (IBX, **4.2**). After addition of *p*-toluenesulfonic acid and Ac_2O (78 g, 0.77 mol, 85 mL) to IBX, the mixture was heated to 80 °C and stirred for 1 h (until it became a clear solution). After cooling to 0 °C, the precipitate was filtered and washed with diethyl ether (5 × 15 mL) to yield DMP (**3.14**, 23 g, 54 mmol, 68%).

Spectroscopic data were identical to those of the literature. [103]

4.2.2 Synthesis of diisopropyl (trimethylsilyl) phosphite (3.12) [75]

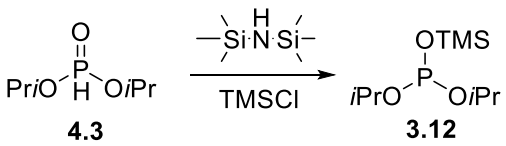

Hexamethyldisilazane (24.2g, 0.15 mol), diisopropyl phosphite (**4.3**, 49.8 g, 0.3 mol) and chlorotrimethylsilane (16.2 g, 0.15 mol) were refluxed in dry *n*-hexane (150 mL) under exclusion of water for two hours. The solvent and ammonium chloride were removed by fractional distillation through a Vigreux column at ambient pressure at 80 °C. Afterwards, the pressure was adjusted to 30 Torr and the temperature was raised gradually from 80 to 140 °C to obtain the desired trimethylsilyl phosphite **3.12** (52 g, 0.22 mol, 73%).

^{1}H NMR (400.27 MHz, d_8-toluene, [4Jul0318/20], TS 42): δ_H = 4.41 (sept, *J* = 6.2 Hz, 1H, CH *i*Pr), 4.40 (sept, *J* = 6.1 Hz, 1H, CH *i*Pr), 1.16 (d, *J* = 6.1 Hz, 6H, 2 × CH_3), 1.15 (d, *J* = 6.2 Hz, 6H, 2 × CH_3), 0.23 (s, 9H, O-TMS).

^{31}P NMR (162.04 MHz, d_8-toluene, [4Jul0318/21]): δ_P = 128.8 (s).

4.2.3 Synthesis of (±)-diisopropyl (2-(benzyloxy)-1-hydroxyethyl)phosphonate [(±)-3.13]

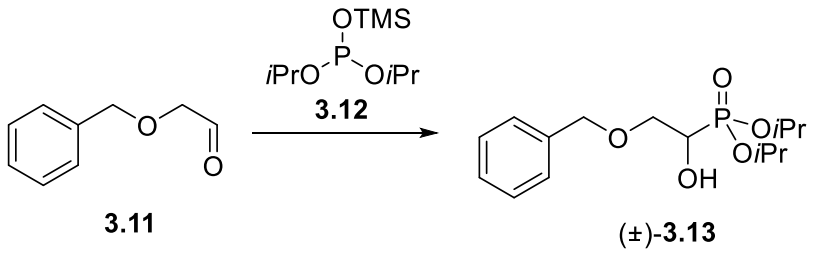

Diisopropyltrimethylsilyl phosphite (**3.12**, 3.58 g, 15 mmol) was added to benzyloxyacetaldehyde (**3.11**, 0.751 g, 5 mmol) under argon in dry toluene (15 mL) and afterwards heated to 80 °C. Completion of the reaction was monitored by TLC [R_f (product) = 0.22, *n*-heptane : EtOAc = 1:1]. After 16 h the solvent was removed *in vacuo*,the residue was dissolved in a mixture of 2 M HCl and THF (1 : 1 ratio) and stirred for 5 h at r.t. The phases were separated and the aqueous phase was then extracted with ethyl acetate (4 × 15 mL). The combined organic portions were dried ($MgSO_4$) and purified by MPLC using a solvent gradient (*n*-heptane/EtOAc; 12% → 100% ethyl acetate) to yield the racemic α-hydroxyphosphonate **3.13** (1.3 g, 4.12 mmol, 82%) as colorless oil.

Spectroscopic data was identical to that of the enantiopure α-hydroxyphosphonate (*S*)-**3.13** (see below).

4.2.4 Synthesis of diisopropyl 2-(benzyloxy)-1-oxoethylphosphonate (**3.15**)

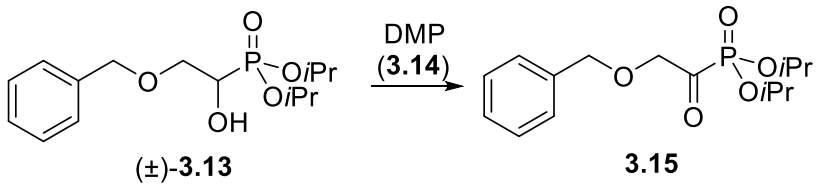

(±)-**3.13** **3.15**

The racemic hydroxyphosphonate (±)-**3.13** (1.58 g, 5 mmol) was dissolved in dry CH_2Cl_2 (30 mL) and cooled to 0 °C. DMP (**3.14**, 3.18 g, 7.5 mmol,) was added and stirring was continued for 30 min. Then, the cooling bath was removed and the reaction mixture was allowed to warm to r.t. The reaction progress was monitored using ^{31}P NMR [δ_P (product) = –5.24 ppm; δ_P (starting material) = 19.84 ppm]. After 4 h at room temperature the solvent was removed *in vacuo* without external heating and the remaining residue was taken up in Et_2O (20 mL). DMP was removed by extraction using a 1:1 mixture of sat. aqueous $NaHCO_3$ and $Na_2S_2O_3$ solutions (3 × 20 mL). The combined organic layers were dried (Na_2SO_4) and the solvent was removed *in vacuo* to yield the desired ketophosphonate **3.15** (1.35 g, 4.3 mmol, 86%) in sufficient purity for the subsequent transformation as a mixture of its keto- and enol-form.

^{1}H NMR of the keto-form (400.27 MHz, $CDCl_3$, [4Nov2618/850], TS 144): δ_H = 7.37-7.25 (m, 5H, 5 × CH_{arom}), 4.83-4.71 (m, 2H, 2 × CH *i*Pr), 4.60 (s, 2H, CH_2 Bn), 4.54 (d, *J* = 2.7 Hz, 2H, $C\underline{H}_2C(O)$-P), 1.35-1.31 (m, 12H, 4 × CH_3).

It was possible to distinguish between the keto- and enol-form in the ^{31}P NMR, but due to overlapping signals they could not be differentiated clearly in the ^{1}H NMR.

^{31}P NMR (162.04 MHz, $CDCl_3$, [4Jul1818/131]): δ_P = 4.42 (s, enol-form, $\int 0.3$), – 5.24 (s, keto-form, $\int 0.7$).

4.2.5 Synthesis of (*S*)- and (*R*)-diisopropyl (2-(benzyloxy)-1-hydroxyethyl)phosphonate [(*S*)-& (*R*)-**3.13**]

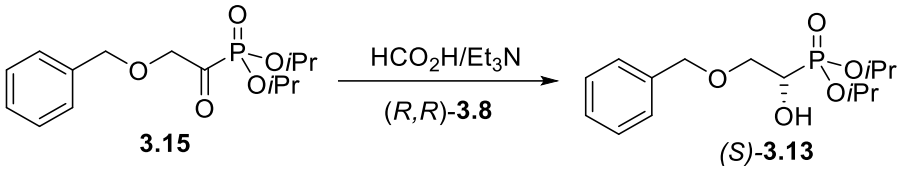

(*R,R*)-RuCl[(*p*-cymene)-TsDPEN] [(*R*,*R*)-**3.7**, 0.054 g, 0.086 mmol] was dissolved in dry CH_2Cl_2 (1 mL) and activated by addition of an aqueous KOH solution (0.48 mL, 0.18 M), whereupon the reaction mixture turned bright purple. The phases were separated and the aqueous layer was washed with CH_2Cl_2 (2 × 1 mL). The combined organic phases were dried (CaH_2).

Meanwhile, formic acid (0.87 g, 0.71 mL, 18.9 mmol) was added dropwise to Et_3N (1.13 g, 1.56 mL, 11.2 mmol) under Ar atmosphere at 0 °C and the resulting solution was stirred for 5 min.

The crude ketophosphonate **3.15** (1.35 g, 4.3 mmol) was dissolved in dry CH_2Cl_2 (10 mL) under Ar and the formic acid/Et_3N mixture was added, followed by the filtered solution of the catalyst. The reaction mixture was stirred at 35 °C for 24 h. The crude product (R_f = 0.22, *n*-heptane : EtOAc = 1:1,) was purified via MPLC using a solvent gradient (*n*-heptane/EtOAc, 12% → 100% EtOAc), to yield hydroxyphosphonate (*S*)-**3.13** (1.1 g, 3.48 mmol, 81%, ee ≥ 98%) as a colorless oil.

^{1}H NMR (600.25 MHz, $CDCl_3$, [6Nov2818/20], TS 79): δ_H = 7.34-7.25 (m, 5H, 5 × CH_{arom}), 4.77-4.70 (m, 2H, 2 × CH *i*Pr), 4.57 (AB-system, dd, J_{AB} = 11.9 Hz, 2H, CH_2 Bn), 4.06 (ddd, J_{XP} = 9.6 Hz, J_{XA} = 3.1 Hz, J_{XB} = 7.8 Hz, 1H, CH-P), 3.75 (ABXP-system, A-part: ddd, J_{AB} = 10.4 Hz, J_{AX} = 3.1 Hz, J_{AP} = 10.4 Hz, 1H; B-part: ddd, J_{AB} = 10.4 Hz, J_{BX} = 7.8 Hz, J_{BP} = 5.2, CH_2CH-P), 1.31 (d, *J* = 6.2 Hz, 3H, CH_3), 1.30 (d, *J* = 5.9 Hz, 3H, CH_3), 1.29 (d, *J* = 5.9 Hz, 3H, CH_3), 1.27 (d, *J* = 6.2 Hz, 3H, CH_3).

^{13}C NMR (150.93 MHz, $CDCl_3$, [6Nov2818/21]): δ_C = 137.62 (s, 1C, C_{arom}), 128.43 (s, 2C, CH_{arom}), 127.84 (s, 2C, CH_{arom}), 127.83 (s, 1C, CH_{arom}), 73.44 (s, 1C, CH_2 Bn), 71.46 (d, *J* = 7.1 Hz, 1C, CH *i*Pr), 71.35 (d, *J* = 6.9Hz, 1C, CH *i*Pr), 70.06 (d, *J* = 5.8 Hz, 1C, -CH_2-O), 68.13 (d, *J* = 162.8 Hz, 1C, -CH-P), 24.13 (d, *J* = 6.4 Hz, 1C, CH_3), 24.11 (d, *J* = 6.5 Hz, 1C, CH_3), 23.94 (d, *J* = 5.0 Hz, 1C, CH_3), 23.89 (d, *J* = 5.4 Hz, 1C, CH_3).

^{31}P NMR (162.03 MHz, $CDCl_3$, [4Aug1418/151]): δ_P = 19.98 (s).

HRMS calculated for $C_{15}H_{25}O_5P$ (316.33 g/mol): $[M+H]^+$ 317.1512, $[M+Na]^+$ 339.1332;

found: $[M+H]^+$ 317.1506, $[M+Na]^+$ 339.1329.

IR (ATR, TS 79): v = 3291, 2979, 1497, 1385, 1229, 1141, 985, 888, 739, 700, 633 cm^{-1}.

NMR of (*S*)-3.13 with chiral solvating agent: δ_P (162.03 MHz, $CDCl_3$) 95.85 [$\int$ 0.52, chiral solvating agent (*S*)-**3.21**], 20.08 [$\int$ 0.48, complex of chiral solvating agent with (*S*)-**3.13**]→ 19.9 [$\int$ 0.01, complex of chiral solvating agent with (*R*)-**3.13**] → ee ≥ 98%.

Specific rotation of (*S*)-**3.13:** α_D^{20} = + 2 (*c* 1.0, CH_2Cl_2).

(*R*)-**3.13** could be obtained similarly starting from **3.15** by using (*S,S*)-RuCl[(*p*-cymene)-TsDPEN] as catalyst. The spectroscopical data were identical to those of the (*S*)-enantiomer.

Specific rotation of (*R*)-**3.13:** α_D^{20} = – 2 (*c* 1.0, CH_2Cl_2).

4.2.6 Synthesis of (*R*)- and (*S*)-diisopropyl(1-azido-2-(benzyloxy)ethyl)phosphonate [(*R*)-& (*S*)-3.16]

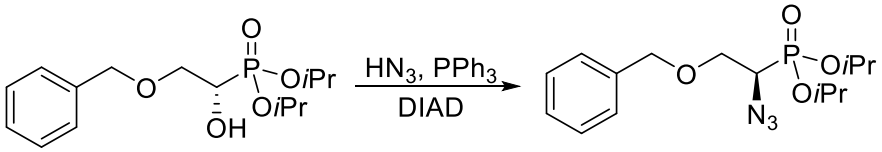

(*S*)-**3.13** (*R*)-**3.16**

Triphenylphosphine (0.63 g, 2.41 mmol) and hydroxyphosphonate (*S*)-**3.13** (0.4 g, 1.27 mmol) were dissolved in dry CH_2Cl_2 (15 mL) and cooled to 0 °C under Ar atmosphere. Then, hydrazoic acid (1.22 mL, 2.41 mmol, 1.97 M in toluene) and DIAD (0.49 g, 0.47 mL, 2.41 mmol) were added simultaneously to the reaction mixture. The cooling bath was removed and after 10 min of stirring at room temperature, the solution was heated to 35 °C. Completion of the reaction was monitored by TLC [R_f (product)= 0.53, *n*-heptane : EtOAc = 1:1] After 18 h the reaction was quenched by addition of methanol (3 mL) and the solvent was removed *in vacuo.* The residue was purified by MPLC with a solvent gradient (*n*-heptane/EtOAc, 12% → 100% EtOAc) to yield azide (*R*)-**3.16** (0.31 g, 0.91 mmol, 72%, ee ≥ 98%) as a colorless oil.

^{1}H NMR (600.25 MHz, $CDCl_3$, [6Dec0418/40], TS146): δ_H = 7.35-7.25 (m, 5H, 5 × CH_{arom}), 4.81-4.68 (m, 2H, CH *i*Pr), 4.57 (AB-system, dd, J_{AB} = 11.8 Hz, 2H, CH_2 Bn), 3.92-3.82 (m, 1H,CH-P), 3.77-3.66 (m, 2H, $C\underline{H}_2$CH-P), 1.324 (d, *J* = 6.2 Hz, 3H, CH_3), 1.319 (d, *J* = 6.2 Hz, 3H, CH_3), 1.31 (d, *J* = 6.2 Hz, 3H, CH_3), 1.28 (d, *J* = 6.2 Hz, 3H, CH_3).

^{13}C NMR (150.93 MHz, $CDCl_3$, [6Dec0418/41]): δ_C = 137.40 (s, 1C, C_{arom}), 128.46 (s, 2C, 2 × CH_{arom}), 127.88 (s, 1C, CH_{arom}), 127.76 (s, 2C, 2 × CH_{arom}), 73.45 (s, 1C, CH_2 Bn), 72.18 (d, *J* = 7.1 Hz, 1C, CH *i*Pr), 71.96 (d, *J* = 6.9Hz, 1C, CH *i*Pr), 68.47 (d, *J* = 5.7 Hz, 1C, CH_2-O), 58.24 (d, *J* = 156.4 Hz, 1C, CH-P), 24.15 (d, *J* = 3.3 Hz, 1C, CH_3), 24.09 (d, *J* = 3.7 Hz, 1C, CH_3), 23.90 (d, *J* = 4.7 Hz, 1C, CH_3), 23.82 (d, *J* = 5.1 Hz, 1C, CH_3).

^{31}P NMR (162.03 MHz, $CDCl_3$, [4Dec0418/281]): δ_P = 16.86 (s).

HRMS calculated for $C_{15}H_{24}N_3O_4P$ (341.15 g/mol): $[M+H]^+$ 342.1577, $[M+Na]^+$ 364.1397; found:$[M+H]^+$342.1563, $[M+Na]^+$ 364.1381

Specific rotation of (*R*)-**3.16:** α_D^{20} = – 13.3 (*c* 1.15, CH_2Cl_2)

NMR of (*R*)-3.16 with chiral solvating agent: δ_P (162.03 MHz, $CDCl_3$) 97.15 [$\int 0.58$, chiral solvating agent (*S*)-**3.21**], 16.86 [$\int 0.42$, complex of chiral solvating agent with (*R*)-**3.16**], 16.51 [$\int 0.001$, complex of chiral solvating agent with (*S*)-**3.16**] → ee ≥ 98%.

(*S*)-**3.16** could be obtained similarly starting from (*R*)-**3.13**. The spectroscopical data were identical to those of the (*R*)-enantiomer.

Specific rotation of (*S*)-**3.16:** α_D^{20} = + 11.7 (*c* 1.09, CH_2Cl_2)

IR (ATR, TS 146): v = 2981, 2361, 2095, 1454, 1386, 1257, 1103, 988, 741, 632 cm^{-1}.

4.2.7 Synthesis of diisopropyl (*R*)-(1-amino-2-hydroxyethyl)phosphonate [(*R*)-**3.17**]

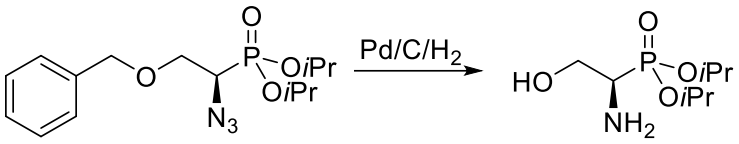

(*R*)-**3.16** (*R*)-**3.17**

The azide (*R*)-**3.16** (0.1 g, 0.3 mmol) was dissolved in ethanol (15 mL) and after addition of 3 drops of HCl (conc.) and Pd/C (0.06 g), it was hydrogenated with shaking in a Parr apparatus at 3 bar for 4 h. The catalyst was removed by filtration over Celite® (moistened with ethanol) and the solvent was evaporated *in vacuo* to yield amine (*R*)-**3.17** (0.065 g, 0.29 mmol, 96%) of sufficient purity for the subsequent deprotection.

^{1}H NMR (400.27 MHz, d_4-methanol, [4Mar2119/150], TS 134): δ_H = 4.94-4.74 (m, 2H, CH *i*Pr), 3.98 (ABXP-system, A-part: ddd, J_{AB} = 11.6 Hz, J_{AX} = 3.9 Hz, J_{AP} = 4.0 Hz, 1H; B-part: ddd, J_{AB} = 11.6 Hz, J_{BX} = 8.2 Hz, J_{BP} = 5.6, CH_2CH-P), 3.58 (ddd, J_{XP} = 12.2 Hz, J_{XA} = 3.9 Hz, J_{XB} = 8.2 Hz, 1H, CH-P), 1.40 (d, *J* = 6.2 Hz, 3H, CH_3), 1.40 (d, *J* = 6.2 Hz, 3H, CH_3), 1.40 (d, *J* = 6.2 Hz, 3H, CH_3), 1.40 (d, *J* = 6.2 Hz, 3H, CH_3).

^{31}P NMR (162.03 MHz, d_4-methanol, [4Mar2119/151]): δ_P = 15.88 (s).

4.2.8 Synthesis of (*R*)-(1-amino-2-hydroxyethyl)phosphonic acid [(*R*)-**3.18**]

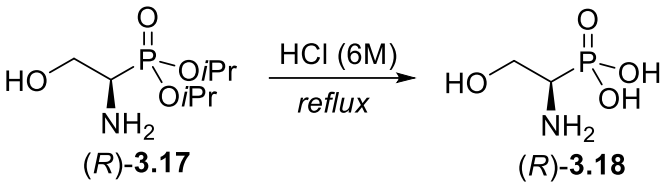

(*R*)-**3.17** (*R*)-**3.18**

The protected amine (*R*)-**3.17** (0.2 g, 0.89 mmol) was refluxed in HCl (10 mL, 6 M) for 8 h. The deprotected phosphonic acid (*R*)-**3.18** was purified by cation exchange chromatography on Dowex 50W × 8 H^+ (column diameter: 1 cm, height: 25 cm) with water as eluent. Ninhydrin positive fractions were pooled and concentrated *in vacuo*. Lyophilisation yielded (*R*)-**3.18** as a colorless solid.

^{1}H NMR (400.27 MHz, D_2O, [4Nov1518/620], TS 137): δ_H = 3.98 (ABXP-system, A-part: ddd, J_{AB} = 12.6 Hz, J_{AX} = 3.7 Hz, J_{AP} = 5.5 Hz, 1H; B-part: ddd, J_{AB} = 12.6 Hz, J_{BX} = 10.3 Hz, J_{BP} = 4.2, CH_2CH-P), 3.47 (ddd, J_{XP} = 13.8 Hz, J_{XA} = 3.7 Hz, J_{XB} = 10.3 Hz, 1H, CH-P).

^{13}C NMR (150.93 MHz, $CDCl_3$, [6Jun2519/90]): δ_C = 51.7 (s, CH-N), 50.8 (s, CH_2-O).

^{31}P NMR (162.04 MHz, D_2O, [4Nov1518/621]): δ_P = 9.71 (s).

Specific rotation: α_D^{20} = – 30.2 (*c* 0.75, H_2O) [lit.: = – 30.2 (c 1.27, H_2O] [88]

Melting range: mp = 95-110 °C (lit.: 95-110 °C) [88]

4.3 Synthesis of (*R*)-phosphacysteine

4.3.1 Synthesis of diisopropyl (2-(benzylthio)acetyl)phosphonate (3.32)

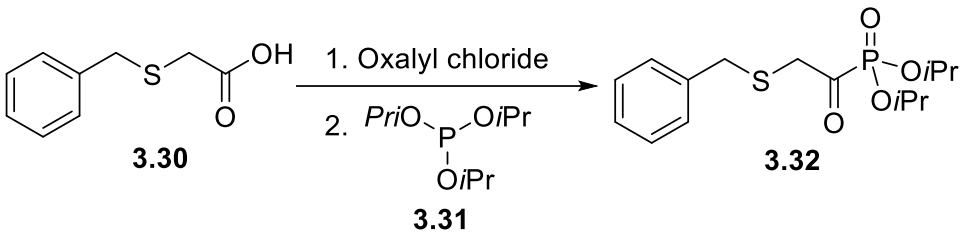

3.30 **3.31** **3.32**

Benzylmercaptoacetic acid (**3.30**, 0.91 g, 5 mmol), was dissolved in dry CH_2Cl_2 (10 mL) under Ar atmosphere. After dropwise addition of oxalyl chloride (0.69 g, 0.47 mL, 5.5 mmol), the reaction mixture was stirred at 35 °C for 5 h. The reaction progress was monitored using ^{1}H NMR [δ_H (starting material, acid proton) = 11.0 ppm]. After removing excess oxalyl chloride *in vacuo*, the obtained crude acyl chloride was purified by distillation *in vacuo* [b.p. 80-100 °C (0.3 mbar]. The purified acyl chloride was then dissolved in dry CH_2Cl_2 (10 mL) under Ar and cooled to 0 °C. The reaction mixture was allowed to warm up to room temperature in the cooling bath after dropwise addition of (iPrO)$_3$P (**3.31**, 1.04 g, 1.23 mL, 5 mmol) and stirring was continued for 3 h. After removal of the solvent, the crude ketophosphonate **3.32** was obtained in good yields (1.5 g, 4.5 mmol, 91%) and sufficient purity for the subsequent steps.

A small analytical sample of **3.32** was purified by crystallization from diisopropyl ether for characterization purposes giving the enol-form.

^{1}H NMR (400.27 MHz, $CDCl_3$, [4Mar2719/80], KS 1141): δ_H = 7.38 – 7.22 (m, 5H, CH_{arom}), 6.05 (d, J = 9.2 Hz 1H, C<u>H</u>=C-P), 5.41 (d, J = 18.7 Hz, O<u>H</u>), 4.64 – 4.52 (m, 2H, 2 × CH iPr), 3.89 (s, 2H, CH_2 Bn), 1.32 (d, J = 6.2, 6H, 2 × CH_3), 1.23 (d, J = 6.2, 6H, 2 × CH_3).

^{31}P NMR (162.03 MHz, D_2O, [4Jun1818/21], TS 33): δ_P = 6.01 (s, enol-form).

4.3.2 Synthesis of diisopropyl (*S*)-(2-(benzylthio)-1-hydroxyethyl)phosphonate [(*S*)-**3.33**]

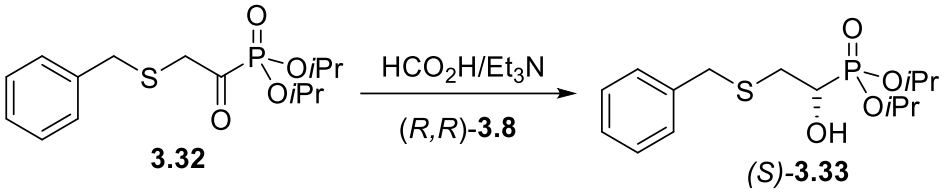

(*R,R*)-RuCl[(*p*-cymene)-TsDPEN] [(*R,R*)-3.7, 0.124 g, 0.19 mmol] was dissolved in CH_2Cl_2 (1 mL) and activated by addition of an aqueous KOH solution (1.1 mL, 0.18 M), whereupon the reaction mixture turned bright purple. The phases were separated and the aqueous layer was washed with CH_2Cl_2 (2 × 1 mL). The combined organic phases were dried (CaH_2) and filtered.

Meanwhile, formic acid (0.79 g, 0.58 mL, 17.16 mmol) was added dropwise to Et_3N (1.0 g, 1.41 mL, 10.14 mmol) under Ar atmosphere at 0 °Cand the resulting solution was stirred for 5 min.

The crude ketophosphonate **3.32** (1.3 g, 3.9 mmol) was dissolved in dry CH_2Cl_2 (10 mL) under Ar and the formic acid/Et_3N mixture was added, followed by the solution of the catalyst. The reaction mixture was stirred at 35 °C for 24 h. The crude product (R_f = 0.24, *n*-heptane : EtOAc = 1:1) was purified via MPLC using a solvent gradient (*n*-heptane/EtOAc, 12% → 100% EtOAc), to yield hydroxyphosphonate (*S*)-**3.33** (0.9 g, 2.7 mmol, 70%, ee ≥ 98%) as slightly reddish oil.

^{1}H NMR (400.27 MHz, $CDCl_3$, [4Jun2618/380], TS 36): δ_H = 7.34 – 7.19 (m, 5H, CH_{arom}), 4.79 – 4.66 (m, 2H, 2 × CH *i*Pr), 3.81 (ddd, J_{AX} = 2.8 Hz, J_{BX} = 10.7 Hz, J_{XP} = 6.8 Hz, 1H, CH-P), 3.75 (AB-System, J_{AB} = 13.5 Hz, 2H, CH_2 Bn), 2.77 (ABXP-System; A-Part: ddd, J_{AB} = 14.3 Hz, J_{AX} = 2.8 Hz, J_{AP} = 4.9 Hz; B-Part: ddd, J_{AB} = 14.3 Hz, J_{BX} = 10.7 Hz, J_{BP} = 10.8 Hz; 2H, C<u>H</u>$_2$-CH-P), 1.30 (d, *J* = 6.1, 3H, CH_3), 1.29 (d, *J* = 6.2, 6H, 2 × CH_3), 1.27 (d, *J* = 6.8, 3H, CH_3).

^{13}C NMR (150.93 MHz, $CDCl_3$, [6Aug0118/51], TS 36): δ_C = 137.81 (s, C_{arom}), 129.19 (s, 2 × CH_{arom}), 128.84 (s, 2 × CH_{arom}), 127.46 (s, CH_{arom}), 71.80 (d, *J* = 7.0 Hz, CH *i*Pr), 71.75 (d, *J* = 7.3 Hz, CH *i*Pr), 66.89 (d, *J* = 162.8 Hz, CH-P), 36.37 (s, CH Bn), 33.86 (d, *J* = 2.2 Hz, <u>C</u>H_2-CH-P), 24.10 (d, *J* = 8.8 Hz, CH_3), 24.33 (d, *J* = 8.8 Hz, CH_3), 24.20 (d, *J* = 7.2 Hz, CH_3), 24.17 (d, *J* = 7.3 Hz, CH_3).

^{31}P NMR (162.03 MHz, $CDCl_3$, [4Jun2618/381], TS 36): δ_P = 20.25 (s).

IR (ATR, TD1.3b): v = 2980, 2374, 2208, 1454, 1232, 988 cm^{-1}.

Specific rotation of (*S*)-**3.32:** α_D^{20}= + 35.8 (*c* 0.76, CH_2Cl_2).

NMR of (*S*)-3.32 with chiral solvating agent: δ_P (162.03 MHz, $CDCl_3$) 96.24 ($\int$ 1.14, chiral solvating agent), 20.42 [$\int$ 0.99, Complex of chiral solvating agent with (*S*)-**3.33**], 20.24 [$\int$ 0.01, Complex of chiral solvating agent with (*R*)-**3.33**] → ee ≥ 98%.

4.3.3 Synthesis of diisopropyl (*R*)-(1-azido-2-(benzylthio)ethyl)phosphonate and diisopropyl (*S*)-(2-azido-1-(benzylthio)ethyl)phosphonate [(*R*)-3.34a and (*S*)-3.34b]

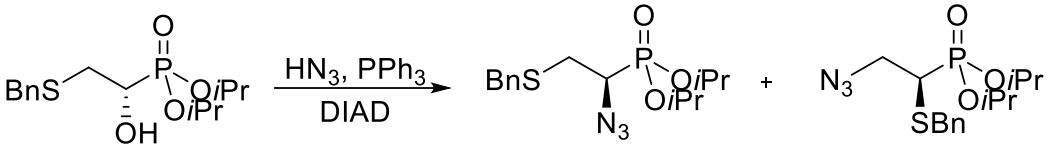

(*S*)-**3.33** (*R*)-**3.34a** (*S*)-**3.34b**

Triphenylphosphine (0.79 g, 3.04 mmol) and hydroxyphosphonate (*S*)-**3.33** (0.7 g, 2.1 mmol) were dissolved in dry THF and cooled to 0 °C under Ar atmosphere. Then, hydrazoic acid (1.54 mL, 3.04 mmol, 1.97 M in toluene) and DIAD (0.61 g, 0.59 mL, 3.04 mmol) were added simultaneously to the reaction mixture. After 10 min the cooling bath was removed and the solution was allowed to warm to r.t. Completion of the reaction was monitored by TLC [R_f (product)= 0.54, CH_2Cl_2 : Et_2O = 19:1]. After 18 h the reaction was quenched by addition of methanol (3 mL) and the solvent was removed *in vacuo.* The residue was purified by three subsequent MPLC runs with a solvent gradient (DCM : Et_2O, 7% → 20% Et_2O) to yield azide (*R*)-**3.34a** (0.42 g, 1.2 mmol, 57%) in admixture with its constitutional isomer (*S*)-**3.34b** (0.18 g, 0.5 mmol, 24%) as colorless oils.

(*R*)-**3.34a:**

^{1}H NMR (400.27 MHz, $CDCl_3$, [4Okt2218/600], TD 1.4b): δ_H = 7.37 – 7.21 (m, 5H, CH_{arom}), 4.79 – 4.65 (m, 2H, 2 × CH *i*Pr), 3.78 (AB-System; J_{AB} = 13,6 Hz, 2H, CH_2 Bn), 3.41 (ddd, J_{AX} = 2.7 Hz, J_{BX} = 11.7 Hz, J_{XP} = 12.5 Hz, 1H, CH-P), 2.73 (ABXP-System; A-Part: ddd, J_{AB} = 14.3 Hz, J_{AX} = 2.7 Hz, J_{AP} = 4.8 Hz; B-Part: ddd, J_{AB} = 14.3 Hz, J_{BX} = 11.7 Hz, J_{BP} = 6.4 Hz; 2H, C$\underline{H}_2$-CH-P), 1.31 (d, *J* = 6.1 Hz, 3H, CH_3), 1.30 (d, *J* = 6.2 Hz, 3H, CH_3), 1.29 (d, *J* = 6.0 Hz, 3H, CH_3), 1.28 (d, *J* = 6.2 Hz, 3H, CH_3).

^{13}C NMR (150.93 MHz, $CDCl_3$, [6Okt2518/61], TD 1.4b): δ_C = 137.96 (s, C_{arom}), 129.20 (s, 2 × CH_{arom}), 128.88 (s, 2 × CH_{arom}), 127.51 (s, CH_{arom}), 72.40 (d, *J* = 6.7 Hz, CH *i*Pr), 72.35 (d, *J* = 7.0 Hz, CH *i*Pr), 58.81 (d, *J* = 152.9 Hz, CH-P), 37.03 (s, CH_2 Bn), 31.27 (d, *J* = 2.3 Hz, $\underline{C}H_2$-CH-P), 24.37 (d, *J* = 3.7 Hz, CH_3), 24.30 (d, *J* = 3.6 Hz, CH_3), 24.17 (d, *J* = 5.1 Hz, CH_3), 24.14 (d, *J* = 5.0 Hz, CH_3).

^{31}P NMR (162.03 MHz, $CDCl_3$, [4Okt2218/601], TD 1.4b): δ_P = 17.43 (s).

HRMS calculated for $C_{15}H_{24}N_3O_3PS$ (357.13 g/mol): $[M+H]^+$ 358.13488, $[M+Na]^+$ 380.11682; found:$[M+H]^+$ 358.1348, $[M+Na]^+$ 380.1168.

IR (ATR, TD1.4b): v = 2979, 2098, 1454, 1385, 1302, 1247, 1104, 982 cm^{-1}.

Specific rotation of (*R*)-**3.34a:** α_D^{20} = – 59.2 (*c* 0.93, $CHCl_3$).

(*S*)-**3.34a** can be obtained similarly starting from (*R*)-**3-.33**. The spectroscopical data were in agreement to those obtained for the (*R*)-enantiomer.

Specific rotation of (*S*)-**2.4a:** α_D^{20} = + 55.1 (*c* 1.00, $CHCl_3$).

(*S*)-**3.34b**[1] (assigned tentatively):

^{1}H NMR (400.27 MHz, $CDCl_3$, [4Okt2318/180] , TD 1.4b 46-50): δ = 7.37 – 7.22 (m, 5H, CH_{arom}), 4.81 – 4.69 (m, 2H, 2 × CH *i*Pr), 4.05-3.91 (m, 2H, CH_2 Bn), 3.67 – 3.60 (m, 1H, CH-P), 3.45 – 2.69 (m, 2H, $C\underline{H}_2$-CH-P), 1.322 (d, *J* = 6.1 Hz, 3H, CH_3), 1.319 (d, *J* = 6.2 Hz, 3H, CH_3), 1.31 (d, *J* = 4.5 Hz, 3H, CH_3), 1.29 (d, *J* = 4.6 Hz, 3H, CH_3).

^{13}C NMR (150.93 MHz, $CDCl_3$, [6Dec1418/61], KS 1091): δ_C = 136.97 (s, C_{arom}), 129.31 (s, 2 × CH_{arom}), 128.61 (s, 2 × CH_{arom}), 127.44 (s, CH_{arom}), 72.11 (d, *J* = 7.2 Hz, CH *i*Pr), 71.70 (d, *J* = 7.3 Hz, CH *i*Pr), 51.66 (d, *J* = 2.9 Hz, $\underline{C}H_2$-CH-P), 40.39 (d, *J* = 148.3 Hz, CH-P), 36.96 (d, *J* = 3.1 Hz, CH_2 Bn), 24.20 (d, *J* = 3.3 Hz, CH_3), 24.10 (d, *J* = 3.7 Hz, CH_3), 23.90 (d, *J* = 5.3 Hz, CH_3), 23.81 (d, *J* = 5.5 Hz, CH_3).

^{31}P NMR (162.03 MHz, $CDCl_3$, [4Okt2318/181], TD 1.4b46-50): δ = 20.08 (s).

[1] Compound **3.34b** was never obtained in 100% purity. There were always traces of (*R*)-**3.34a** remaining in the sample, for which the relevant NMR signals can be found above.

Specific rotation of (*S*)-**3.34b:** α_D^{20} = – 32.91 (*c* 1.10, $CHCl_3$).

HRMS calculated for $C_{15}H_{24}N_3O_3PS$ (357.13 g/mol): $[M+H]^+$ 358.13488, $[M+Na]^+$ 380.11682; found:$[M+H]^+$ 358.1346, $[M+Na]^+$ 380.1167.

4.3.4 Synthesis of Benzyl-protected *tert*-butyl carbamate [(*R*)-3.35a]

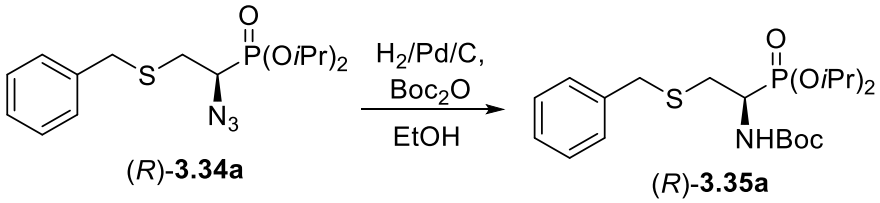

(*R*)-**3.34a** (*R*)-**3.35a**

A mixture of the azide (*R*)-**3.34a** (0.2 g, 0.56 mmol) with Pd/C (0.18 g) and di-*tert*-butyl-dicarbonate (0.16 g, 0.73 mmol) was dissolved in ethanol (30 mL) and the resulting reaction mixture was degassed. The reaction mixture was hydrogenated using a H_2-filled balloon for 24 h under continuous stirring. The catalyst was removed by filtration over Celite® and the solvent was evaporated *in vacuo* to obtain the crude product (*R*)-**3.35a** (R_f = 0.58, CH_2Cl_2 : Et_2O = 4:1). After purification via MPLC using a solvent gradient (CH_2Cl_2 : Et_2O, 7% → 40% Et_2O), the Boc-protected amine (*R*)-**3.35a** (0.2 g, 0.46 mmol, 83%) was obtained as a colorless oil.

^{1}H NMR (400.27 MHz, $CDCl_3$, [4Nov0718/40], TS B): δ_H = 7.36 – 7.17 (m, 5H, CH_{arom}), 4.77 – 4.58 (m, 3H, 2 × CH *i*Pr), 4.22 – 4.07 (m, 1H, CH-P), 3.73 (s, 2H, CH_2 Bn), 2.67 (ABXP-System; A-Part: ddd, J_{AB} = 14.1 Hz, J_{AX} = 3.8 Hz, J_{AP} = 7.1 Hz; B-Part: ddd, J_{AB} = 14.1 Hz, J_{BX} = 10.8 Hz, J_{BP} = 7.7 Hz; 2H, C<u>H</u>$_2$-CH-P), 1.45 (s, 9H, 3 × CH_3 Boc), 1.30 (d, J = 6.2, 3H, CH_3 *i*Pr), 1.27 (d, *J* = 5.8 Hz, 3H, CH_3 *i*Pr), 1.26 (d, *J* = 5.9 Hz, 3H, CH_3 *i*Pr), 1.23 (d, *J* = 6.2 Hz, 3H, CH_3 *i*Pr).

^{13}C NMR (150.93 MHz, $CDCl_3$, [6Nov1618/71], TD 7): δ_C = 137.96 (s, C_{arom}), 129.30 (s, 2 × CH_{arom}), 128.72 (s, 2 × CH_{arom}), 127.25 (s, CH_{arom}), 72.01 (d, *J* = 7.3 Hz, CH *i*Pr), 71.53 (d, *J* = 7.0 Hz, CH *i*Pr), 46.64 (d, *J* = 156.7 Hz, CH-P), 35.98 (s, CH_2 Bn), 32.47 (d, *J* = 7.4 Hz, <u>C</u>H$_2$-CH-P), 28.54 (s, 3 × CH_3 Boc), 24.42 (d, *J* = 3.1 Hz, CH_3), 24.27 (d, *J* = 3.4 Hz, CH_3), 24.11 (d, *J* = 4.6 Hz, CH_3), 24.00 (d, *J* = 4.7 Hz, CH_3).

^{31}P NMR (162.03 MHz, $CDCl_3$, [4Nov0718/41], TS B): δ_P = 21.13 (s).

4.3.5 Synthesis of deprotected *tert*-butyl carbamate [(*R*)-3.36a]

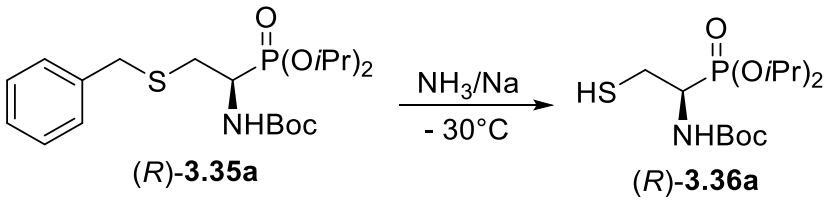

(*R*)-**3.35a** (*R*)-**3.36a**

Benzylthiocarbamate (*R*)-**3.35a** (0.285 g, 0.66 mmol), dissolved in dry Et_2O (3 mL), was added to liquid NH_3 (25 mL) at –30°C. Sodium metal (0.042 g, 1.83 mmol) was added in portions until a blue color persisted. The reaction was quenched by addition of NH_4Cl (0.087 g, 1.64 mmol) whereupon it became colorless again. Ammonia was allowed to evaporate in a fume hood to yield the desired mercaptocarbamate (*R*)-**3.36a** in sufficient purity for the final deprotection.

^{1}H NMR (400.27 MHz, d_4-methanol, [4Nov0818/190], TS 132): δ_H = 4.77-4.63 (m, 2H, 2 × CH *i*Pr), 4.02-3.88 (m, 1H, CH-P), 2.97-2.87 (m, 1H, $\underline{CH_2}$-CH-P), 2.73-2.61 (m, 1H, $\underline{CH_2}$-CH-P), 1.47 (s, 9H, 3 × CH_3 Boc), 1.36-1.30 (m, 12 H, 4 × CH_3).

^{31}P NMR (162.03 MHz, d_4-methanol, [4Nov0818/191]): δ_P = 20.96 (s).

4.3.6 Synthesis of (*R*)-(1-amino-2-mercaptoethyl)phosphonic acid [(*R*)-3.37a]

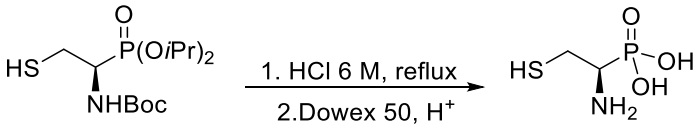

(*R*)-**3.36a** (*R*)-**3.37a**

The crude product (*R*)-**3.36a** was refluxed in HCl (10 mL, 6 M) for 8 h. The solvent was removed under reduced pressure and the residue was purified by cation exchange chromatography using Dowex 50W × 8 H^+ (column diameter: 1 cm, height: 24 cm) with water as eluent. Ninhydrin positive fractions were pooled and concentrated *in vacuo.* The solid residue was recrystallized from water/EtOH and dried by lyophilisation to yield the crystalline product (*R*)-**3.37a** (0.068 g, 0.43 mmol, 62% over two steps).

^{1}H NMR (600.25 MHz, D_2O, [6Nov0918/80], TD 9): δ_H = 3.35 (ddd, J_{AX} = 3.9 Hz, J_{BX} = 10.3 Hz, J_{XP} = 14.1, 1H, CH-P), 3.03 (ABXP-System; A-Part: ddd, J_{AB} = 14.9 Hz, J_{AX} = 3.9 Hz J_{AP} = 8.0 Hz; B-Part: ddd, J_{AB} = 14.9 Hz, J_{BX} = 10.3 Hz, J_{BP} = 6.9 Hz, 2H, C$\underline{H_2}$-CH-P).

^{13}C NMR (150.93 MHz, D_2O, [6Nov0918/81]): δ_C = 51.56 (d, *J* = 136.9 Hz, CH-P), 23.15 (s, $\underline{C}H_2$-CH-P).

^{31}P NMR (162.03 MHz, D_2O, [4Nov0918/461], TD 9): δ = 10.58 (s).

Specific rotation of (*R*)-**3.37a:** $[\alpha]_D^{20}$ = – 58.5 (*c* 0.545, H_2O).

HRMS calculated for $C_2H_8NO_3PS$ (166.00 g/mol): $[M–H]^-$ 155.98897, found: $[M–H]^-$ 155.9893

Melting range: m.p. = 245-248 °C (decomp.).

Compound (*S)*-**3.37b** was isolated after elution of the ion exchange column with formic acid (2 %). Ninhydrine positive fractions were pooled and treated as described for (*R*)-**3.37a**. However, only small fractions of the unwanted regioisomer were obtained and the purity was not sufficient for characterization.

4.4 Synthesis of deuterated phosphaisoserine {(*R*)-1-[$^2H_1$]-**3.44**}

4.4.1 Synthesis of 1-[$^2H_1$] formic acid {1-[$^2H_1$]-**4.5**} [105]

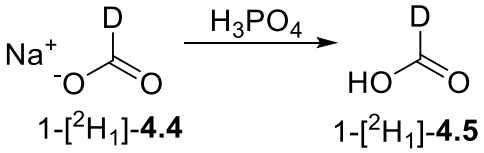

1-[$^2H_1$]-**4.4** 1-[$^2H_1$]-**4.5**

Deuterated sodium formate (1-[$^2H_1$]-**4.4**, 3 g, 44.11 mmol) was melted together with phosphoric acid (99%, 25 g, 257.73 mmol) at 45 °C in a distillation apparature. Afterwards the reaction mixture was heated to 70 °C *in vacuo* (0.3 mbar) whereupon distillation of formic acid occured. Formic acid was collected at –196 °C and heating was continued for 2 h until no further distillation of deuterated formic acid was observed. The pure deuterated formic acid ([$^2H_1$]-**4.5**, 1.4 g, 30.43 mmol, 69%) was obtained as colorless liquid.

^{1}H NMR (600.25 MHz, $CDCl_3$, [6Sep0518/30], TS 81): δ_H = 8.20 (s, C(O)OH).

^{13}C NMR (150.93 MHz, $CDCl_3$, [6Sep0518/31]): δ_C = 165.46 (t, C(O)OH).

4.4.2 Synthesis of 2-phthalimidoacetic acid (**3.40**) [106]

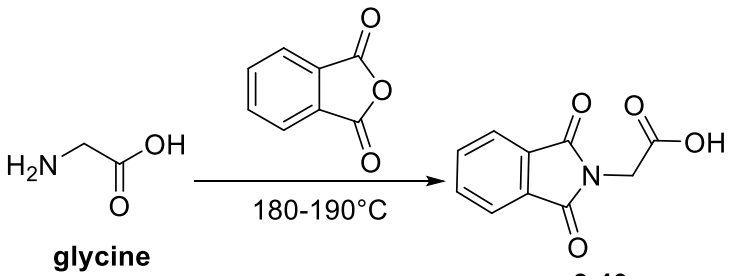

glycine **3.40**

A mixture of glycine (7.5 g, 100 mmol) and phthalic anhydride (15.1 g, 102 mmol) was heated to 190 °C, whereupon the mixture solidified and was subsequently cooled down to room temperature again. The solid product was recrystallized from water to yield phthalyl-protected glycine (**3.40**, 16 g, 78 mmol, 78%) as slightly brownish crystals.

^{1}H NMR (400.27 MHz, *d_6*-dimethyl sulfoxide, [4Jun2218/481], TS 37): δ_H = 8.39-8.32 (m, 4H, CH_{arom}), 4.87 (s, 1H, CH_2), 3.68 (s, 1H, C(O)OH).

4.4.3 Synthesis of 2-phthalimodoacetyl chloride (3.40) [106]

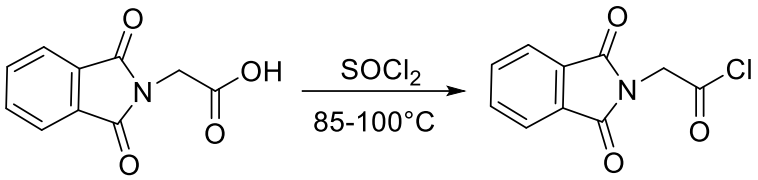

3.40 **3.41**

3.40 (16 g, 78 mmol) was refluxed with $SOCl_2$ (68.78 g, 41.94 mL, 578 mmol) at 100 °C for 2 h. After cooling to room temperature, excess $SOCl_2$ was removed *in vacuo* and the crude product was crystallized from *n*-heptane/toluene to yield the acyl chloride **3.41** (14 g, 62.61 mmol, 80%).

^{1}H NMR (400.27 MHz, $CDCl_3$, [4Jun2518/200], TS 37): δ_H = 7.93-7.87 (m, 2H, CH_{arom}), 7.80-7.74 (m, 2H, CH_{arom}), 4.80 (s, 2H, CH_2).

4.4.4 Synthesis of diisopropyl 1-oxo-2-phthalimidoethyl phosphonate (3.42) [106]

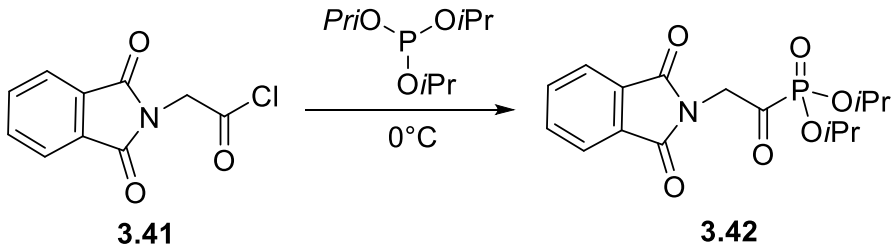

3.41 **3.42**

The acyl chloride **3.41** (11.2 g, 50 mmol) was dissolved in dry CH_2Cl_2 under argon atmosphere and cooled to 0 °C. After addition of triisopropyl phosphite (10.9 g, 13.45 mL, 52.2 mmol), the cooling bath was removed and the reaction mixture was allowed to warm to room temperature. Stirring was continued for 2 h until the ^{1}H NMR showed complete consumption of the starting material. The solvent was removed *in vacuo* and the crude product was taken up in *n*-heptane, whereupon it crystallized. The solution was heated up and diisopropyl ether was added until the solution became clear. The ketophosphonate **3.42** (14.5 g, 41 mmol, 82%) was collected by filtration as slightly yellowish crystals.

^{1}H NMR (400.27 MHz, $CDCl_3$, [4Jun2718/300], TS 40): δ_H = 7.88-7.83 (m, 2H, CH_{arom}), 7.75-7.70 (m, 2H, CH_{arom}), 4.88 (d, *J* = 3.6 Hz, 1H, CH_2), 4.82 (sept, *J* = 6.2 Hz, 1H, CH *i*Pr), 4.80 (sept, *J* = 6.0 Hz, 1H, CH *i*Pr), 1.38 (d, *J* = 6.2 Hz, 6H, 2 × CH_3), 1.37 (d, *J* = 6.2 Hz, 6H, 2 × CH_3).

^{31}P NMR (162.03 MHz, $CDCl_3$, [4Jun2718/301]): δ = – 5.84 (s).

4.4.5 Synthesis of diisopropyl (*R*)-1-[$^{2}H_1$]-1-hydroxy-2-phthalimido)-ethylphosphonate {(*R*)-1-[$^{2}H_1$]-**3.43**} [106]

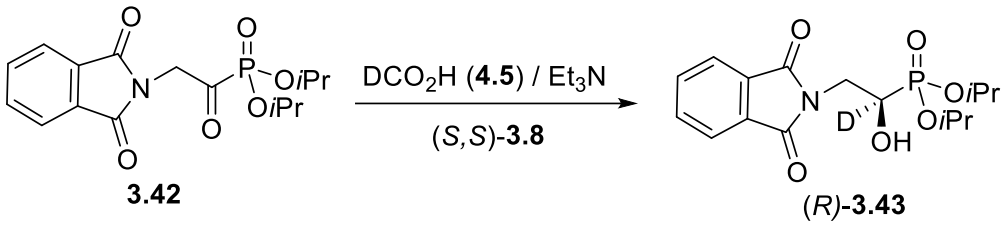

3.42 (*R*)-**3.43**

(*S,S*)-RuCl[(*p*-cymene)-TsDPEN] [(*S,S*)-**3.7**, 0.053 g, 0.083 mmol] was dissolved in CH_2Cl_2 (1 mL) and activated by addition of an aqueous KOH solution (0.46 mL, 0.18 M), whereupon the reaction mixture turned bright purple. The phases were separated and the aqueous layer was washed with CH_2Cl_2 (2 × 1 mL). The combined organic phases were dried (CaH_2) and filtered.

Meanwhile, deuterated formic acid (**4.5**, 0.25 g, 0.21 mL, 5.45 mmol) was added dropwise to Et_3N (0.55 g, 0.76 mL, 5.45 mmol) under Ar atmosphere at 0 °Cand the resulting solution was stirred for 5 min. The crude ketophosphonate **3.42** (0.74 g, 2.1 mmol) was dissolved in dry CH_2Cl_2 (10 mL) under Ar and the deuterated formic acid/Et_3N mixture was added, followed by the solution of the catalyst. The reaction mixture was stirred at 35 °C for 18 h. The crude product (R_f = 0.24, *n*-heptane : EtOAc = 1:1) was purified via MPLC using a solvent gradient (*n*-heptane/EtOAc, 12% → 100% EtOAc), to yield the desired deuterated hydroxyphosphonate (*R*)-1-[$^{2}H_1$]-**3.43** (0.58 g, 1.63 mmol, 78%) as a white powder.

^{1}H NMR (400.27 MHz, $CDCl_3$, [4Oct0318/20], TS 82): δ_H = 7.86-7.81 (m, 2H, CH_{arom}), 7.72-7.67 (m, 2H, CH_{arom}), 4.81-4.69 (m, 2H, CH *i*Pr), 4.03 (ABP-System; A-Part: dd, J_{AB} = 14.5 Hz, J_{AP} = 7.4 Hz; B-Part: dd, J_{AB} = 14.5 Hz, J_{BP} = 7.0 Hz, 2H, $C\underline{H}_2$-CD-P), 3.26 (s, 1H, OH), 1.35 (d, *J* = 6.2 Hz, 3H, CH_3), 1.314 (d, *J* = 6.2 Hz, 3H, CH_3), 1.312 (d, *J* = 6.2 Hz, 3H, CH_3), 1.29 (d, *J* = 6.2 Hz, 3H, CH_3).

^{31}P NMR (162.03 MHz, $CDCl_3$, [4Oct0318/21]): δ = – 5.84 (s).

4.4.6 Synthesis of (*R*)-1-[$^2H_1$]-2-amino-1-hydroxyethylphosphonic acid {(*R*)-1-[$^2H_1$]-**3.45**}

[106]

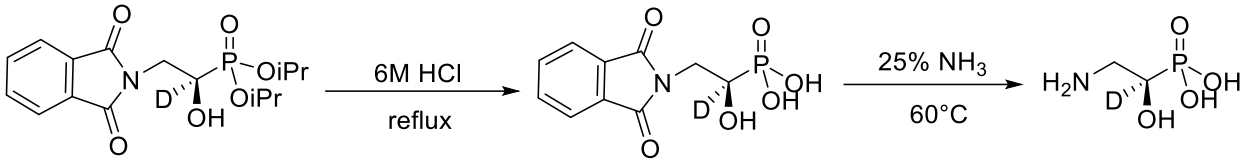

(*R*)-1-[$^2H_1$]-**3.43** (*R*)-1-[$^2H_1$]-**3.44** (R)-1-[$^2H_1$]-**3.45**

The hydroxyphosphonate (*R*)-1-[$^2H_1$]-**3.43** (0.86 g, 2.42 mmol) was dissolved in 30 mL HCl (6M) and refluxed for 18 h. After removing excess HCl by evaporation with water, the residue was taken up in an aqueous NH_3 solution (20 mL, 25 %) and stirred at 60 °C for 24 h with a condenser attached to the reaction flask. Ammonia was removed *in vacuo*, the residue was taken up in water and extracted with EtOAc. The crude product was purified by cation exchange chromatography over Dowex 50W × 8 H^+ (column diameter: 1 cm, height: 35 cm) with water as eluent. The ninhydrin positive fractions were pooled and concentrated *in vacuo.* The remaining solid was recrystallized from water/EtOH to yield pure (*R*)- 1-[$^2H_1$]-2-amino-1-hydroxyethylphosphonic acid ((*R*)-1-[$^2H_1$]-**3.45**, 0.32g, 2.22 mmol, 92%).

^{1}H NMR (400.27 MHz, $CDCl_3$, [4May1619/340], TS 162): δ_H = 3.31 (ABP-System; A-Part: dd, J_{AB} = 13.35 Hz, J_{AP} = 6.6 Hz; B-Part: dd, J_{AB} = 13.35 Hz, J_{BP} = 6.5 Hz, 2H, C$\underline{H}_2$-CD-P).

^{31}P NMR (162.03 MHz, $CDCl_3$, [4Oct0318/21]): δ = 15.00 (s).

Specific rotation of (*R*)-**3.44:** α_D^{20} = – 30.6 (*c* 0.51, H_2O).

Spectroscopic data was in agreement to those reported in the literature. [107]

4.5 Attempted synthesis of (*R*)-*N*-(*sec*-butyl)-1-(2-chloropyridin-3-yl)-*N*-methyl-2,6-naphthyridine-3-carboxamide [(*R*)-**3.55**]

4.5.1 Synthesis of (*Z*)-3-(2-nitroprop-1-en-yl)pyridine [(*Z*)-**3.57**] [99]

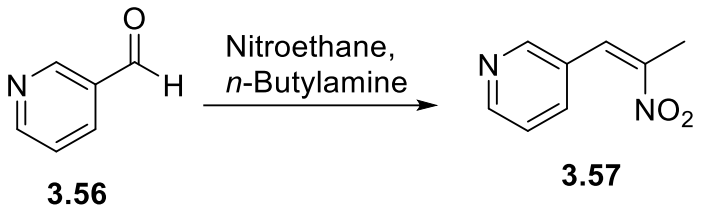

3.56 **3.57**

Nicotinic aldehyde (**3.56**, 10.7 g, 9.38 mL, 100 mmol) was refluxed with nitroethane (7.5 g, 7.14 mL, 100 mmol) and *n*-butylamine (0.37 g, 0.5 mL, 5 mmol) for 6 days at 120°C. After evaporating the solvent, the crude product was purified by flash column chromatography [R_f (product) = 0.38, CH_2Cl_2 : acetone = 19 : 1] to yield the desired nitropyridine **3.57** (13.8 g, 84.12 mmol, 84%). [108]

^{1}H NMR (400.27 MHz, $CDCl_3$, [4Oct0318/80], TS 95): δ_H = 8.67 (d, *J* = 1.9 Hz, 1H, N-CH_{arom}), 8.63 (dd, J = 4.8 Hz, *J* = 1.6 Hz, 1H, N-CH_{arom}), 8.01 (s, 1H, CH), 7.72 (ddd, *J* = 7.9 Hz, J = 1.6 Hz, *J* = 1.9 Hz, 1H, CH_{arom}), 7.38 (ddd, *J* = 7.9 Hz, J = 4.8 Hz, *J* = 0.4 Hz, 1H, CH_{arom}), 2.44 (d, *J* = 1.0 Hz, 3H, CH_3).

Spectroscopic data were in agreement to those reported in the literature. [99]

4.5.2 Synthesis of 1-(pyridin-3-yl)propan-2-amine (**3.58**) [99]

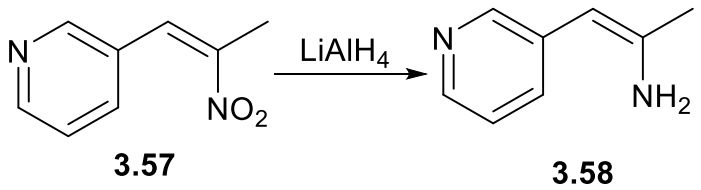

3.57 **3.58**

The nitropyridine **3.57** (0.5 g, 3.05 mmol) was dissolved in dry THF (20 mL) and cooled to 0 °C under Ar atmosphere. After careful addition of $LiAlH_4$ solution (9.15 mL, 1 M in THF), the reaction mixture was allowed to warm to r.t. The reaction was quenched with H_2O after 2 h of monitoring the reaction progress by ^{1}H NMR [δ_H (product) = 3.13, 2.69 ppm; δ_H (side product) = 3.00, 2.59 ppm]. The reaction mixture was filtered over Celite® and the solvent was removed *in vacuo*. The

crude product was purified by flash column chromatography [R_f (product) = 0.1, 4% conc. NH_3 in EtOH] to yield the desired amine **3.58** (0.25 g, 1.84 mmol, 60%) as colorless oil.

^{1}H NMR (400.27 MHz, d_4-methanol, [4Oct2918/430], TS 125): δ_H = 8.40 (d, *J* = 1.7 Hz, 1H, N-CH_{arom}), 8.39 (dd, *J* = 4.8 Hz, J = 1.6 Hz, 1H, N-CH_{arom}), 7.71 (ddd, *J* = 7.8 Hz, J = 1.7 Hz, *J* = 1.6 Hz, 1H, CH_{arom}), 7.38 (ddd, *J* = 7.8 Hz, *J* = 4.8 Hz, *J* = 0.5 Hz, 1H, CH_{arom}), 3.13 (ABX-system, J_{AX} = 6.7 Hz, J_{BX} = 6.8 Hz, 1H, N-CH), 2.69 (ABX-system, A-part: dd, J_{AB} = 13.5 Hz, J_{AX} = 6.7 Hz, 1H; B-part: dd, J_{AB} = 13.5 Hz, J_{BX} = 6.8 Hz, CH_2CH-N), 1.08 (d, *J* = 6.4 Hz, 3H, CH_3).

4.5.3 Synthesis of 2-chloro-*N*-(1-(pyridin-3-yl)propan-2-yl)nicotinamide (3.60)

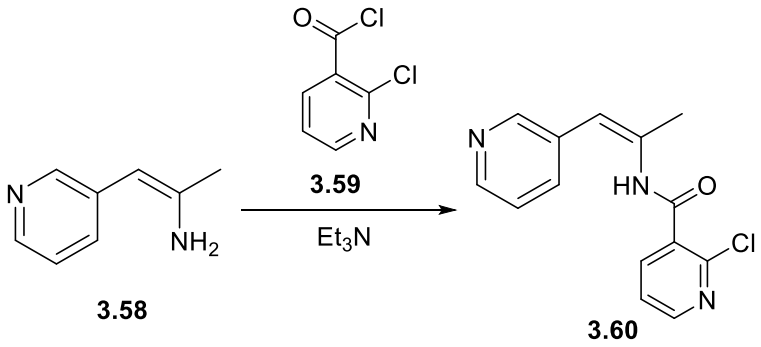

2-Chloronicotinoyl chloride (**3.59**, 0.32 g, 1.84 mmol) was dissolved in dry CH_2Cl_2 under Ar atmosphere and the amine **3.58** (0.25 g, 1.84 mmol) was added to the solution. After dropwise addition of Et_3N (0.56 g, 0.77 mL, 5.52 mmol), the reaction was stirred at 35 °C for 2 days and the reaction progress was monitored by ^{1}H NMR [δ_H (product) = 2.9 ppm]. The reaction mixture was concentrated *in vacuo* and purified by MPLC using a solvent gradient (EtOAc/MeOH, 0% → 2% methanol) to yield the amide **3.60** (0.26 g, 0.94 mmol, 51%) as colorless crystals. [109]

^{1}H NMR (400.27 MHz, $CDCl_3$, [4Oct0318/80], TS 123): δ_H = 8.46 (dd, *J* = 4.8, *J* = 1.7 Hz, 1H, N-CH_{arom1}), 8.44 (d, *J* = 1.9 Hz, 1H, N-CH_{arom2}), 8.41 (dd, *J* = 4.8, J = 1.9, 1H, Cl-C-N-CH_{arom1}), 7.96 (dd, *J* = 7.6 Hz, *J* = 1.9 Hz, 1H, CH_{arom1}) 7.59 (ddd, *J* = 7.8 Hz, J = 1.9 Hz, *J* = 1.9 Hz, 1H, CH_{arom2}), 7.29 (dd, *J* = 7.6 Hz, *J* = 4.8 Hz, 1H, CH_{arom2}), 7.23 (ddd, *J* = 7.8 Hz, *J* = 4.8 Hz, *J* = 0.5 Hz, 1H, CH_{arom1}), 6.38 (d, *J* = 7.4 Hz, 1H, NH), 4.52-4.41 (m, 1H, NH-CH), 2.90 (ABX-system, A-part: dd, J_{AB} = 13.8 Hz, J_{AX} = 6.5 Hz, 1H; B-part: dd, J_{AB} = 13.8 Hz, J_{BX} = 6.9 Hz, CH_2C-N), 1.26 (d, *J* = 6.7 Hz, 3H, CH_3).

^{13}C NMR (150.93 MHz, *d_6*- dimethyl sulfoxide, [6Dec0718/11]): δ_C = 164.22 (s, 1C, C=O), 150.27 (s, 1C, N-CH_{arom1}), 150.02 (s, 1C, N-CH_{arom2}), 147.40 (s, 1C, N-CH_{arom1}), 146.39 (s, 1C, C_{arom2}), 137.65 (s, 1C, CH_{arom2}), 136.65 (s, 1C, C_{arom2}), 134.23 (s, 1C, CH_{arom1}),133.33 (s, 1C, CH_{arom2}), 123.27 (s, 1C, CH_{arom1}), 122.99 (s, 1C, C_{arom1}), 46.16 (s, 1C, N-CH), 38.50 (s, 1C, CH_2), 20.14 (s, 1C, CH_3).

HRMS calculated for $C_{14}H_{14}ClN_3O$ (275.08 g/mol): $[M+H]^+$ 276.7435, $[M+Na]^+$ 298.7252; found:$[M+H]^+$ 276.0895, $[M+Na]^+$ 298.0705.

IR (ATR, TS 53): v = 3402, 3210, 1708, 1581, 1548, 1425, 1361, 1223, 1170, 1070, 702, 620 cm^{-1}.

5. Abstracts

5.1 English Abstract

This master thesis deals with the synthesis of different compounds, which have a high potential for future applications in medicine as well as in the chemical industry. The thesis can be divided into two main chapters.

The first chapter deals with the synthesis of α-aminophosphonates, having a potential as future mechanism-based enzyme inhibitor drugs. Furthermore, they can be used as substrates for biochemical studies on the enzymatic steps involved in the biodegradation of phosphonates. I could successfully synthesize the α-aminophosphonic acid analogs to the proteinogenic amino acids serine and cysteine: (*R*)-(1-amino-2-hydroxyethyl)phosphonic acid [(*R*)-**3.18**] and (*R*)-(1-amino-2-mercaptoethyl)phosphonic acid [(*R*)-**3.39a**]. These compounds could be synthesized by slightly adapting the same general synthetic procedure. Currently it is optimized to enable the synthesis of all phosphonic acid analogues to the 21 proteinogenic α-aminophosphonates as pure enantiomers. The key steps of this route include a Noyori type transfer-hydrogenation of an α-oxophosphonate to an α-hydroxyphosphonate and a subsequent substitution of the hydroxyl-group by an azide in a Mitsunobu reaction under inversion of configuration. In case of (*R*)-(1-amino-2-mercaptoethyl)phosphonic acid, this is the first non-racemic synthesis to be reported. It could be accomplished by using an alternative deprotection step (Birch reduction).

An adaption of this method using deuterated formic acid further made (*R*)-1-[$^{2}H_{1}$]-2-amino-1-hydroxyethylphosphonic acid {(*R*)-1-[$^{2}H_{1}$]-**3.45**} easily accessible in the same number of steps as its non-deuterated analogue.

The second chapter of this work was dealing with the synthesis of a novel TSPO ligand: (*R*)-*N*-(*sec*-butyl)-1-(2-chloropyridin-3-yl)-*N*-methyl-2,6-naphthyridine-3-carboxamide[(*R*)-**3.55**]. This compound is a potential TSPO ligand with a possible future application in PET diagnosis of TSPO-related neurodegenerative diseases. It is anticipated to have a better binding behavior compared to other TSPO ligands. The presence of an additional pyridine ring, will hopefully lower the lipophilicity of the tracer considerably. However, this additional nitrogen-atom made the design

and development of a completely new synthetic pathway necessary. (A Heck reaction cannot be used successfully here). The new approach relied on a Bischler-Napieralski reaction for ring closure. However, this approach did not lead to the desired product. In order to overcome these difficulties another completely new synthesis approach has already been developed and will be tested soon.

5.2 Deutsche Zusammenfassung

Im Zuge dieser Masterarbeit wurden verschiedene Verbindungen hergestellt, welche ein enormes Potential für zukünftige Anwendungen sowohl im medizinischen Feld als auch in der Industrie haben. Die Arbeit kann in zwei Themenschwerpunkte unterteilt werden.

Zum einen wurde an der Synthese von chiralen α-Aminophosphonaten, die großes Potential als zukünftige mechanismus-basierte Enzyminhibitoren haben gearbeitet. Ein mögliches Anwendungsgebiet für diese Verbindungen ist als Substrate für biochemische Studien zur Erforschung des enzymkatalisierten Phosphatabbaus. Es war mir möglich die α-Aminophosphonsäureanaloga der proteinogenen Aminosäuren Serin und Cystein herzusellen: (*R*)-(1-amino-2-hydroxyethyl)phosphonsäure [(*R*)-**3.18**] und (*R*)-(1-amino-2-mercaptoethyl)phosphonsäure [(*R*)-**3.37a**]. Diese Verbindungen konnten mithilfe eines leicht modifizierten Syntheseschemas, zur Herstellung der Analoga der 21 proteinogenen Aminosäuren in enantiomerenreiner Form, erhalten werden. Die Schlüsselschritte dieser Syntheseroute beinhalten eine Noyori Transferydrierung eines α-Oxophosphonats zu einem α-Hydroxyphosphonat und in weiterer Folge eine Mitsunobu Reaktion mit Substitution der Hydroxylgruppe durch ein Azid, wodurch eine Inversion der Konfiguration erfolgt.

Im Falle der (*R*)-(1-Amino-2-mercaptoethyl)phosphonsäure [(*R*)-**3.37a**] war es die erste nicht-racemische Synthese dieser Verbindung. Diese wurde durch einen alternativen Entschützungsschritt (Birch reduktion) möglich.

Des Weiteren war es mit dieser Methode möglich, unter Verwendung deuterierter Ameisensäure (*R*)-1-[$^{2}H_{1}$]-2-Amino-1-hydroxyethylphosphonsäure {(*R*)-1-[$^{2}H_{1}$]-**3.45**} in der gleichen Anzahl an Schritten herzustellen wie ihr nicht-deuteriertes Analogon.

Der zweite Teil dieser Arbeit beschäftigt sich mit der Synthese eines neuen TSPO Liganden: (*R*)-*N*-(*sec*-butyl)-1-(2-chloropyridin-3-yl)-*N*-methyl-2,6-naphthyridine-3-carboxamide[(*R*)-**3.56**].
Dieser hat Potential als zukünftiger PET Tracer in der Diagnostik verschiedenster neurodegerativer Erkrankungen. Dieser neue Ligand sollte ein verbessertes Bindungsverhalten zu TSPO zeigen als bisher etablierte Liganden. Ein weiterer Pyridinring soll zu niedrigerer Lipophilie führen. Allerdings erfordert der zusätzliche Stickstoff in einem der Ringe die Entwicklung eines komplett neuen Synthesewegs (Es ist keine Heck Reaktion mit Pyridinringen möglich). Im neuen Syntheseplan sollte der Ringschluss mittels Bischler-Napieralski Reaktion erfolgen. Da diese Reaktion es nicht möglich machte das gewünschte Produkt zu erhalten, wurde ein ganz neuer Syntheseweg entwickelt, welcher bald getestet werden kann.

7. References

[1] K. Ashley, D. Cordell and D. Mavinic, "A brief history of phosphorus: From the philosopher's stone to nutrient recovery and reuse," *Chemosphere,* vol. 84, no. 6, pp. 737-746, 2011.

[2] D. Corbridge, Phosphorus: Chemistry, Biochemistry and Technology, FL: Taylor & Francis Group, 2013.

[3] B.-M. M. and A. M., Basic and Clinical Toxicology of Organophosphorus Compounds, London: Springer, 2014.

[4] J. W. McGrath, J. P. Chin and J. P. Quinn, "Organophosphonates revealed: new insights into the microbial metabolism of ancient molecules," *Nature Reviews Microbiology,* vol. 11, no. 6, pp. 412-419, 2013.

[5] M. Horiguchi and M. Kandatstu, "Isolation of 2-Aminoethane Phosphonic Acid from Rumen Protozoa," *Nature,* vol. 184, pp. 901-902, 1959.

[6] T. O. Rogers and J. Birnbaum, "Biosynthesis of Fosfomycin by Streptomyces fradiae," *Antimicrobial Agents and Chemotherapy,* vol. 5, pp. 121-132, 1974.

[7] D. Hendlin, E. Stapley, M. Jackson, H. Wallick, A. K. Miller, F. J. Wolf and S. Mochales, "Phosphonomycin, a New Antibiotic Produced by Strains of Streptomyces," *Science,* vol. 166, p. 122–123., 1969.

[8] D. s. M. Mazzacurati, "Advanced Studies on the Synthesis of Organophosphorus Compounds (Doctoral dissertation)," Universita di Bologna.

[9] W. W. Metcalf and W. A. van der Donk, "Biosynthesis of Phosphonic and Phosphinic Acid Natural Products," *Annual Review of Biochemistry,* vol. 78, no. 1, pp. 65-94, 2009.

[10] K.-S. J. et al, "Discovery of phosphonic acid natural products by mining the genomes of 10,000 actinomycetes," *PNAS,* vol. 112, no. 39, pp. 12175-12180, 2015.

[11] G. P. Horsman and D. L. Zechel, "Phosphonate Biochemistry," *Chemical Reviews,* vol. 117, p. 5704−5783, 2017.

[12] D. Schwartz, S. Berger, E. Heinzelmann, K. Muschko, K. Welzel and W. Wohlleben, "Biosynthetic Gene Cluster of the Herbicide Phosphinothricin Tripeptide from Streptomyces viridochromogenes Tü494 Tripeptide from Streptomyces viridochromogenes Tu¨494," *Applied and Environmental Microbiology,* p. 7093–7102, 2004.

[13] D. D. Schoepp and B. G. Johnson, "Inhibition of Excitatory Amino Acid-Stimulated Phosphoinositide Hydrolysis in the Neonatal Rat Hippocampus by 2-Amino-3-Phosphonopropionate," *Journal of Neurochemistry,* vol. 53, pp. 1865-1870, 1989.

[14] F. Orsini, G. Sello and M. Sisti, "Aminophosphonic Acids and Derivatives. Synthesis and Biological Applications," *Current Medicinal Chemistry,* vol. 17, pp. 264-289, 2010.

[15] F. M. Kahan, J. S. Kahan, P. J. Cassidy and H. Kropp, "The mechanism of action of fosfomycin," *Annals of the New York Academy of Sciences,* vol. 235, pp. 364-386, 1974.

[16] M. E. Falagas, E. K. Vouloumanou, G. Samonis and K. Z. Vardakasa, "Fosfomycin," *Clinical Microbiology Reviews,* vol. 29, no. 2, pp. 321-347, 2016.

[17] L. L. Silver, "Fosfomycin: Mechanism and Resistance," *Cold Spring Harbor Perspectives in Medicine,* vol. 7, no. 2, pp. 1-11, 2017.

[18] G. Hoerlein, "Glufosinate (Phosphinothricin), A Natural Amino Acid with Unexpected Herbicidal Properties," *Reviews of Environmental Contamination and Toxicology,* vol. 138, p. 73–145, 1994.

[19] C. Wendler and A. Wild, "Effect of Phosphinothricin (Glufosinate) on Photosynthesis and Photorespiration," *Zeitschrift Für Naturforschung,* vol. 45, no. 5, p. 535–537, 1990.

[20] M. Drath, N. Kloft, A. Batschauer, K. Marin, J. Novak and K. Forchhammer, "Ammonia Triggers Photodamage of Photosystem II in the Cyanobacterium Synechocystis sp. Strain PCC 6803," *PLANT PHYSIOLOGY,* vol. 147, no. 1, p. 206–215, 2008.

[21] W. M. Kazmierski, Antiviral Drugs: From Basic Discovery Through Clinical Trials, John Wiley & Sons, 2011.

[22] B. P. Kearney, J. F. Flaherty and J. Shah, "Tenofovir Disoproxil Fumarate," *Clinical Pharmacology and Pharmacokinetics,* vol. 43, no. 9, p. 595–612, 2004.

[23] E. D. Clercq and A. Holý, "Acyclic Nucleoside Phosphonates: A Key Class of Antiviral Drugs," *Nature Reviews,* vol. 4, pp. 928-940, 2005.

[24] A. Hörnberg, A.-K. Tunemalm and F. Ekström, "Crystal Structures of Acetylcholinesterase in Complex with Organophosphorus Compounds Suggest that the Acyl Pocket Modulates the Aging Reaction by Precluding the Formation of the Trigonal Bipyramidal Transition State," *Biochemistry,* vol. 46, pp. 4815-4825, 2007.

[25] P. A. Lamden and L. A. Bartlett, "Inhibition of Chymotrypsin by Phosphonate and Phosphonamidate Peptide Analogs," *Bioorganic Chemistry,* vol. 14, pp. 356-377, 1986.

[26] J. Balzarini, A. Ford, N. Maguire, J. John, K. Das, E. Arnold, W. Dehaen and A. Maguire, "Alpha-carboxynucleoside phosphonates: direct-acting inhibitors of viral DNA polymerases," *Future Medicinal Chemistry,* vol. 11, no. 2, 2019.

[27] D. Bartee, S. Sanders, P. D. Phillips, M. J. Harrison, A. T. Koppisch and C. L. F. Meyers, "Enamide Prodrugs of Acetyl Phosphonate Deoxy-d-xylulose-5-phosphate Synthase Inhibitors as Potent Antibacterial Agents," *ACS Infectious Diseases,* vol. 5, no. 3, pp. 406-417, 2019.

[28] H. Ohtake, H. Wu, K. Imazu, Y. Anbe, J. Kato and A. Kuroda, "Bacterial phosphonate degradation, phosphite oxidation and polyphosphate accumulation," *Resources, Conservation and Recycling,* vol. 18, pp. 125-134, 1996.

[29] L. L. Clark, E. D. Ingall and R. Benner, "Marine phosphorus is selectively remineralized," *Nature,* vol. 393, no. 4, pp. 426-427, 1998.

[30] J. W. McGrath and J. P. Quinn, "Expression of the Phosphonoalanine-Degradative Gene Cluster From Variovorax Sp. Pal2 Is Induced by Growth on Phosphonoalanine and Phosphonopyruvate. FEMS," *Microbiology Letters,* vol. 292, p. 100−106, 2009.

[31] J. M. La Nauze, J. R. Coggins and H. B. Dixon, "Aldolase-Like Imine Formation in the Mechanism of Action of Phosphonoacetaldehyde Hydrolase," *Biochemical Journal,* vol. 165, p. 409−411, 1977.

[32] A. S. Baker, M. J. Ciocci, W. W. Metcalf, J. Kim, P. C. Babbitt, B. L. Wanner, B. M. Martin and D. Dunaway-Mariano, "Insights into the Mechanism of Catalysis by the P−C Bond-Cleaving Enzyme Phosphonoacetaldehyde Hydrolase Derived from Gene Sequence Analysis and Mutagenesis," *Biochemistry,* vol. 37, no. 9, pp. 305-315, 1998.

[33] J. F. Villarreal-Chiu, J. P. Quinn and J. W. McGrath, "The Genes and Enzymes of Phosphonate Metabolism by Bacteria, and Their Distribution in the Marine Environment," *Frontiers in Microbiology,* vol. 19, no. 3, pp. 1-13, 2012.

[34] G. McMullan and J. P. Quinn, "Detection of a Novel Carbon-Phosphorus Bond Cleavage Activity in Cell-Free Extracts of an Environmental Pseudomonas Fluorescens Isolate," *Biochemical and Biophysical Research Communications,* vol. 184, p. 1022−1027, 1992.

[35] J. W. Frost, S. Loo, M. L. Cordeiro and D. Li, "Radical-Based Dephosphorylation and Organophosphonate Biodegradation," *Journal of the American Chemical Society,* vol. 109, p. 2166−2171, 1987.

[36] B. Hove-Jensen, D. L. Zechel and B. Jochimsena, "Utilization of Glyphosate as Phosphate Source: Biochemistry and Genetics of Bacterial Carbon-Phosphorus Lyase," *Microbiology and Molecular Biology Reviews,* vol. 78, no. 1, p. 176 –197, 2014.

[37] D. J. Repeta, S. Ferrón, O. A. Sosa, C. G. Johnson, L. D. Repeta, M. Acker, E. F. DeLong and D. M. Karl, "Marine methane paradox explained by bacterial degradation of dissolved organic matter," *Nature Geoscience,* vol. 9, p. 884–887, 2016.

[38] D. M. Karl, L. Beversdorf, K. M. Björkman, M. J. Church, A. Martinez and E. F. DeLong, "Aerobic Production of Methane in the Sea," *Nature Geoscience,* vol. 1, p. 473−478, 2008.

[39] W. W. Metcalf, B. M. Griffin, R. M. Cicchillo, J. Gao, S. C. Janga, H. A. Cooke, B. T. Circello, B. S. Evans, W. Martens-Habbena, D. A. Stahl and e. al., "Synthesis of Methylphosphonic Acid by Marine Microbes: a Source for Methane in the Aerobic Ocean," *Science,* vol. 337, p. 1104−1107, 2012.

[40] H. A. Cooke, S. C. Peck, B. S. Evans and W. A. v. d. Donk, "Mechanistic Investigation of Methylphosphonate Synthase, a NonHeme Iron-Dependent Oxygenase," *Journal of the American Chemical Society,* vol. 134, no. 38, p. 15660–15663, 2012.

[41] D. A. Born, E. C. Ulrich, K.-S. Ju, S. C. Peck, W. A. v. d. Donk and C. L. Drennan, "Structural basis for methylphosphonate biosynthesis," *Science,* vol. 358, no. 8, p. 1336–1339, 2017.

[42] F. R. McSorley, P. B. Wyatt, A. Martinez, E. F. DeLong, B. Hove-Jensen and D. L. Zechel, "PhnY and PhnZ Comprise a New Oxidative Pathway for Enzymatic Cleavage of a Carbon-Phosphorus Bond," *Journal of the American Chemical Society,* vol. 134, p. 8364−8367, 2012.

[43] S. R. Gama, M. Vogt, T. Kalina, K. Hupp, F. Hammerschmidt, K. Pallitsch and D. L. Zechel, "An Oxidative Pathway for Microbial Utilization of Methylphosphonic Acid as a Phosphate Source," *ACS Chemical Biology,* vol. 14, no. 4, pp. 735-741, 2019.

[44] E. Miele, G. P. Spinelli, F. Tomao, A. Zullo, F. D. Marinis, G. Pasciuti, L. Rossi, F. Zoratto and S. Tomao, "Positron Emission Tomography (PET) radiotracers in oncology – utility of 18F-Fluoro-deoxy-glucose (FDG)-PET in the management of patients with non-small-cell lung cancer (NSCLC)," *Journal of Experimental & Clinical Cancer Research,* vol. 27, no. 52, pp. 1-10, 2008.

[45] A. Berger, "Positron emission tomography," *British Medical Journal,* vol. 326, pp. 1449-1450, 2003.

[46] K. Tanaka and K. Fukase, "PET (positron emission tomography) imaging of biomolecules using metal–DOTA complexes: a new collaborative challenge by chemists, biologists, and physicians for future diagnostics and exploration of in vivo dynamics," *Organic and Biomolecular Chemistry,* vol. 6, p. 815–828, 2008.

[47] B. H. Mock, G. K. Mulholland and M. T. Vavrek, "Convenient Gas Phase Bromination of [11C]Methane and Production of [11C]Methyl Triflate," *Nuclear Medicine & Biology,* vol. 26, p. 467–471, 1999.

[48] D. M. Jewett, "A Simple Synthesis of [11C]Methyl Triflate," *Applied Radiation and Isotopes,* vol. 43, no. 11, pp. 1383-1385, 1992.

[49] E. A. Rabiner and M. Laruelle, "Imaging the D3 receptor in humans in vivo using [11C](+)-PHNO positron emission tomography (PET)," *International Journal of Neuropsychopharmacology,* vol. 13, no. 3, p. 289–290, 2010.

[50] N. Ginovart, L. Galineau, M. Willeit, R. Mizrahi, P. M. Bloomfield, P. Seeman, S. Houle, S. Kapur and A. A. Wilson, "Binding characteristics and sensitivity to endogenous dopamineof [11C]-(+)-PHNO, a new agonist radiotracer for imaging thehigh-affinity state of D2receptorsin vivousing positronemission tomography," *Journal of Neurochemistry,* vol. 97, p. 1089–1103, 2006.

[51] S. M. Austin, A. Galonsky, J.Bortins and C. Wolk, "A batch process for the production of 13N-labelled nitrogen gas," *Nuclear Instruments and Methods,* vol. 126, no. 3, pp. 373-379, 1975.

[52] A. E. A. International, "Cyclotron Produced Radionuclides: Operation and Maintenance of Gas and Liquid Targets," in *IAEA Radioisotopes and radiopharmaceuticals No. 4*, Vienna, IAEA, 2012.

[53] P. Som and H. Atkins, "A fluorinated glucose analog, 2-fluoro-2-deoxy-D-glucose (F-18): Nontoxic tracer for rapid tumor detection," *Journal of Nuclear Medicine ,* vol. 21, no. 7, p. 670–675, 1980.

[54] B. M. Burt, John L Humm, D. A. Kooby, O. D. Squire, S. Mastorides, S. M. Larson and Y. Fong, "Using Positron Emission Tomography with [18F]FDG to Predict Tumor Behavior in Experimental Colorectal Cancer," *Neoplasia,* vol. 3, no. 3, p. 189–195, 2001.

[55] S. R.Cherry, J. A.Sorenson and M. E.Phelps, "Positron Emission Tomography," in *Physics in Nuclear Medicine*, Elsevier, 2012, pp. 307-343.

[56] V. Papadopoulos and a. et, "Translocator protein (18kDa): new nomenclature for the peripheral-type benzodiazepine receptor based on its structure and molecular function," *TRENDS in Pharmacological Sciences,* vol. 27, no. 8, pp. 402-409, 2006.

[57] R. Rupprecht, V. Papadopoulos, G. Rammes, T. C. Baghai, J. Fan, N. Akula, G. Groyer, D. Adams and M. Schumacher, "Translocator protein (18 kDa) (TSPO) as a therapeutic target for neurological and psychiatric disorders," *Nature Rewievs Drug Discovery,* vol. 9, no. 12, pp. 971-988, 2010.

[58] M. Imaizumi and H. Kim, "PET imaging with [11C]PBR28 can localize and quantify upregulated peripheral benzodiazepine receptors associated with cerebral ischemia in rat," *Neuroscience Letters,* vol. 411, no. 3, pp. 200-205, 2007.

[59] F. Shah, S. P. Hume, V. W. Pike, S. Ashworth and J. McDermott, "Synthesis of the Enantiomers of [N-Methyl-11C]PK 11195 and Comparison of Their Behaviours as Radioligands for PK Binding Sites in Rats," *Nuclear Medicine and Biology ,* vol. 21, no. 4, pp. 573-581, 1994.

[60] F. Chauveau, H. Boutin, N. Van Camp, F. Dollé and B. Tavitian, "Nuclear imaging of neuroinflammation: a comprehensive review of [11C]PK11195 challengers," *European Journal of Nuclear Medicine and Molecular Imaging,* vol. 35, no. 12, p. 2304–2319, 2008.

[61] D. R. Owen, Q. Guo, E. A. Rabiner and R. N. Gunn, "The impact of the rs6971 polymorphism in TSPO for quantification and study design," *Clinical and Translational Imaging,* vol. 3, no. 6, p. 417–422, 2015.

[62] R. Mizrahi, P. M. Rusjan, J. Kennedy, B. Pollock, B. Mulsant, I. Suridjan, V. D. Luca, A. A. Wilson and S. Houle, "Translocator protein (18 kDa) polymorphism (rs6971) explains in-vivo brain binding affinity of the PET radioligand [18F]-FEPPA," *The Journal of Cerebral Blood Flow and Metabolism,* vol. 32, no. 6, p. 968–972, 2012.

[63] M. Kobayashi, P. Zanotti-Fregonara, L. Dickstein, S. Zoghbi, T. Lohith, D. Rallis-Frutos, S. Telu, V. Pike, M. Fujita and R. Innis, "Influence of polymorphism rs6971 on [11C]DPA-713 imaging in human brain," *Journal of Nuclear Medicine,* vol. 55, no. 1, pp. 320-325, 2014.

[64] D. R. Owen, A. J. Yeo, R. N. Gunn, K. Song, G. Wadsworth, A. Lewis, C. Rhodes, D. J. Pulford, I. Bennacef, C. A. Parker and e. al., "An 18-kDa translocator protein (TSPO) polymorphism explains differences in binding affinity of the PET radioligand PBR28," *Journal of Cerebral Blood Flow and Metabolism,* vol. 32, pp. 1-5, Jan 2012.

[65] D. R. Owen and a. et, "., Yeo, A. J., Gunn, R. N., Song, K., Wadsworth, G., LAn 18-kDa Translocator Protein (TSPO) Polymorphism Explains Differences in Binding Affinity of the PET Radioligand PBR28," *Journal of Cerebral Blood Flow & Metabolism,* vol. 32, no. 1, pp. 1-5, 2011.

[66] M. Ikawa, T. G. Lohith, S. Shrestha, S. Telu, S. S. Zoghbi, S. Castellano, S. Taliani, F. D. Settimo, M. Fujita, V. W. Pike and R. B., "11C-ER176, a Radioligand for 18-kDa Translocator Protein, Has Adequate Sensitivity to Robustly Image All Three Affinity Genotypes in Human Brain," *Journal of Nuclear Medicine,* vol. 58, no. 2, p. 320–325, 2017.

[67] T. Kalina, N. Berroterán-Infante, S. Schmitl, C. Vraka, M. Hacker, M. Mitterhauser, W. Wadsak and K. Pallitsch, "Synthesis and in vitro evaluation of new translocator protein ligands designed for positron emission tomography," *Future medicinal chemistry,* vol. 11, 2019.

[68] E. Council of, "Radiopharmaceutical preparations," in *European pharmacopoeia*, Vienna, Verlag Österreich GmbH, 2008, p. 995.

[69] B.-I. N., K. T., F. L., J. V., V. R., V. C., H. M., H. AR., P. K., W. W. and M. M., "(R)-[18F]NEBIFQUINIDE: A promising new PET tracer for TSPO imaging," *European Journal of Medicinal Chemistry,* vol. 176, pp. 410-418, 2019.

[70] R. Qian, T. Kalina, J. Horak, S. Giberti and G. Forlani, "Preparation of Phosphonic Acid Analogues of Proline and Proline," *American Chemical Society,* vol. 3, pp. 4441-4452, 2018.

[71] M. T. J. J. S. Corbett, "Diametric Stereocontrol in Dynamic Catalytic Reduction of Racemic Acyl Phosphonates: Divergence from α-Keto Ester Congeners," *Journal of the American Chemical Society,* vol. 135, no. 2, p. 594–597, 2013.

[72] T. Yokomatsu, T. Yamagishi and S. Shibuya, "Enantioselective synthesis of α-hydroxyphosphonates through asymmetric Pudovik reactions with chiral lanthanoid and titanium alkoxides," *Journal of the Chemical Society, Perkins Transitions,* pp. 1527-1534, 1997.

[73] G. Keglevich and E. Bálint, "The Kabachnik–Fields Reaction: Mechanism and Synthetic Use," *Molecules,* vol. 17, no. 11, pp. 12821-12835, 2012.

[74] X. Ma, Q. Xu, H. Li, C. Su, L. Yu and X. Zhang, "Alcohol-based Michaelis–Arbuzov reaction: an efficient and environmentally-benign method for C–P(O) bond formation," *Green Chemistry,* vol. 20, no. 15, pp. 3408-3413 , 2018.

[75] F. Hammerschmidt, "Addition von Dialkylphosphiten und Dialkyl(trimethylsily1)phosphiten an 2-(Benzyloxy)propanal," *Liebigs Annalien der Chemie,* pp. 469-475, 1991.

[76] A. Schröckeneder, D. Stichnoth, P. Mayer and D. Trauner, "The crystal structure of the Dess–Martin periodinane," *Beilstein Journal of Organic Chemistry,* vol. 8, p. 1523–1527, 2012.

[77] J. Morrison and H. Mosher, Asymmetric Organic Reactions, Minnesota: Prentice-Hall, 1971.

[78] R. Noyori, I. Tomino, Y. Tanimoto and M. Nishizawa, "Rational Designing of Efficient Chiral Reducing Agents," *Journal of the American Chemical Society,* vol. 106, pp. 6709-6716, 1984.

[79] R. Noyori and S. Hashiguchi, "Asymmetric Transfer Hydrogenation Catalyzed by Chiral Ruthenium Complexes," *Accounts of Chemical Research,* vol. 30, pp. 97-102, 1997.

[80] S. T. Marino, D. Stachurska-Buczek, D. A. Huggins, B. M. Krywult, C. S. Sheehan, T. Nguyen, N. Choi, J. G. Parsons, P. G. Griffiths, I. W. James, A. M. Bray, J. M. White and R. S. Boyce, "Synthesis of Chiral Building Blocks for Use in Drug Discovery," *Molecules,* vol. 9, p. 405–426, 2004.

[81] R. Noyori, "Asymmetric Catalysis: Science and Opportunities," *Angewandte Chemie Internationale Edition,* vol. 41, pp. 2008-2022, 2002.

[82] T. S. Manikandan, S. Saranya and R. Ramesh, "Synthesis and catalytic evaluation of ruthenium(II) benzhydrazonecomplex in transfer hydrogenation of ketones," *Tetrahedron Letters,* vol. 57, p. 3764–3769, 2016.

[83] A. Fujii, S. Hashiguchi, N. Uematsu, T. Ikariya and R. Noyori, "Ruthenium(II)-Catalyzed Asymmetric Transfer Hydrogenation of Ketones Using a Formic Acid-Triethylamine Mixture," *Journal of the American Chemical Society,* vol. 118, pp. 2521-2522, 1996.

[84] O. Mitsunobu and M. Yamada, "Preparation of Esters of Carboxylic and Phosphoric Acid via Quaternary Phosphonium Salts," *Bulletin of the Chemical Society of Japan,* vol. 40, pp. 2380-238, 1967.

[85] T. Y. S. But and P. H. Toy, "The Mitsunobu Reaction: Origin, Mechanism, Improvements, and Applications," *Chemistry – An Asian Journal ,* vol. 2, p. 1340 – 1355, 2007.

[86] P. J. Kocienski, Protecting Groups, Stuttgart: Georg Thieme Verlag, 2005.

[87] F. Hammerschmidt and H. Völlenkle, "Absolute Konfiguration der (2-Amino-1-hydroxyethy1)phosphonsaure aus Acanthamoeba castellanii (Neff) - Darstellung der Phosphonsaure-Analoga von (+)- und (-)-Serin," *Liebigs Annalen der Chemie,* vol. 6, pp. 577-583, 1989.

[88] H. Wise, "Mechanisms of catalyst poisoning by sulfur species," *Catalyst Deactivation,* pp. 497-504, 1991.

[89] M. Hesse, H. Meier and B. Zeeh, Spektroskopische Methoden in der organischen Chemie, Zürich: Thieme, 2005.

[90] A. J. Birch, "Reduction by dissolving metals. Part I.," *Journal of the Chemical Society,* vol. 0, pp. 430-436, 1944.

[91] E. J. Corey and A. X. Huang, "A Short Enantioselective Total Synthesis of the Third-Generation Oral Contraceptive Desogestrel," *Journal of the American Chemial Society,* vol. 121, no. 710, pp. 710-714, 1999,.

[92] L. A., A. Borbás and B. I., "Protecting Group Manipulations in Carbohydrate Synthesis," *Comprehensive Glycoscience,* vol. 1, pp. 203-259, 2007.

[93] P. W. Rabideau and Z. Marcinow, "The Birch Reduction of Aromatic Compounds," *Organic Reactions,* vol. 42, 1992.

[94] W. Y., "Protection of the amino group," in *The Chemistry of the Amino Group*, Wiley & Sons Ltd., 1968, pp. 670-690.

[95] A. K. Bose, F. Greer and C. C. Price, "A Procedure for Phthaloylation under Mild Conditions," *Journal of Organic Chemistry,* vol. 23, pp. 1335-1338, 1958.

[96] L. M. v. Staalduinen, F. R. McSorley, K. Schiessl, J. Séguin, P. B. Wyatt, F. Hammerschmidt, D. L. Zechel and Z. Jia, "Crystal structure of PhnZ in complex with substrate reveals a di-iron oxygenase mechanism for catabolism of organophosphonates," *Proceedings of the National Academy of Sciences,* vol. 111, no. 14, pp. 5171-5176, 2014.

[97] A. Lockhart, B. Davis, J. C. Matthews, G. Hong, A. Gee, D. Earnshaw and J. Brown, *Nuclear Medicine and Biology,* vol. 30, pp. 199-206, 2003.

[98] M. Rodriguez-Mata, V. Gotor-Vernandez, J. Gonzales-Sabin, F. Rebolledo and V. Gotor, "Straightforward preparation of biologically active 1-aryl- and 1-heteroarylpropan-2-amines in enantioenriched form," *Organic and Biomolecular Chemistry,* vol. 9, pp. 2274-2275, 2011.

[99] A. Foucaud, C. Razorilalana-Rabearivony, E. Loukakou and a. H. Person, "Studies of 2,2'-bipyridyl N,N'-dioxides," *Journal of Organic Chemistry,* vol. 48, no. 3, pp. 283-289, 1983.

[100] M. Movassaghi and M. D. Hill, "A Versatile Cyclodehydration Reaction for the Synthesis of Isoquinoline and β-Carboline Derivatives," *Organic Letters,* vol. 10, pp. 3485-3488, 2008.

[101] E. Awuah and A. Caprett, "Strategies and Synthetic Methods Directed Toward the Preparation of Libraries of Substituted Isoquinolines," *Journal of Organic Chemistry,* vol. 75, pp. 5627-5634, 2010.

[102] H. Wang, J. Zhang and M. Xi, "Facile Formation of Dehydroalanine From S-Nitrosocysteines," *Journal of the American Chemical Society,* no. 131, pp. 13238-13239, 2009.

[103] R. E. Ireland and L. Liu, "An improved procedure for the preparation of the Dess-Martin periodinane," *Journal of Organic Chemistry,* vol. 58, no. 10, pp. 2899-2900, 1993.

[104] F. Hammerschmidt and H. Völlenkle, "Absolute Konfiguration der (2-Amino-1-hydroxyethy1)phosphonsaure aus Acanthamoeba castellanii (Neff) - Darstellung der Phosphonsaure-Analoga von (+)- und (-)-Serin," *Liebigs Annalen der Chemie,* vol. 6, pp. 577-583, 1989.

[105] G. A. Ropp and C. Melton, "Studies Involving Isotopically Labelled Formic Acid and its Derivatives," *Journal of the American Chemical Society,* vol. 82, no. 4, pp. 842-852, 1960.

[106] L. M. v. Staalduinen, F. R. McSorley, K. Schiessl, J. Séguin, P. B. Wyatt, F. Hammerschmidt, D. L. Zechel and Z. Jia, "Crystal structure of PhnZ in complex with substrate reveals a di-iron oxygenase mechanism for catabolism of organophosphonates," *PNAS,* vol. 111, no. 14, pp. 5171-5176, 2014.

[107] S. R. Gama, B. S. Y. Lo, J. Séguin, F. H. Katharina Pallitsch and D. L. Zechel, "C-H Bond Cleavage is Rate Limiting for Oxidative C-P Bond Cleavage By the Mixed Valence Diiron Dependent Oxygenase PhnZ," *Biochemistry,* pp. 1-44, 2019.

[108] A. Foucaud, C. Razorilalana-Rabearivony, E. Loukakou and H. Person, "[1 + 4] Cycloaddition of Isocyanides with l-Aryl-2-nitro- 1-propenes, Methyl 2-Nitro-3-arylpropenoates, and Methyl 2-Nitro-2,4-pentadienoates.," *Journal of Organic Chemistry,* vol. 48, no. 21, pp. 3639-3644, 1983.

[109] M. Rodriguez-Mata, V. Gotor-Vernandez, J. Gonzales-Sabin, F. Rebolledo and V. Gotor, "Straightforward preparation of biologically active 1-aryl- and 1-heteroarylpropan-2-amines in enantioenriched form," *Organic and Biomolecular Chemistry,* vol. 9, pp. 2274-2275, 2011.

[110] F. Hammerschmidt, W. Lindner, F. Wuggenig and E. Zarbl, "Enzymes in organic chemistry. Part 10 Chemo-enzymatic synthesis of l-phosphaserine and l-phosphaisoserine and enantioseparation of amino-hydroxyethylphosphonic acids by non-aqueous capillary electrophoresis with quinine carbamate as chiral ion pair agent," *Tetrahedron: Asymmetry,* pp. 2955-2964, 2000.

[111] R. Engl, in *Handbook of Organophosphorus Chemistry*, 1992, pp. 67-69.

[112] P. J. Murphy, in *Organophosphorus Reagents*, 2004, pp. 194-195.

[113] D. A. Born, E. C. Ulrich, K.-S. Ju, S. C. Peck, W. A. v. d. Donk and C. L. Drennan, "Structural basis for methylphosphonate biosynthesis," *Science,* vol. 358, no. 6368, pp. 1336-1339, 2017.